Manuel Tomberger, BSc

Adhesion of Thin Dielectric Films applied in Semiconductor Industry

MASTER THESIS

For obtaining the academic degree
Diplom-Ingenieur

Master Programme of
Advanced Materials Science

Graz University of Technology

Supervisor:

Ao.Univ.-Prof. Dipl.-Ing. Dr.techn. tit.Univ.-Prof. Adolf Winkler

Institute of Solid State Physics

In cooperation with

Infineon Technologies Austria AG, Villach

Graz, November 2012

Deutsche Fassung:
Beschluss der Curricula-Kommission für Bachelor-, Master- und Diplomstudien vom 10.11.2008
Genehmigung des Senates am 1.12.2008

EIDESSTATTLICHE ERKLÄRUNG

Ich erkläre an Eides statt, dass ich die vorliegende Arbeit selbstständig verfasst, andere als die angegebenen Quellen/Hilfsmittel nicht benutzt, und die den benutzten Quellen wörtlich und inhaltlich entnommene Stellen als solche kenntlich gemacht habe.

Graz, am ………………………………   ……………………………………………………………..
(Unterschrift)

Englische Fassung:

STATUTORY DECLARATION

I declare that I have authored this thesis independently, that I have not used other than the declared sources / resources, and that I have explicitly marked all material which has been quoted either literally or by content from the used sources.

………………………………   ……………………………………………………………..
date   (signature)

To my parents with thanks.

To my grandfather in memory.

There are agents in nature able to make the particles of joints stick together by very strong attraction and it is the business of experimental philosophy to find them out.

Sir Isaac Newton

Abstract

In semiconductor industry new technologies are steadily emerging and offering novel applications for the fabricated electronic devices. To ensure the best possible functionalities of these products great demands are made on the applied materials and all the single unit processes, including a significant percentage of thin film processes.

One major reliability and quality factor is the proper adhesion of the fabricated films to the substrate material and within the individual films. For this reason quickly applicable, reproducible and quantitative methods for determining adhesion of thin, predominantly dielectric films have to be found. It should be examined whether a method is more suitable for being applied for purposes of process and product development either or even as occasionally applicable quality tests during mass production. Besides the investigation of materials like thermally grown silicon oxide, chemical vapour deposited oxides and nitrides, as well as doped and undoped silica glasses, also nitrogen-doped hydrogenated amorphous carbon films were inspected, concerning their adhesion to different substrate materials. The adhesion of such thin films, strongly affected by thermo-mechanically induced film stresses which determine the long term durability of the devices, is a delicate topic in semiconductor industry.

In this work two testing methods have been applied to monitor the adhesion of the investigated films: the “stud pull-off test” and the “tape test”. The pull-off test was found to be a straightforward test providing numerical values for the adhesion within the examined interface, in case the metering capacity of the used instrument is not exceeded. The tape test, which has been modified for instant purposes according to an ASTM (American Society of Testing Materials) standardised testing procedure, however, just yields comparative results. Nevertheless, none of these two tests was judged to be suitable for quality inspections because they are destructive and to tedious to be prepared, but suitable for developing new products and processes.

Kurzfassung

In der Halbleiterindustrie treten ständig neuartige Technologien hervor und eröffnen neue Anwendungsmöglichkeiten für die hergestellten Bauteile. Um die bestmögliche Funktionsweise dieser Produkte gewährleisten zu können, werden große Anforderungen an die verarbeiteten Materialien sowie an alle involvierten Einzelprozesse gestellt, einen großen Anteil an Dünnschichtprozessen miteinbezogen.

Ein tragender Zuverlässigkeits- sowie Qualitätsfaktor ist in diesem Zusammenhang die Haftung der prozessierten Schichten auf dem jeweiligen Substrat. Aus diesem Grund sollten im Zuge dieser Arbeit schnell anwendbare, reproduzierbare und quantitative Methoden gefunden werden, um die Haftung der dünnen, vorwiegend dielektrischen Schichten zu bestimmen. Dabei sollte beurteilt werden, ob sich diese Methoden nur für Produkt- oder Prozessentwicklungszwecke eignen, oder auch für gelegentliche Qualitätskontrollen während der Massenanfertigung eignen. Neben den untersuchten Schichten wie thermisch gewachsenem Siliziumoxid, aus der chemischen Gasphase abgeschiedenen Oxiden und Nitriden, als auch dotierten sowie nicht-dotierten Silikat Gläsern, wurden auch stickstoff-dotierte amorphe Kohlenstoffschichten hinsichtlich ihrer Haftung auf dem Substrat untersucht. Die Haftung solcher Schichten, die von thermomechanisch induzierten Spannungen verursacht wird, ist in der Halbleiterindustrie in Bezug auf die Langzeitbeständigkeit ein prekäres Thema.

Im Zuge der vorliegenden Diplomarbeit wurden zwei Methoden angewandt, um die Haftung der untersuchten Schichten und Schichtsysteme zu bestimmen: der „Stempel-Abzugstest“ und der „Tape Test“. Der Stempeltest ist ein unkomplizierter Test, der numerische Ergebnisse für die Haftung innerhalb der untersuchten Grenzschicht liefert, jedoch müssen die Messwerte innerhalb des Messbereichs der verwendeten Apparatur liegen. Der Tape-Test, der anhand eines ASTM-genormten (American Society of Testing Materials) Testverfahrens auf unsere Zwecke angepasst worden ist, liefert jedoch nur Vergleichswerte für die Haftung einer Schicht. Obwohl keines der beiden Testverfahren für permanente Qualitätskontrollen als zweckmäßig beurteilt werden konnte, eigenen sie sich, um aufbauend auf die erhaltenen Ergebnisse, neue Prozesse sowie Produkte zu entwickeln oder zu verbessern.

Contents

List of Figures.......... V
List of Tables.......... IX
Index of Appendices.......... XI
List of Abbreviations.......... XIII
1. Introduction.......... 1
2. Adhesion – Theories, Issues, Testing Methods.......... 5
  2.1 Adhesion Theories.......... 6
    2.1.1 Mechanical Theory.......... 9
    2.1.2 Electrostatic Theory.......... 10
    2.1.3 Diffusion Theory.......... 10
    2.1.4 Adsorption or Thermodynamic Theory.......... 11
    2.1.5 Weak-Bonding-Layer (WBL) – Theory.......... 12
    2.1.6 Chemical Bonding Theory.......... 13
    2.1.7 Polarisation Theory.......... 13
  2.2 Challenges of Measuring Adhesion.......... 14
  2.3 Testing Methods.......... 16
    2.3.1 Mechanical Methods.......... 20
    2.3.1.1 Direct Pull-Off Method.......... 20
    2.3.1.2 Momentum or Topple Test.......... 21
    2.3.1.3 Ultra Centrifugal Method.......... 22
    2.3.1.4 Ultrasonic Method.......... 23
    2.3.1.5 Scotch Tape Test.......... 24
    2.3.1.6 Peel Test.......... 24
    2.3.1.7 Tangential or Lap Shear Test.......... 26
    2.3.1.8 Scratch and Indentation Test.......... 27
    2.3.1.9 Blister Method.......... 29
    2.3.2 Nucleation Methods.......... 29
    2.3.3 Miscellaneous Techniques.......... 30
    2.3.3.1 Thermal Method.......... 30
    2.3.3.2 X-Ray Method.......... 30
    2.3.3.3 Capacitance Method.......... 31
    2.3.3.4 Cathodic Treatment Method.......... 31
    2.3.3.5 Pulsed Laser or Electron-Beam Method.......... 31
    2.3.3.6 Scanning Thermal Microscopy (SThM).......... 32
    2.3.4 Abrasion Method.......... 32

3. Thin Films 33
3.1 Dielectric Films 34
3.2 Physical Properties of Thin Films 35
3.2.1 Mechanical Properties of Thin Films 35
3.2.1.1 Different Interfaces 35
3.2.1.2 Internal / Intrinsic Stress 38
3.2.1.3 Hardness of Thin Films 41
3.3 Thin Film Technologies 41
3.4 Film Properties affecting Adhesion 41
3.4.1 Substrate Properties affecting Adhesion 43
4. CVD – Chemical Vapour Deposition 45
4.1 General Process Principles 45
4.2 Methods of CVD 48
4.2.1 Thermal CVD 49
4.2.2 Atmospheric Pressure CVD (AP-CVD) 50
4.2.3 Low Pressure CVD (LP-CVD) 51
4.3 Plasma-Enhanced CVD (PE-CVD) 53
4.4 CVD Thin Films 55
4.4.1 Silicon Dioxide 55
4.4.2 Silicon Nitride 58
4.4.3 Silicon Oxinitride 59
4.4.4 Carbon Films 59
4.5 Cleaning Process/Cleaning Chemistry 60
5. CVD Reactors 63
5.1 P5000 65
5.2 Producer 67
5.3 Centura 69
5.4 Watkins Johnson 70
6. Investigated CVD Films 73
6.1 Boron and Phosphorous doped Silicon Glass (BPSG) on Silicon processed on different Machinery 73
6.2 Copper-Nitride Interface (CuNIT) on a product specific substrate with varying roughness of the copper surface 74
6.3 Silicon Nitride (SNIT) Films on assorted product-related Oxide Substrates 75
6.4 Amorphous hydrogenated nitrogen-doped Carbon (a-C:H:N) affected by substrate and pre-deposition plasma treatment 78
7. In-line Measurements and Processes 81
7.1 Opti-Probe: Film Thickness Measurements 81

7.2 MX 204: Film Stress Measurements 82
7.3 RFA-2: Doping Level....85
7.4 Annealing and Furnace Processes 86
8. Applied Testing Methods....87
8.1 Adhesion Pull-Off Test....87
8.2 Tape Test 92
8.3 Adjusting the Adhesion Pull-Off Test....95
9. Measurement Results and Discussion....99
9.1 Boron and Phosphor doped Silicon Glass on silicon 100
9.2 Copper-Nitride Interface on a product-specific Substrate 103
9.3 Silicon Nitride Films on assorted Substrates 108
9.4 Amorphous hydrogenated nitrogen-doped Carbon with different Plasma pre-treatment 115
10. Summary and Conclusions....123
11. Forecast....127
Acknowledgements....129
Bibliography....131
Appendix....i

List of Figures

Figure 1: Liquid-vapour (a), liquid-solid (b), and solid-vapour (c) “elastic membranes” in mechanical equilibrium at the contact line (d). The vectors generally used to present the forces in Young’s equation are shown in (e). 12

Figure 2: Schematic depiction of some of the most common and simplest mechanical adhesion tests. 17

Figure 3: Possible set-up of a pull-off test. 20

Figure 4: Diagram showing the arrangement for the moment or topple method. 21

Figure 5: Diagram of ultra-centrifugal arrangement for measuring adhesion. 22

Figure 6: (a) Diagram of the apparatus for stripping or peeling experiments using a kind of backing material, and (b) diagram for peeling experiments on unsupported films.. 25

Figure 7: Arrangement of the lap shear test for measuring adhesion, where the arrow shows the direction of the applied shear force. 26

Figure 8: (a) Schematic layout of the scratch or stylus test, and (b) the functional principle of such a scratch test. 27

Figure 9: The functional principle of a (nano-) indentation test. 28

Figure 10: Schematic illustration of the interfacial region between substrate and coating. a) mechanical interlocking, b) monolayer on monolayer, c) chemical bonding or compound interface, d) diffusion interface, e) pseudo-diffusion interface. 36

Figure 11: Sequence of events leading to (a) residual tensile stress in film; (b) residual compressive stress in film.. 39

Figure 12: Stresses in silver-lithium thin films: (a) Tensile film failures during deposition; (b) compressive film failures during aging in Ar.. 40

Figure 13: Possible profiles of conformity and edge coverage. 46

Figure 14: Sequence of gas transport and reaction processes contributing to CVD film growth. 46

Figure 15: Schematic diagram of the chemical, transport, and geometrical complexities involved in modelling CVD processes. 47

Figure 16: Pressure and temperature regimes of the most popular and well established processes in fields of Chemical Vapour Deposition as applied at INFINEON Technologies in Villach. 49

Figure 17: Schematic diagrams of AP-CVD reactors employed, among others, in epitaxial Si and CVD deposition processes. (a) Horizontal tube reactor; (b) pancake reactor; (c) barrel reactor; and (d) gas-injection reactor, operating continuously. 50

Figure 18: Different design of typical hot-wall multiple wafer LP-CVD reactors with a separate closure head (a) or with a closure head which is permanently fixed to the wafer carrier “boat”. 52
Figure 19: Reinberg-type cylindrical radial-flow plasma reactor for the deposition of – in this case – a silicon-nitride film. 54
Figure 20: Ternary phase diagram of bonding in amorphous carbon hydrogen alloys. 60
Figure 21: Schematic image of the P5000 mainframe showing the arrangement of the process chambers around the load lock chamber in the centre. 65
Figure 22: Schematic image of a P5000 process chamber. In this case the “chuck” is lamp heated and used for plasma-enhanced CVD, indicated by the blue RF-plasma cloud. 66
Figure 23: Schematic image of a P5000 process chamber. In this case the “chuck” is resistive heated and again used for plasma-enhanced CVD, indicated by the blue RF-plasma cloud. 67
Figure 24: Schematic image of Producer mainframe with its three individual twin chambers arranged around the loadlock chamber. 68
Figure 25: Schematic image of CVD Centura mainframe including the process chambers, the orienter chamber and the cool down chamber, as well as the load lock station. 69
Figure 26: Schematic image of HDP Centura mainframe. Process chamber D is completely missing, and chambers C and A are equipped with a special type of vacuum pump required for HDP deposition processes. 70
Figure 27: Schematic image of the “process muffle” of a Watkins Johnson applied for AP-CVD processes. 71
Figure 28: Film stack of boron and phosphorous doped silicon oxide on a bare silicon wafer. 74
Figure 29: Film stack of the Copper Nitride showing the thickness of each deposited film. ...75
Figure 30: Film stack of Silicon Nitride on the subjacent oxide film. 76
Figure 31: Schematic depiction of the D-Sound microphone, including the active and passive parts. The purple arrow indicates the gap, where the a-C:H:N film has been removed. 78
Figure 32: Film stack of a-C:H:N on either furnace POLY or furnace TEOS. 80
Figure 33: Wafer geometry and wafer centring station of the E+H MX204 measuring device, determining bow, stress and warp. 83
Figure 34: Triplet of local delta warp points used to determine the film stress. 84
Figure 35: RFA hardware components including the optical path of the X-rays. 85
Figure 36: Image of the PosiTest AT-M Manual adhesion tester. 87
Figure 37: Image of the quick-coupling system of the PosiTest showing the main feature of the self-alignment system. 88

Figure 38: Schematic drawing of the completely prepared sample stack placed on the heating plate......90
Figure 39: Illustration of the sawing pattern that has been used for the Tape Test showing the width of the single trace respectively. 95
Figure 40: Comparison of the maximum applied strain for differently treated rear sides of the utilized dollies......97
Figure 41: Compound strength for BPSG film obtained from tests with differently treated 10 mm dollies. 100
Figure 42: Compound strength for BPSG film obtained from tests with differently treated 14 mm dollies. 101
Figure 43: Compound strength for the copper-nitride interface obtained from tests with differently treated 10 mm dollies......105
Figure 44: Compound strength for the copper-nitride interface obtained from tests with differently treated 14 mm dollies. The arrows indicate those values at which some film material was pulled-off by the actuator. 105
Figure 45: Pictures of sample sites where the film stack has been pulled off and the silicon compound of the wafer was broken in succession......106
Figure 46: Pictures of the 160*160 µm grid where the CuNIT stack has completely peeled off from the silicon wafer (a) and of a 500 µm broad track where the CuNIT stack did not delaminate during the sawing process......107
Figure 47: Maximum values of the compound strength for Silicon Nitride on various substrates......111
Figure 48: ASTM grading of the adhesion for Silicon Nitride films on various substrates. ...112
Figure 49: Comparison of SNIT on a silicon wafer (# 04) and SNIT on EOX (#06). 300*300 µm grid size, magnification factor 2.5, scale 1000 µm. 113
Figure 50: Comparison of SNIT on SNIT with 3 weeks storage inside the cleanroom (#04) and SNIT on SNIT without storing wafer (#06). The red circles indicate regions at the sawing edges where delamination slightly took place. 500*500 µm grid size, magnification factor 2.5, scale 1000 µm......114
Figure 51: Significant values for the compound strength describing the adhesion of amorphous carbon films on their substrate layer, affected by the post-tempering process and strongly depending on the kind of plasma pre-treatment. 117
Figure 52: Images of some successful pull-offs of the amorphous carbon film from the subjacent POLY film, during testing with a 10 mm dolly. The red circle indicates the diameter of 10 mm. 118

Figure 53: Images of some successful pull-offs of the amorphous carbon film from the subjacent TEOS film, during testing with 10 mm (a) as well as with 14 mm dollies. One sample in (a) is magnified in insert (c). The green circles indicate the diameter of 14 mm (b), the red circle that of 10 mm (c). 119
Figure 54: ASTM grading of the adhesion of amorphous hydrogenated nitrogen-doped carbon, depending on executed pre- and post-treatments. 120
Figure 55: Comparison of the results gained by the tape test for an as-deposited (#14) and a tempered (#20) amorphous carbon film, on N_2O plasma treated POLY. 121
Figure 56: Comparison of the results gained by the tape test for an as-deposited (#17) and a tempered (#23) amorphous carbon film, on N_2O plasma treated TEOS. 122

List of Tables

Table 1: Classification along the purposes of investigation and the measured parameters or properties. 19
Table 2: Pressure and temperature regimes in CVD Reactors applied for Silicon Oxide Deposition. 56
Table 3: Overview across the Applied Materials equipment hardware. 64
Table 4: Sample specifications – BPSG on different equipments. 74
Table 5: Specifications of the substrate material and substrate films of Silicon Nitride. 74
Table 6: Split plan for the a-C:H:N film on POLY or TEOS including different plasma pre-treatments and different post-deposition treatments. 76
Table 7: Priming pressures and maximum pull rates according to the dolly diameter. 91
Table 8: Classification of the adhesion test results. 93
Table 9: Compound strength of boron and phosphor doped silicon oxide obtained from different dolly-sizes with variably treated rear sides. 98
Table 10: Compound strength of the copper-nitride interface obtained from different dolly-sizes with variably treated rear sides. 100
Table 11: Compound strength of Silicon Nitride on various and differently treated substrates gained from different dolly-sizes with alumina blasted rear sides. 98
Table 12: Compound strength of Silicon Nitride on various and differently treated substrates gained from different dolly-sizes with alumina blasted rear sides. 105
Table 13: Sample denotation and sequential arrangement of the films appropriate to figure 46. 112
Table 14: Compound strength of the a-C:H:N films with respect to the kind of plasma cleaning before and the type of post-treatment after depositing the particular carbon film. .111
Table 15: Sample denotation and sequential arrangement of the individual process steps.120

Index of Appendices

Appendix 1: Measurements of the BPSG film parameters. iii
Appendix 2: Measurments of the tempered BPSG films before and after the tempering process. v
Appendix 3: Percentual reduction of the BPSG film thickness during the tempering process. vi
Appendix 4: Impact of several film deposition and one tempering process on the wafer bow. vii

List of Abbreviations

a-C:H:N	amorphous hydrogenated nitrogen-doped Carbon
AFM	Atomic Force Microscope
ALD	Atomic Layer Deposition
AMAT	Applied Materials
AP-CVD	Atmospheric Pressure Chemical Vapour Deposition
ASTM	American Society of Testing Materials
BPSG	Boron and Phosphorous doped Silicon Glass
BSG	Boron doped Silicon Glass
CuNIT	Copper Nitride
CVD	Chemical Vapour Deposition
DARC	Dielectric Anti-Reflection Coating
DLC	Dielectric-Like Carbon
EOX	“Erst-Oxid” – fist oxide layer of process route
HDP	High Density Plasma
LE-CVD	Laser-Enhanced Chemical Vapour Deposition
LP-CVD	Low Pressure Chemical Vapour Deposition
MO-CVD	Metal Oxide Chemical Vapour Deposition
PE-CVD	Plasma-Enhanced Chemical Vapour Deposition
PSG	Phosphorous doped Silicon Glass
PVD	Physical Vapour Deposition
RF-power	Radio Frequency power
RT-CVD	Rapid Thermal Chemical Vapour Deposition
SA-CVD	Sub-Atmospheric Chemical Vapour Deposition
SEM	Scanning Electron Microscope
SNIT	Silicon Nitride
STM	Scanning Tunnelling Microscope
TC-bond	Thermo Compression bond
TEB	Triethylborate, $B(C_2H_5O)_3$
TEOS	Tetraethyorthosilicate or Tetraethyloxisilane, $Si(C_2H_5O)_4$
TEPO	Triethylphosphate, $PO(C_2H_5O)_3$
USG	Undoped Silicon Glass

1. Introduction

Energy Efficiency, Mobility, Safety – these are just some of the major aspects upon which the development and production of innovative semiconductor solutions and products is based. For this reason many companies have committed themselves to searching and providing the best solutions in focus areas that centrally challenge modern lifestyle and society: energy efficiency, mobility and security. Energy efficiency, for instance, takes on special significance because natural resources melt away and energy requirements steadily rise. Therefore advanced semiconductor solutions, as assembled and established by Infineon Technologies Austria AG, afford cutting-edge technologies to generate, transmit, and utilize the available energy.

The recent focuses are located on semiconductor solutions to be applied in the automotive, industrial and security sectors, include key products like novel systems for measuring tire pressure, microchips for engine management systems, chips for energy efficiency, or contactless security products necessary for identification cards.

As the world's population is growing, more and more megacities are arising and therefore the demand for energy proceeds to wind up across the terrestrial globe. Additionally, the growing demand for protecting the climate claims for approaches to novel solutions for numerous aspects of everyday's life. As we go ahead, life quality will always be addicted to innovative technologies bringing more energy efficiency to already existing applications and systems, mobility concepts to be made more flexible and digital ways of communications more secure. Powerful semiconductors can provide valuable building blocks for the rapidly growing markets. To being able to embrace all these requirements and to succeed and to persist at all mentioned sectors one major and even primary goal is to ensure zero-defect products, including chips and electrical circuits. In the automotive sector safety is especially relevant, wherefore electronic defects regardless of which type are not tolerable at all. These zero-defect demands are also necessary with respect to the transport sector, e.g. trains and airplanes, which requires long-term endurance. All these electronic components are produced and tested on silicon wafers in various complexities and technologies in more than 400 single process steps, whereas the challenge is to manage dimensions of structures down to magnitudes of 200 nm.

As a leading global provider of semiconductor and system solutions that enable applications to influence and improve tomorrow's world in the titled focus areas of energy efficiency, mobility and security, Infineon also has to persist in the daily increasing competition. This can just be achieved and the zero-defect policy can be maintained, if all the various frontend process steps are perfectly adjusted on one another, resulting in devices being characterized by their functionality, their high performance, their quality and their long term durability. Particularly with regards to quality and long term durability, the adhesion between the various films is a quite determinative factor.

The process route of a common semiconductor device consists of many different process steps and process types, such as furnace technologies, deposition processes including sputtering and epitaxial film growth, photo lithography for structuring and passivation purposes. Moreover there are implantation processes, for doping certain materials and etch processes, either by plasma or wet chemicals, followed by inline inspections and reverse side processes, until the completely processed chips are separated by cutting in the backend area. Because of the diversity of the applied process types this thesis focuses on films processed during chemical vapour deposition (CVD) processes.

The major purpose of the presented thesis was to compile and develop quickly applicable, reproducible and quantitative methods which can be applied to determine the adhesion of thin dielectric films to each other. The initial plan was to investigate films like thermally grown silicon oxides, CVD oxides and nitrides with various specifications and even imide films. A checklist for the tested materials as well as for suitable testing methods had to be established to be utilized as reliable reference, and the influence of specific surface treatments had to be investigated. This field is of such great scientific interest, as up to now no method could be established as a standard to be suitable for almost every field of application. Apparently, all the recently known and applied methods have advantages and disadvantages. Therefore, at the beginning, an overview across many different methods of testing adhesion will be given, pointing out the preferences, boundaries and issues of the several testing methods.

Adhesion of thin films is, in the course of long term durability, a delicate topic in fields of semiconductor processing and technology.

Therefore, one has to find suitable ways to measure the adhesion for the instant film stacks. But before that one has to be aware of what adhesion is, how it can be defined and upon which phenomena and theories it is based. In the course of this thesis information about available testing methods have been collected, methods which are available to be executed at Infineon Technology Austria AG, Villach had to be discovered and their functionality had to be compared to experiments which have already been executed in literature. Finally, two methods for testing adhesion have been found, showing different operating principles: the Adhesion Pull-Off Test, a quantitative method being similar to the stud or direct pull method, and the TLM Tape Test, a more qualitative method based upon an ASTM (American Society for Testing Materials) standard, whose preparation procedure had to be adjusted for our purposes and is executed similar to Tape or Peel tests.

These two destructive methods finally have been applied to judge the adhesion of assorted and selected sample lots, processed with various methods of CVD and with different types of equipment, whereas the process steps have been extracted from recent process plans of typical semiconductor products. As sample lots such product types have been chosen, whose incorporated process steps are essential for many different types of devices and products manufactured at Infineon in Villach. An additional aspect taken into consideration while deciding to prepare certain samples was their importance and the relevance of their examination for gaining new insights in fields of product and technology developments.

Considering the mentioned aspects the following samples have been investigated with respect to their adhesive properties and features:

We started off with a lot of Boron and Phosphorous doped Silicon Oxide (BPSG) at low doping levels of boron and phosphor with the same critical film thickness of 1800 nm, to study the effect of being processed on different equipments. Once via sub-atmospheric pressure chemical vapour deposition (SA-CVD) on an equipment called “Centura”, and once on a “Watkins Johnson” running atmospheric pressure chemical vapour deposition (AP-CVD). When the BPSG films are processed via SA-CVD up to the critical film thickness they tend to show cracks and start delaminating from the subjacent film.

The second investigation deals with the adhesion of plasma-enhanced chemical vapour deposited Silicon Nitride (PE-CVD SNIT) on copper films. The intention is to investigate how good the SNIT adheres to copper substrates. Aluminum, which has originally been used for these purpose shall be replaced by copper due to its better electrical properties.

The third sample lot has been studied because of some uncertainties concerning the adhesion of silicon nitride processed via plasma-enhanced CVD by using silane (SiH_4) on several substrate layers. As there have been several problems concerning the adhesion of silicon nitride (SNIT) films on diamond-like carbon (DLC) and especially on oxide films, silicon nitride has been deposited on various oxide films to figure out whether the composition and the way of production of the respective substrate have an influence on the adhesion.

And finally an amorphous hydrogenated nitrogen-doped carbon (a-C:H:N) film has been deposited on two different substrates, POLY and TEOS. The main intention of this lot has been the examination of the effect of different surface treatments on the adhesion. For this reason the particular surface – POLY or TEOS – was treated either without any plasma, with N_2O plasma or with NH_3 plasma, before the a-C:H:N film has been deposited. It has been assumed that the N_2O plasma has a worsening effect on the adhesion, as during post-tempering processes the oxygen from the N_2O and the carbon from the a-C:H:N film start reacting with each other at the considered interface forming carbon monoxide or carbon dioxide (CO and CO_2). This a priori statement should be verified with this series of experiments, also incorporating a chemical aspect.

2. Adhesion – Theories, Issues, Testing Methods

Adhesion, also denoted as adhesive force or adhesive strength, is the physical state of a boundary layer which forms between two condensed phases getting into contact with one another, as well as between solid state bodies and liquids with negligible vapour pressure. The main properties of this state, the mechanical cohesion of the involved phases, are generated by the molecular interactions inside the boundary layer. The forces affecting this mechanical cohesion are not completely studied for which reason there appear several adhesion theories.

The term “adhesion” or “adhesive strength” is, practically, defined as the power and strength of a bonding between two materials.

The *American Society of Testing and Materials* (ASTM) defines “adhesive strength” as a state where two surfaces are held together by valence bonds, mechanical clamping or both of them. Quantitatively and physically the adhesive strength σ_A can be defined as follows: [1]

$$\sigma_A = \frac{F_i}{A_r} \tag{1}$$

F_i is the experimentally not measurable internal force per elementary area and A_r is the real surface created in case of fracture. There is no testing method which can directly and exclusively measure the above stated internal force.

The sum of all the adhesive strengths results in a new expression, the bond or compound strength σ_C. This is the ratio between the outer (measurable) force F_A per unit area and the geometric surface A_g: [1]

$$\sigma_C = \frac{F_m}{A_g} \tag{2}$$

Adhesion itself is also defined as the state of a boundary layer that builds between two condensed phases of matter which are in contact to each other. This adhesion is characterized by the mechanic coherence of the involved phases, induced by molecular and atomic interactions, called primary and secondary valence bonds.

When looking at the ranges and binding energies of all the possible interactions, it seems obvious that on the one hand close contact between different phases is necessary, and on the other hand the appearance of chemical bonds should result in high bond strength.

2.1 Adhesion Theories

Generally, adhesion and the associated theories can simply be divided into three different kinds: basic adhesion, thermodynamic adhesion, and practical adhesion. [2], [3]

Basic adhesion is the work which has to be applied to overcome the largest tension inside the boundary layer of the solid compound.

The thermodynamic adhesion W_A denotes the required work to separate two solid phases of matter as:

$$\mathrm{W_A} = \gamma_\mathrm{f} + \gamma_\mathrm{s} + \gamma_\mathrm{fs} \tag{3}$$

In this formula γ_f is the surface energy of the film, γ_s the surface energy of the substrate and γ_{fs} the surface energy of the boundary between these two phases.

The practical adhesion W_{prac}, in contrary to the basic adhesion, considers conditions that might occur in practical exercise like relations of stress throughout the coating, the film thickness and the mechanical properties of the substrate.

$$\mathrm{W_{prac}} = \mathrm{W_A} + \mathrm{U_f} + \mathrm{U_s} + \mathrm{U_{fric}} \tag{4}$$

W_{prac} is the practical adhesion strength which is the toughness of the interface, U_f and U_s are the energies released during plastic deformation of the film and the substrate, U_{fric} is the amount of energy converted into heat and other forms of energy.

As there are quite some definitions, there are as many or even more options for grouping the known types or better said theories of adhesion.

In one reference it seems sufficient just to distinguish between “chemical bonding” and “mechanical bonding” to be the reason for adhesion in terms of “liquid adhesion” or “wetting”. [4] In this case one means chemical adhesion by ionic bonding that occurs when one atom loses one of its electrons and another atom gains this electron resulting in strong Coulomb forces. In case of two atoms sharing two electrons covalent bonding arises. Both types of bonds, ionic and covalent, occur in atoms or molecules with few free electrons. Most of these materials show low electrical conductivities and they are brittle. In metallic materials which have a good electrical conductivity the bonding is provided by atoms being surrounded by lots of free electrons. In some materials atoms are held together not only by one single but by different types of bondings. Between atoms and non-polar molecules Van-der-Waals or dispersion bonding occurs as an alterable dipole of one molecule induces a dipole in another molecule, leading to an interaction and causing the bonding. When dealing with mechanical bonding adhesion is caused by mechanical interlocking of the two considered surfaces. Therefore the one or the other material has to be deformed for bonding or ruptured when separated. Mechanical bonding requires the deposited film to be consistent with the rough surface without any voids, porosities or bad contacting areas at the coated interface.

Others divide present theories of adhesion into "practical adhesion" and "fundamental adhesion".[5] In this context some authors thought that practical and fundamental adhesion were the same and handled it as such. Practical adhesion deals with the dimension of the force or energy necessary to break an adhesive bond. According to this context *Mattox* and *Rigney* state: *"Practical adhesion may be defined as the physical strength of an interface between two regions of a material system."* [6]

Fundamental adhesion, in the contrary, deals with all mechanisms and forces on the molecular scale which connects different components appearing in an adhesive bond.

Whenever, in consideration of fundamental adhesion, an adhesive junction fails a certain amount of energy will have to be supplied to break the bonds and to create two new surfaces. These broken bonds, according to the circumstances, have been primary or secondary bonds. This amount of energy needed to form new surfaces is called surface energy. If the failure occurs at the interphase between phase 1 and phase 2, the appropriate surface energy term resembles the work of adhesion, W_A:

$$\mathrm{W_A} = \gamma_1 + \gamma_2 - \gamma_{12} \tag{5}$$

γ_1 and γ_2 are the surface energies of the two materials, both in contact with the surrounding air, and γ_{12} being the interfacial energy between the two phases 1 and 2. An adhesive bond often fails cohesively within one component rather than at the interface. Under these circumstances the corresponding term will be the work of cohesion Wc, given by (for failure within phase 1):

$$\mathrm{W_C} = 2 * \gamma_1 \tag{6}$$

In practice the magnitude of the fracture energy G is (almost) always considered to be greater than the surface energy term W_A or W_C – now written as G_0 – which are defined by the equations above. G_0 may be some average value of W_W or W_C depending on the place of failure. All the above equations are thermodynamic equations and fracture of an adhesive bond will seldom, if ever be considered to be reversible as thermodynamics requires. During the fracture process other energy-absorbing processes like plastic and visco-elastic deformations (e.g. reconstruction, adsorption) might occur.

Therefore

$$\mathrm{G} = \mathrm{G}_0 + \Psi \tag{7}$$

where Ψ represents all these other processes that absorb part of the released energy.

The already mentioned surface energy is the result of non-symmetric bonds of the surface atoms or surface molecules which are in contact with vapour (gaseous phase) and it is measured as energy per unit area. If there isn't any elastic or plastic strain applied in some way (Ψ=0), the fracture energy *G* one would have to apply to create two new surfaces from the interface in the fracture area of the solid compound, would just be the surface energy itself. (Compare [5], p.14f.) Solid matters always try to reduce their surface energy to a minimum and they manage this by several reaction and adsorption processes.

Probably the most common and comfortable way to classify adhesion might be mechanical adhesion, based on physical and mechanical forces, and specific adhesion due to chemically, physically and thermodynamically based forces.[4] For both of these types of adhesion there exist separate adhesion theories, which were developed independently from one another. But according to today's level of knowledge the mechanical and the specific adhesion kind of resemble to each other.

Mechanical adhesion in this context refers to the clamping or interlocking of glue into the microscopically small porosities and slots of a solid state body. In the past this has been the way of explaining adhesion but the cohesion between a solid body and a smooth surface cannot be explained that way.

Therefore theories of specific adhesion were developed and studied, because all the theories about mechanical adhesion have not been sufficient to explain the cohesion of a solid body with a smooth surface in a plausible way. The different theories of specific adhesion and the theory of mechanical adhesion do not totally exclude each other, but they complement one another.

Many authors have written about the different divisions and types of adhesion and all their different theories. But there is no uniform classification especially when dealing with the specific theories, whereas the mechanical theory always has to be considered up to a certain extent. It gets even more confusing as all the different theories dealing with adhesion are not always subdivided into equivalent categories.

All documents used for this thesis have a common classification concerning four theories that are discussed in [5], [7] and [8].

- Mechanical theory
- Electrostatic theory
- Diffusion theory
- Adsorption (or Thermodynamic) theory

Beside these, let's call them "quintessential theories" there exist two other theories dealing with different aspects of reasons for adhesive bonding.

- Weak-Bonding-Layer theory [5], [8]
- Chemical bonding theory [8]

As this should not be sufficient there is even a 7th grouping to be found in literature [9], the

- Polarisation theory

2.1.1 Mechanical Theory

This theory, also called mechanical interlocking or keying, is said to be the oldest explanation for adhesion and it describes mechanical interlocking to be the reason for adhesion when adhesives flow into an irregularity (porosities, cavities, pores or asperities) of the substrate surface, and, thus, being the major factor to determine and to influence the adhesive strength of the compound. Similarly as for the push-button principle some molten metal or an adhesive flows into porosities or any warping of the substrate, forming a positive locking surface after solidification and becomes no more extractable except by breaking one of the adhered materials. Nevertheless, the theory of mechanical interlocking cannot be universally applied when trying to establish good adhesion between two smooth surfaces. For this purpose the effects of the mechanical interlocking, as well as the thermodynamic interactions between interfaces have to be kept in mind, resulting in a relation for the joint strength *G*:

$$\begin{aligned} \mathrm{G} = (\mathrm{constant}) * (\mathrm{mechanical\ keying\ component}) \\ * (\mathrm{interfacial\ interaction\ component}) \end{aligned} \tag{8}$$

According to this equation a good adhesion could be achieved by improving the morphology of the surface as well as the physiochemical properties of the substrate and the applied adhesive.[7]

2.1.2 Electrostatic Theory

This theory states that an electrical double layer arises at any arbitrary interface, consequently Coulomb forces start acting. These electrostatic forces are said to enforce the adhesive strength in a significant way. Applying this theory a substrate/coating system is seen as a capacitor that gets charged as soon as two different materials get into contact. Trying to separate the two plates of the capacitor leads to an increase of the potential difference until a discharge occurs. Therefore it seems obvious that the attractive electrostatic forces operating across such electrical double layers lead to the adhesive strength. This theory can be represented by the Theory of *Derjaguin*, indicating that the energy needed to separate the interface G_e is related to the discharge potential V_e as follows:

$$\mathrm{G_e} = \frac{\mathrm{h}\varepsilon_\mathrm{d}}{8\pi}\left(\frac{\partial \mathrm{V_e}}{\partial \mathrm{h}}\right)^2 \tag{9}$$

where h is the discharge distance, ε_d the dielectric constant and V_e the electric potential between the two capacitor plates. Furthermore, according to the approach made above, the adhesive strength might vary with the gas pressure while a measurement is performed.

In a descriptive way one can imagine the effect of the electrostatic theory to be the adhesion of a thin electrostatically charged plastic film on a sheet of paper.[7]

2.1.3 Diffusion Theory

According to the diffusion theory an inter-diffusion process of the adhesive and the adherent across the interface between them is the reason for adhesion. Adhesion is considered to be a 3-dimensional process taking place inside a certain volume, rather than being a 2-dimensional surface process. This theory can especially be applied for polymeric materials where the adhesives and the adherent must be thermodynamically compatible to each other, leading to interfacial diffusion. In such a case the adhesion is based on the assumption that the adhesive strength of polymers to themselves (denoted as “autohesion”) or to each other results from mutual diffusion (inter-diffusion) of macromolecules across the interface. For some adhesion problems (healing, welding) this is very important for which reason, when dealing with inter-diffusion phenomena, the joint strength often depends on factors like contact time, temperature, nature and molecular weight of the involved polymers. A quantitative model for this diffusion theory of adhesion was developed from Fick’s first law, outlining the amount of a certain material w which diffuses in a given direction x across a plane of unit area due to $\delta c/\delta x$, the concentration gradient.[7]

$$\partial w = -D_f \, \partial t \, \frac{\partial c}{\partial x} \quad \leftrightarrow \quad \frac{\partial w}{\partial t} = D_f \, \nabla j \tag{10}$$

With:

$$-\frac{\partial c}{\partial x} = \nabla j \tag{11}$$

2.1.4 Adsorption or Thermodynamic Theory

For interfacial adhesion the adsorption theory is most widely applied. Though the generation of an interface between a liquid and a solid face and the mechanisms of adhesion differ quite a lot from those interfaces formed during thin film deposition processes, this theory contains some interesting basics. It states that surface forces are involved while polar molecules are orientated in such a way that the surface molecules of the adhesive and the adherent get into contact. Because of interatomic and intermolecular forces an intimate contact between the molecules or atoms is achieved at the interface, so the materials will adhere to each other.

During interfacial bonding the magnitude of these interatomic and intermolecular forces can be explained by fundamental thermodynamic quantities like the surface free energies of adherent and adhesive. [7], [8]

The criteria for good adhesion are equivalent with the criteria of equally good wetting being a necessary rather than a sufficient condition.[10] This process of wetting a surface by a fluid can be described by Young's equation:

$$\gamma_{LV} \cos\theta = \gamma_{SV} - \gamma_{SL} \tag{12}$$

This equation relates the interfacial tensions (γ) between the phase solid-vapour (γ_{SV}), liquid-vapour (γ_{LV}) and liquid-solid (γ_{SL}) to the contact angle θ adjusting at the state of equilibrium between the tension vectors γ_{LV} and γ_{SL}, as illustrated in figure 1. Therein images of the mechanical balance of the "contacting skins", the "stretched membranes", or the "elastic membranes" are shown. Liquid/vapor (a), solid/liquid (b), and solid/vapor (c) tensions balance one another (d) to generate an equilibrium contact angle. In (e) the common depiction of vectors that are used to represent forces in Young's statement are shown. [10]

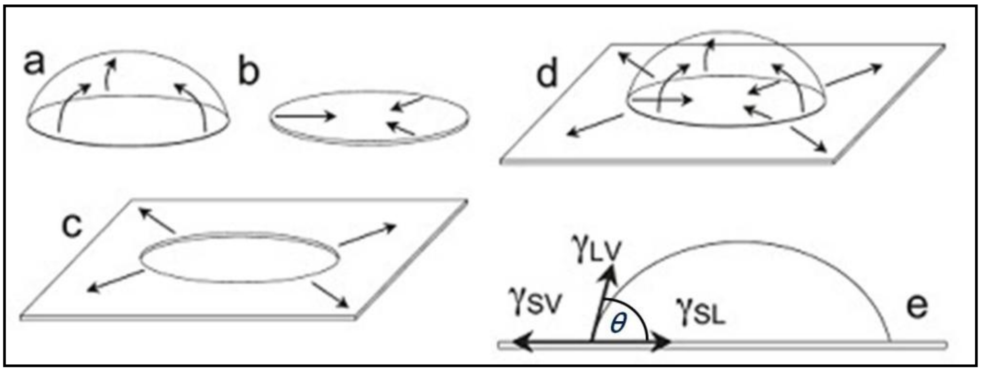

Figure 1: Liquid-vapour (a), liquid-solid (b), and solid-vapour (c) “elastic membranes” in mechanical equilibrium at the contact line (d). The vectors generally used to present the forces in Young’s equation are shown in (e).

The surfaces morphology, the fluids viscosity and Young’s equation are three major factors that influence the rate of spreading of the fluid. The spreading rate can be increased due to capillary effects when the surface is roughened or by decreasing the viscosity of the fluid.
For the case we deal with, thus, for systems of solid-liquid interfaces, the work of adhesion W_{SL} can now be derived including Young’s equation (equation 12):

$$W_{SL} = \gamma_{SV} + \gamma_{LV} - \gamma_{SL} = \gamma_{LV} * (1 + \cos\theta) \tag{13}$$

2.1.5 Weak-Bonding-Layer (WBL) – Theory

From the past till now it got more and more obvious that varieties and modifications of adhesives can be found in the surrounding area of an interface causing an interfacial zone to form which shows different properties as the surrounding bulk materials. The main factor for the determination of the adhesion level is said to be the cohesive strength of a Weak Boundary Layer (WBL). Therefore the energy of adhesion *G* equals the cohesive energy G_c *(WBL)* of the weaker interface. If fracture of the composite occurs one cannot expect that it just spreads out along the interface between adhesive and substrate. More often this failure in cohesive adhesion occurs within the weaker material – in this case adhesive or adherent material – somewhere near the interface. The fact that the distribution and the concentration of internal stresses near the crack tip somehow support the statement that the fracture has to propagate close to but not at the interface substrate-adhesive. Anyhow, the creation of interfacial layers become of such high interest, leading to the concept of “thick interface” or “interphase” whose thickness ranges from the molecular level (few angstroms or nanometres) up to the microscopic scale (few microns or even more). The formation of such interfaces can strongly be influenced by physical, physio-chemical or chemical phenomena like the orientation of chemical groups, the growth of transcrystalline structures or the modification of thermodynamics and kinetics of the polymerization process. [5], [8]

2.1.6 Chemical Bonding Theory

The basis for this theory is that real chemical bonds tend to arise at the interface between both of the involved materials at a microscopic range of size. The chemical bonds forming across an interface can strongly influence, even being crucial, for the level and quality of adhesion between both materials. Such bonds are denoted as “primary” bonds compared to the other kind of bonds, the physical interactions like Van-der-Waals bonds representing the “secondary” bonds. In this context the terms “primary” as well as “secondary” refer to the bond energy and the relative strength of each type of interaction taken into account. Obviously the formation of these chemical bonds depends on how reactive both materials, the substrate and the coating, are. Ionic and covalent bonds, representing the primary bonds are of great interest and have been explored a lot. In the same context several studies have been analysing the influence of these bonds on the joint strength G or the intrinsic fracture energy of adhesion G_0, explained previously. Also a very important field of adhesion, making use of the discussed chemical bonds, applies coupling agents improving the joint strength of the bonded materials. [8]

2.1.7 Polarisation Theory

The principle of this theory is that a compact adhesive bond is only formed if both materials have polar groups of atoms which are the origin of dipole forces leading to the adhesion of a compound. So, this theory takes advantage of the dipole character of certain molecules. Beside the dipole interaction it is important to pay attention that on certain surfaces thin oxi-hydrate layers can be present. Consequently, hydrogen bonds are formed between both materials which are in close contact.

This can be characterised by the Lewis Theory of the interaction between acid and chemical base, if the chemical base – acting as electron donor or proton acceptor – interacts with the acid. A qualitative classification separates the compounds into hard and soft chemical bases and acids, whereupon the acid is a particle with an empty outer orbital which can easily accept an electron by forming a covalent bond. A Lewis-acid, hence, has an “electron pair hole” which can be occupied by a free electron (Lewis-acids are electron pair acceptors). On the other hand a Lewis-base has a free pair of electrons that can be shared with a Lewis-acid to form a bonding (Lewis-bases are electron pair donators). The interaction between two materials, therefore, is induced by the interaction and the covalent bonding of electrons in the lowest unoccupied molecular orbital (LUMO) of the acid and the highest occupied molecular orbital (HOMO) of the chemical base. [9]

2.2 Challenges of Measuring Adhesion

The adhesive force is an important parameter for coating processes. The determination of their magnitude, though, has been and still is quite a challenge from the physical point of view. To achieve an ideal coating, one has to afford many trials before, including a proper correlation between wetting and adhesive strength.
During coating processes some questions are of great importance:

1. How a surface has to be conditioned to achieve the highest possible adhesion?
2. How can one measure this ideal state of the surface?
3. How good does the coating finally adhere to that surface?

Dealing with question one, there are many methods of treating a surface to improve adhesion, but it is not well established how a surface has to look like, which properties it should have to achieve a high adhesion. Therefore, the reasons and sources for adhesion have to be explained properly, but this has not happened up to now, as adhesion mechanism and adhesion theories are always discussed in a controversial way. The biggest problem in this regard is the fact that adhesion is based on that many different mechanisms, which can be lead back to the following fundamental mechanisms: primary and secondary valence bonds, mechanical interlocking, diffusion processes and electrical double layers. How high the percentage of the contribution of each single mechanism definitely is, is not well known and it differs depending on which kind of coating shall adhere to what kind of surface. So there is no generally valid statement about how a surface has to be structured to achieve the highest possible adhesion.
This directly leads us to the second question – how the ideal surface state can be measured: if an ideal state of the surface to be coated, leading to the maximal adhesive force does not even exist, it cannot be determined either. This, let’s call it idea – seeming to be a contradiction in itself – somehow disagrees with the theory of wetting, which cannot be applied to explain such a high magnitude of adhesion being expected from today’s coating technologies. Because of this statement, based on the observation of different wettability of surfaces, the “thermodynamic adhesion theory” started to develop with Dupré. The adhesion of different compounds to one another should be explained thereby. According to this theory,

one would always expect good adhesive properties for small wetting angles and for large magnitudes of surface tension of the solid matter. The performance of the surface pre-treatment is also judged through high surface tension, gained by a certain procedure of surface conditioning.

The reason for the adhesion theory not being suitable to explain a high magnitude of adhesive strength is that Duprè's statements about adhesion are based on reversible processes like the surface tension of a water droplet which adheres to a plate. If the droplet is removed, the plate is arranged in its original state, but this primitive state can normally not be achieved when dealing with real-live coatings showing a good adhesion. Here adhesion itself does not fail, the fracture takes place inside the coating or the base material and, hence, the original state is never accomplished again. Therefore the premise of this theory, namely the reversibility of the process is not implemented at all. Another problem is that fractures mostly occur in regions near the interface of the coating which cannot be explicitly identified as cohesive fractures.

Furthermore, the wetting theory can only cover and determine the magnitude of adhesion that results from electrical interactions (secondary valency and electrical double layers). The influence and the impact of diffusion processes, the formation of primary bonds, as well as the effect of micromechanical interlocking can neither be characterised while verifying the wettability, nor explained by such a reversible wetting process.

As adhesion leads to bonding of two materials to each another, operating inside the molecular range, it cannot be directly measured. So adhesion has to be measured indirectly via the adhesive strength between two types of matter, leading to a laminar consideration of that problem. Though such an area can be very small, many single adhesive bonds are stressed at the same time but not all of them are acting in a similar way and the forces applied on the tested surface are not equally distributed. Another important aspect that has to be taken into consideration is the ductility of the coating material, as the distribution of the applied forces strongly influences the sample, as well as the direction of these forces, either if they are applied parallel or perpendicular to the surface. For this reasons one attempts to gain a comparative value for the adhesive strength by dividing the tensile strength by the examined surface area, resulting in the adhesive strength:

$$\text{adhesive strength} = \frac{\text{tensile strength}}{\text{geometrical bonding area}} \tag{14}$$

The magnitude for the adhesive strength of the examined compound is neither an all-over proven nor constant value, more an average value whose magnitude lies below the maximum load to be applied to the compound. An additional big issue during the determination of the adhesive strength of a compound is the used area where adhesion occurs. Not the real surface area is taken into account but the geometrically ideal area, being much smaller than the real one, because the adhesive area is spatial, rather than planar. Hence, the adhesive strength is not a grade for the actual adhesion, but more for the compound strength, for which reason one might gain different results from different testing methods.

Therefore it is not astonishing at all, that different testing methods being used for the same substrate and coating material lead to different values for the adhesive strength.

Because of all this it was and still is difficult to compare gained results from different testing methods as well as identifying one single testing method to be applied to determine the adhesion for all fields of application and research. So one cannot really tell precisely how well any type of coating adheres to a certain surface area.

2.3 Testing Methods

The compound strength that is determined experimentally and which can be explained by one or more of the adhesion theories depends on various adhesion mechanisms. Additionally, it can strongly be influenced by the testing procedure, size and geometry of the sample as well as on the surrounding conditions at which the test is performed. The adhesion calculated theoretically must, however, not be compared to the one determined experimentally. For exactly this reason adhesion is likely to be classified as “practical adhesion” and “fundamental adhesion” (compare section “adhesion theories”) and, moreover, Mittal tends to talk about practical or even experimental adhesion. [3] To characterise the adhesive strength of thin films many different methods are known, though there is not a single procedure to be applied for explicitly determining the adhesive strength and without any limitation. The established methods for measuring adhesion can be separated in many different ways, qualitative and quantitative, mechanical and non-contact methods, or destructive and non-destructive methods.

Testing adhesion is either used to monitor the reproducibility of a process and a product or for the acceptance of the product as well. Such testing can be performed at several processing stages to find a process or process step that is degrading the adhesive properties and the adhesive strength. Normally, adhesion is tested by so called lot sampling on either product samples or witness samples, being representative for a certain product or process group. One should consider the properties of the used substrate material and the procedure of surface preparation to have a great effect on the measured adhesive strength or compound strength. Therefore the material of the witness sample, if utilized, and its preparation must resemble to the product processing.

As one will only gain comparative rather than absolute results one will obtain different results when executing different tests even showing different failure modes. The best test, among the hundreds, if not even thousands of various adhesion tests, should be executed under the same conditions appearing during processing, storage and service of the examined sample.

The simplest way to divide the adhesion tests are the different methods by which force or stress is applied to the film. Such adhesion tests include mechanical methods like tensile tests, peel tests, shear tests, deformation tests, energy deposition tests, fatigue (mechanical or thermal) tests, and many miscellaneous others. (compare [3], [4])

Some of the most common and simplest mechanical adhesion tests are depicted in figure 2. [4]

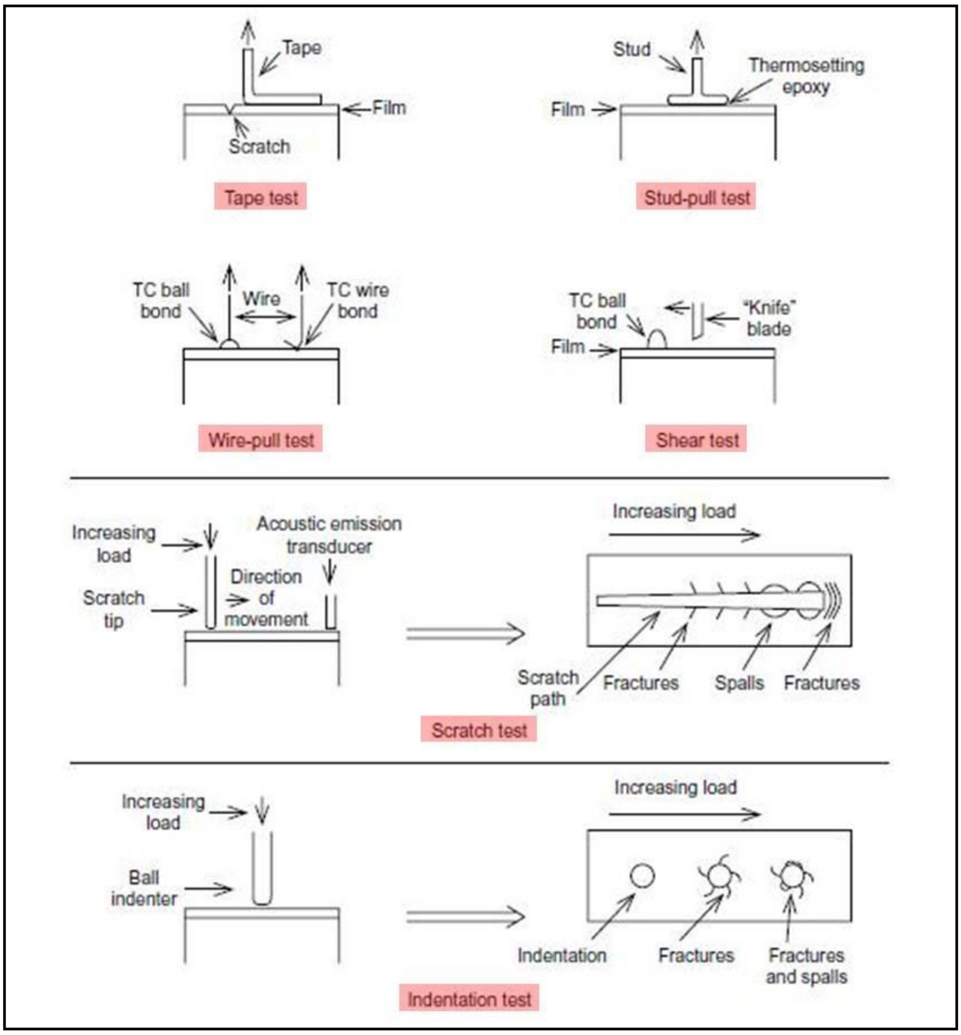
Tape
Film
Scratch
Tape test
Stud
Thermosetting epoxy
Film
Stud-pull test
TC ball bond
Wire
TC wire bond
Wire-pull test
TC ball bond
"Knife" blade
Film
Shear test
Increasing load
Acoustic emission transducer
Scratch tip
Direction of movement
Increasing load
Scratch path
Fractures
Spalls
Fractures
Scratch test
Increasing load
Ball indenter
Increasing load
Indentation
Fractures
Fractures and spalls
Indentation test

Figure 2: Schematic depiction of some of the most common and simplest mechanical adhesion tests. After *Mattox* [4].

According to figure 2 and in their simplest manner these mentioned tests are performed as follows: for the tape test, which is a variation of the peel test, an adhesive tape is stuck onto the surface of the examined film and pulled off for performing the test; a pull-off test (stud-pull test) is performed by bonding a die or stud to the thin films surface by using some kind of adhesive and pulling off the stud until the adhesion fails in any kind; when using a wire-pull test wires are joined to the film surface by so called thermo-compression (TC) ball or wire bonds and then pulled off to evaluate adhesion; a die shear test or push-off shear test is generally done by pushing off a bump which has been bonded to the film while the applied shear fore is measured with a load cell; for the scratch test a needle or stylus is skimmed over the surface of the film with increasing load until the coating peels of the substrate; similar to that indentation tests are used by varying the applied load and the tip geometries while observing the area around the indentation for fracture.

For purposes of this master thesis it is not sufficient just to talk about common and simple methods to test adhesion, as applicable methods for determining the adhesion of various thin dielectric chemical vapour deposited (D-CVD) films shall be identified upon the existing methods. And consequently also one or even some of the discussed methods might be applied for performing adhesion tests in mass production. Therefore many different methods – some being more others being less known and reproducible – must be studied more detailed, pointing out their properties, fields of application, advantages and disadvantages, especially in regard to their force of expression.

For being able to find an applicable method to examine the adhesive strength of a compound one has to consider all the parameters being present during the (atomistic) deposition process at which the films are processed. Not only the process parameters have to be observed but also the adhesion of such deposited thin films has to be studied for some aspects. (Compare [6], [3])

As the methods for testing adhesion are as versatile as the different definitions of adhesion and its provoking theories, *Jacobsson* was quite right when he stated the following: *“As no method has been found, so far, which can be applied universally, it is important to select the correct method for each particular case under investigation.”* [11]

Therefore, if someone wants to investigate the adhesion of a coating or film to the substrate underneath it is of great importance to define the intention of the upcoming measurement, because this will determine whether a method is suitable or not. An allocation of these methods is displayed in table 1. After Jacobsson [11].

Table 1: Classification along the purposes of investigation and the measured parameters or properties.

purpose of Investigation	*parameter or property measured*
physics and chemistry of thin film adhesion	binding energy
thin film deposition process development	binding energy or force of adhesion
product quality testing	durability, environmental stability, etc.

Regardless for what purpose a thin film might be used, its functional characteristics, its performance and properties in action as well as its structure strongly depend on the adhesion between the thin film and the substrate or the subjacent film stack.

Before covering the many different methods of adhesion testing it should be pointed out that the units in which the values for the determined adhesion, adhesion strength or compound strength are expressed, are not very consistent, as many different units have been and still are used. This hinders a comparison of the qualitative and especially quantitative results gained by different methods and obtained by different operators.

For his purpose of enumerating and explaining the different methods being applied to determine a proper value for adhesion *Mittal* treats adhesion in three different forms: basic adhesion, thermodynamic or reversible adhesion, and experimental or practical adhesion [3] (in more common terms of “bond strength” or “adhesion strength”).

According to this experimental point of view one can determine adhesion – according to *Mittal* – in two ways: (1) *in terms of the forces, defining the work of adhesion as the maximum force per unit area exerted when two materials are separated,* and (2) *alternatively, in terms of work or energy, defining the work of adhesion as the work done in separating or detaching two materials from one another*. [3]

For this reason locating the position at which the two materials are separated is very important. Some other things are important to point out beforehand: practical adhesion is not just determined by directly measuring the basic adhesion as it is defined by Mittal; one must not compare the values for experimental adhesion determined by different methods in a direct way though they might be quantitative and similar in their order of magnitude; and there are many different ways to be used to categorize the various methods to measure adhesion such as quantitative/qualitative methods, destructive/non-destructive methods, mechanical/non-mechanical methods which are the most pleasant ways of separation. Other categories include the state of development of a certain method, its interest for practical application or academic researches and how much is known or published about that method.

2.3.1 Mechanical Methods [3]

All the mechanical methods are based on the principle of removing the film from the substrate by an external force applied either normal or lateral to the interface. For methods involving a detachment of the film normal to the interface a maximum force is applied and measured or adhesion is somehow characterised by criteria concerning the magnitude of the area where the film has been detached. In case this whole area is not torn off simultaneously it might get complex to analyse all the acting forces which then have resulted in the obtained value for adhesion.

2.3.1.1 Direct Pull-Off Method

This method is based on the principle of attaching some sort of pulling device like a die, a brass pin, an aluminium dolly or a steel cylinder to the back of the film and another one to the substrate by using an adhesive, a cement or some kind of solder. Then these two pulling devices are pulled in perpendicular direction with a so-called tensile tester machine displaying either the tensile strength or the applied force, always considering the size of the pulling devices surface which is attached to the sample. Figure 3 shows two possible ways how the set-up of such a pull-off test might look like, (a) and (b), and schematic diagram of a cross sectional cut through the cylinder, the cement film, the film to be measured and the substrate (c). [3], [11]

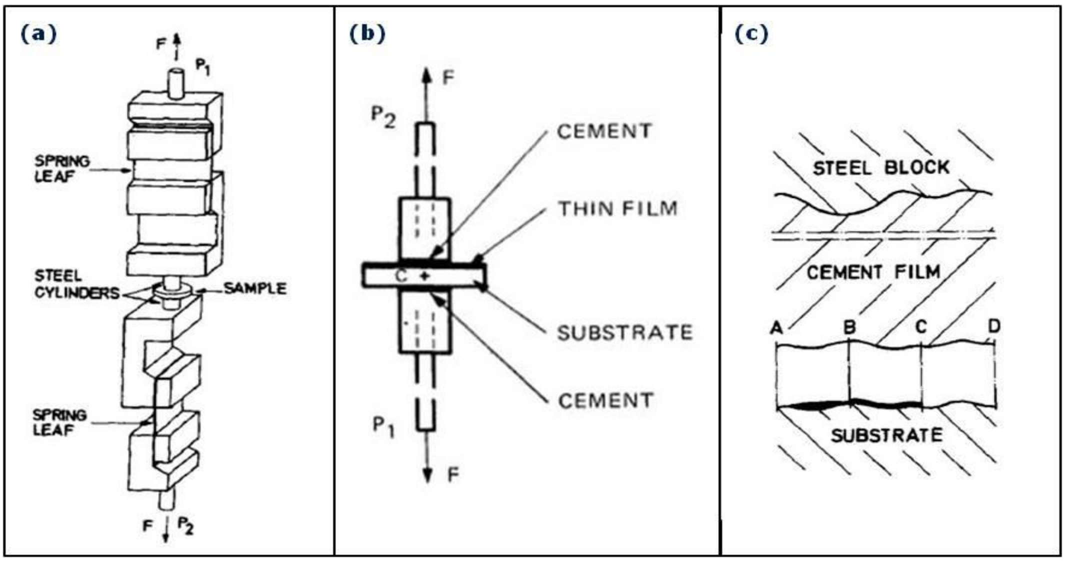

Figure 3: Possible set-up of a pull-off test.
(a) The arrangement for adhesion measurement by the direct pull method. [11] (b) Detail adhesion test by application of a normal pulling force. [3] (c) Schematic diagram of a section through a steel cylinder, the cement film, the film to be measured and the substrate. [11]

Within the pull-off test some difficulties might influence the adhesion strength which is finally measured. These influences are the mixture of tensile and shear forces within the setup, not always aligned perfectly; the magnitude of the adhesion force that one is interested in, is limited by the strength of the used adhesive, cement or solder. The solder can also penetrate into and therefore influence the interface between the film and the substrate, during preparation of the solder stresses could be induced before the testing load is applied and the external stresses are not applied in a uniform way.

2.3.1.2 Momentum or Topple Test

This test is a slight variation of the pull-off method as the force is applied horizontally instead of vertically to the interface via a rod glued to the film. The adhesion then is determined according to the momentum of force that has to be applied to detach the film from the substrate. Compared to the direct pull of test, the topple method offers some advantages: in this method the substrate is less deformed or stressed because there is no force applied perpendicular to the plane of the substrate and the alignment is not as critical in regard to the direction of the pulling forces. In this alignment, as depicted in figure 4, the end of the rod to be attached to the film is cut to form two “legs”. To calculate the results of this test one assumes tensile stresses under one and compressive stress under the other leg, handling them as being equal in magnitude.

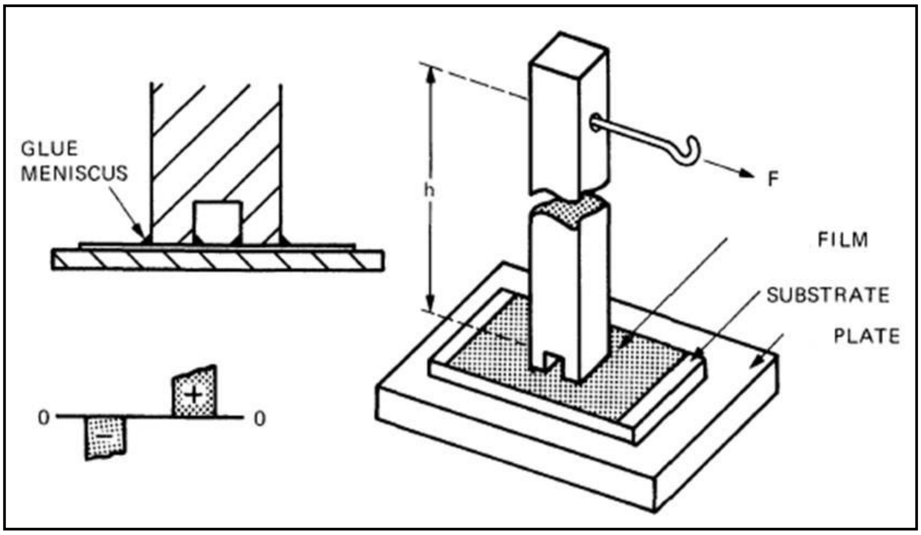

Figure 4: Diagram showing the arrangement for the moment or topple method. [3]

The exceptions or issues in executing this method are the used adhesives or solders influencing the results gained for the adhesion in the same way as for the pull-off method.

2.3.1.3 Ultra Centrifugal Method

The direct pull-off method and in some cases also the topple method suffer from the fact, that some kind of adhesive has to be applied to attach any kind of pulling device to the sample. The use of an adhesive is not always allowed. In such a case the UCM can be applied. For this method the specimen, acting as the rotor, is spun at a very high speed to produce the high centrifugal forces needed, like it is illustrated in figure 5. The coating to be investigated in terms of its adhesion to the substrate can no longer resist that high stresses and is finally detached at a critical rotation speed (angular speeds can reach 80.000 rps).

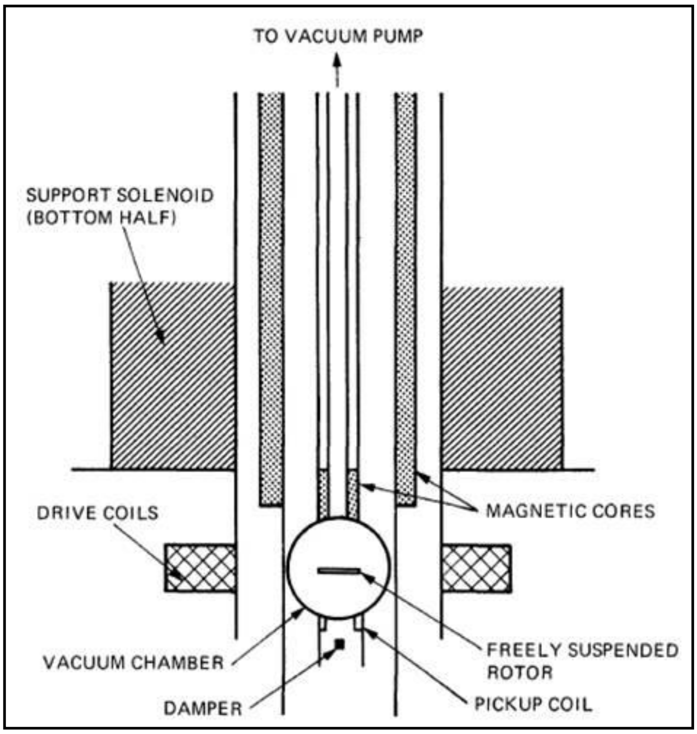
TO VACUUM PUMP
SUPPORT SOLENOID (BOTTOM HALF)
DRIVE COILS
MAGNETIC CORES
VACUUM CHAMBER
DAMPER
FREELY SUSPENDED ROTOR
PICKUP COIL

Figure 5: Diagram of ultra-centrifugal arrangement for measuring adhesion. [3]

In this ultra-centrifugal system the forces acting on the coating are given by the following equation: [12]

$$4\pi^2 N^2 R^2 d = T + \frac{AR}{h} \tag{15.1}$$

where *N* is the critical rotor speed in s^{-1}, *R* is the rotor radius in cm, *d* is the density of the coating in $g*cm^{-3}$, *h* the thin-film thickness in cm, *T* the tensile strength of the film in $g*cm^{-1}*s^{-2}$, and *A* the adhesion in $g*cm^{-1}*s^{-2}$. (Compare [3], [12]) It can be observed that the second term on the right side of equation (15) contains R/h, while the first term does not, so by experimenting with rotors having different radii, the magnitude of the tensile strength as well as of the adhesion can be gained. In case the adhesion of the examined film is vanishingly small, the expression from equation (15.1) turns to

$$4\pi^2N^2R^2d = T \tag{15.2}$$

showing that the measured tensile strength is no longer depending on the film thickness.

Otherwise, in case the hoop stress T vanishes, for the case the material is directly deposited on the rotors surface in circumferentially disconnected patches, the value for the adhesion of the thin film to the substrate can be determined by the following equation: [12]

$$A = 4\pi^2N^2Rhd \tag{15.3}$$

Some of the concerns about this method have been the ferromagnetic rotor limiting the investigation of coatings deposited only on some substrates. If the materials for the specimen resembling the rotor are selected properly, the ultracentrifugal methods seems to be quite versatile as many different coatings can be studied then, but paying attention the higher centrifugal forces required to investigate thinner films.

2.3.1.4 Ultrasonic Method

Before explaining the functional principle of this method, it should be pointed out that the ultrasonic method has often been applied to study the adhesive properties of relatively thick films of paint.

In this method the force acting normal to the interface is provided by the inertia of the coating material itself because of fast rebounds of motion induced by ultrasonic frequencies. A film which is attached to the loose end of the vibrating cylinder will separate from the substrate as soon as the force caused by the acceleration gets higher than the adhesive force at the interface. This accelerating force can be calculated from the amplitude and the ultrasonic frequency of the vibrations and of course by area, mass and thickness of the film under investigation. The amplitude of the vibrations is determined from the applied input voltage. The effective force acting can be increased by altering the mass, and essentially the thickness of the film, but film stresses in thick vacuum deposited films affect the adhesion and sometimes lead to the films peel off the substrate. Hence, a lot of further research will be necessary before this method can be applied for thinner films.

Besides methods where the coating is detached by a normally applied stress, there exist also methods where the application of lateral stresses causes the detachment of the film from the substrate. Plenty of these methods might lead to a cohesive cracking of the film. However, a carful inspection sometimes leads to the conclusion that the roughness of the developed crack pattern can directly be related to the inadequacy of adhesion. Within these techniques only those methods showing good results for testing the adhesion of thin films are mentioned and explained in the following.

2.3.1.5 Scotch Tape Test

For executing this test a pressure sensitive tape is cemented onto the film at any place of interest and then quickly pulled off, whereas the film can either be removed from the substrate completely, or only parts of the film are removed, or the film is not removed from the substrate at all. These three possibilities show that this is a highly qualitative test and, therefore, can be applied to monitor cases of very poor adhesion up to appreciable good adhesion. Despite the fact that this test is qualitative in such a way, it offers quite some mentionable advantages: it is cheap and can be executed very quickly; it can be used for studying the influence of temperature, humidity and other environmental factors on the adhesive strength of the film on the substrate. As a disadvantage one has to note that because of its highly qualitative nature no numerical values can be obtained. Further issues are the influence of type of tape, applied pressure to attach the tape on the film, the speed and way of stripping off the tape, as well as the limitation in cases the adhesion of the film to the substrate being greater than the adhesion of the tape to the film.

2.3.1.6 Peel Test

For this kind of adhesion test one can use various types of set ups – two of them depicted in figure 6 – and it can be executed in two different ways: (1) either by peeling off the film from the substrate by holding onto the coating or film directly, or (2) by using some kind of backing material attached to the film and holding onto the backing material for pulling off the film. For the test shown in figure 6 (a), peeling of a specified width of the film is necessary for a proper execution, but it is almost impossible to define the area really being involved during testing. The result of the applied force is measured and expressed as energy or work per unit area.

However, the monitored results have too little significance to be directly compared with results gained from other techniques. The applicability of this method is, furthermore, limited by the fact that the film hast to be removed from the substrate completely in order to be able to gain any useful result in terms of force per unit area. So only interfaces, which are expected to have an innately bad adhesion can be investigated.

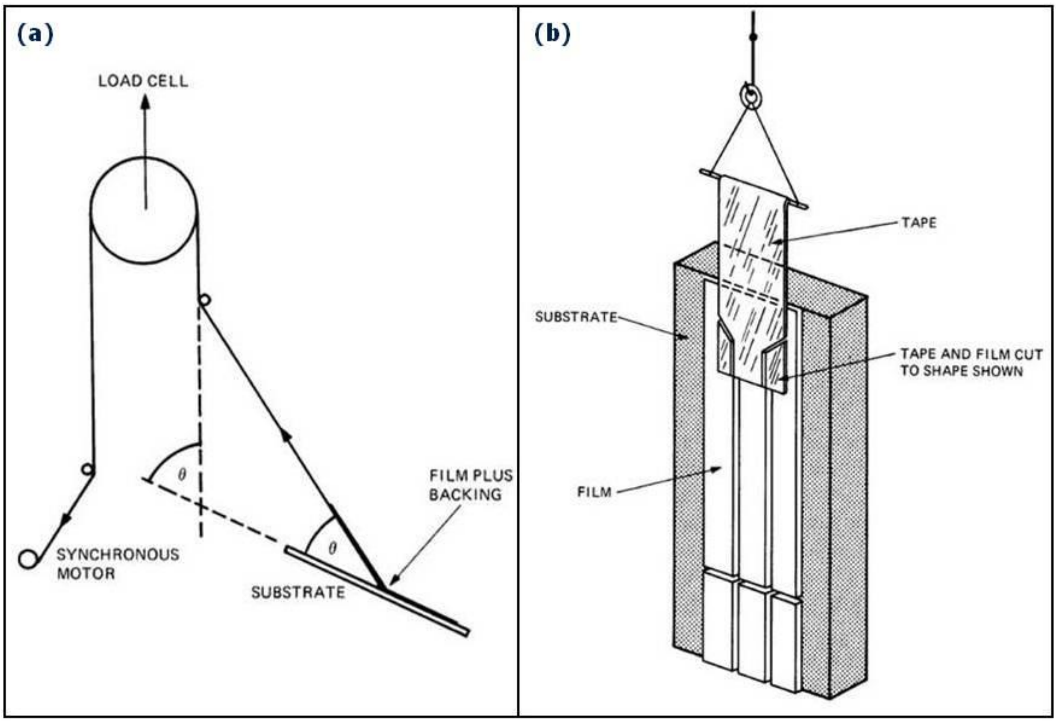

Figure 6: (a) Diagram of the apparatus for stripping or peeling experiments using a kind of backing material, and (b) diagram for peeling experiments on unsupported films. After Mittal [3].

A more quantitative version of executing the Scotch tape test is the mechanical stripping method offering two different ways to be performed, either using supported or unsupported films. Consequently, two different experimental arrangements can be applied: (1) in this first case the tape is firmly attached to the back of the film and then this tape is again attached to a winding string – similar to what is shown in figure 6 (a). While executing the test, both, the film and the tape are removed from the substrate; (2) for the second case the tape is attached to the first front part of the film and film and tape are then traced with a razor blade in the depicted shape scalpel as shown in figure 6 (b). The stripping process then takes place starting at a region where tape and film are stripped off together to the unsupported film only, so the actual measurement is executed only on the unsupported part of the film. The measured peeling or stripping energies gained through the mentioned arrangements of this method partially consist of an amount of true adhesion energy, due to intermolecular interactions, and partially of a certain amount of energy spent in inelastic deformations of the film itself.

2.3.1.7 Tangential or Lap Shear Test

This method for testing adhesion has not been that popular as the direct pull-off method, but for some cases the lap shear test leads to more meaningful results, as it better replicates the application conditions of the investigated film, which are actually prevailing. The experimental setup of such a test, where the measured shear stress is the tangential force per unit area needed to break the bond between substrate and film, is schematically shown in figure 7. A piece of a glass microscope slide is glued to the surface of the film which was deposited on a certain substrate, and then the film and the substrate are fixed in the proper position so no inelastic deformations can occur. For testing the adhesion a shear force is applied parallel to the film by pulling weights ensuring a normal load with a stiff steel wire. The values for the applied shear stress can be determined by dividing the required force to detach the film and the substrate by the contact area achieved by a fast-set adhesive.

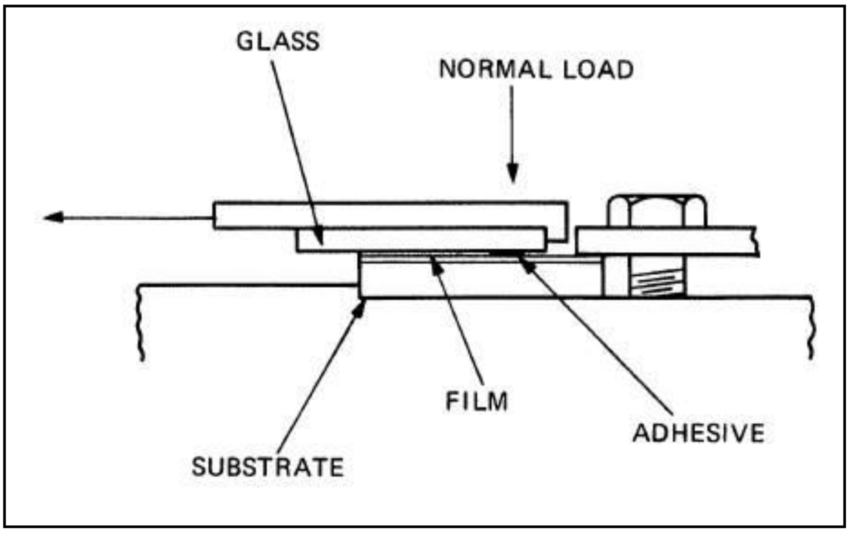

Figure 7: Arrangement of the lap shear test for measuring adhesion, where the arrow shows the direction of the applied shear force. [3]

As for the pull-off method an adhesive is used to glue the glass plate to the surface of the deposited film, so this technique suffers from the same weakness pointed out also for the pull-off method. To achieve usable results the adhesion at the interface film-substrate must not be greater than the adhesive strength of the used glue. Despite this problems the shear test avoids severe substrate deformations, the applied stress is less concentrated as the applied forces are distributed over a larger surface area and it can be approximated by the “pure” shear force. With regard to the opportunity of comparing quantitative values measured with different methods, one has to notice that the values for the shear stress are about 100 times smaller than the stresses which are measured for forces applied perpendicular to the interface. All this can be explained by the fact that forces acting parallel to a surface can remove a film more easily than forces applied perpendicular to the same surface (theoretically a 1:4 ratio between shear and tensile stresses is predicted). This method was not frequently used to study the adhesion of thin films, due to the lack of difficulties and fundamental objections, it nevertheless can be applied for scientific purposes.

2.3.1.8 Scratch and Indentation Test

For the scratch test, also named stylus test or scribe test, which has evolved from the scrape test, a loaded point or tip (rounded chrome steel, tungsten carbide or diamond tip, similar to those tips used for hardness measurements) is drawn over the surface of the film while the load, which is vertically applied, is steadily increased until the film is completely removed. The result is a clear channel or even a crack, depending on the coating, and the magnitude of the critical load which has caused the detachment is considered as a measure for the adhesion of the investigated film-substrate interface. The failure modes of the thin film can be observed by using a Scanning Electron Microscope (SEM) that is capable to do in situ scratch tests, offering the advanced opportunity of observing the failure and the material transfer without any environmental effects. A schematic layout of this test is depicted in figure 8 (a) [3] and the functional principle in figure 8 (b) [4].

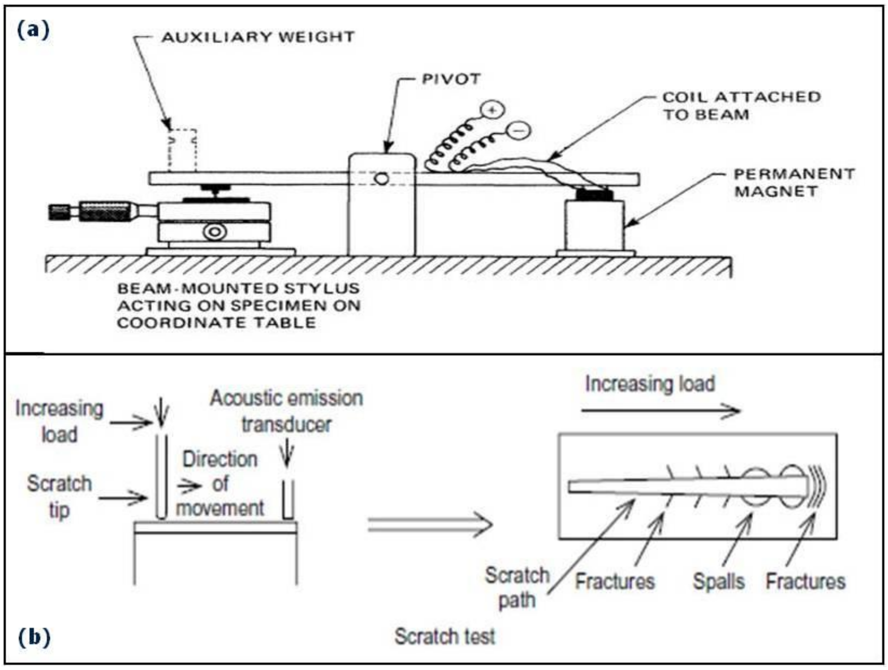
(a)
AUXILIARY WEIGHT
PIVOT
COIL ATTACHED TO BEAM
PERMANENT MAGNET
BEAM-MOUNTED STYLUS ACTING ON SPECIMEN ON COORDINATE TABLE
Increasing load
Acoustic emission transducer
Direction of movement
Scratch tip
Increasing load
Scratch path
Fractures
Spalls
Fractures
(b)
Scratch test

Figure 8: (a) Schematic layout of the scratch or stylus test, [3], and (b) the functional principle of such a scratch test. [4]

While the tip is drawn over the film surface always plastic deformation of the substrate material occurs producing a shearing force at the interface film-substrate around the region of indentation defined by the tip, its size and the load. This leads to a simple relationship opening up the opportunity to calculate the adhesion as shearing force *F*: [3]

$$\mathrm{F} = \frac{\mathrm{AP}}{\sqrt{\mathrm{r}^2 - \mathrm{a}^2}} \tag{16.1}$$

$$\mathrm{A} = \sqrt{\frac{\mathrm{W}}{\pi \mathrm{P}}} \tag{16.2}$$

W is the critical load, *r* is the tip radius, *F* is the shearing force per unit area due to surface deformations, *a* is the radius of the contact circle of the tip and *P* is the substrates indentation hardness.

Similar to the scratch test, the indentation test also uses a loaded tip to test the adhesion of a film. During adhesion testing the indentations are made by altering the load. Then one observes the area around the indentation for de-adhesion, flaking, fracture or peeling off of the film from the substrate. Common hardness testers operating the same way, via indentation, are often used instruments for performing this test whose functional principle is shown in figure 9 below. [4]

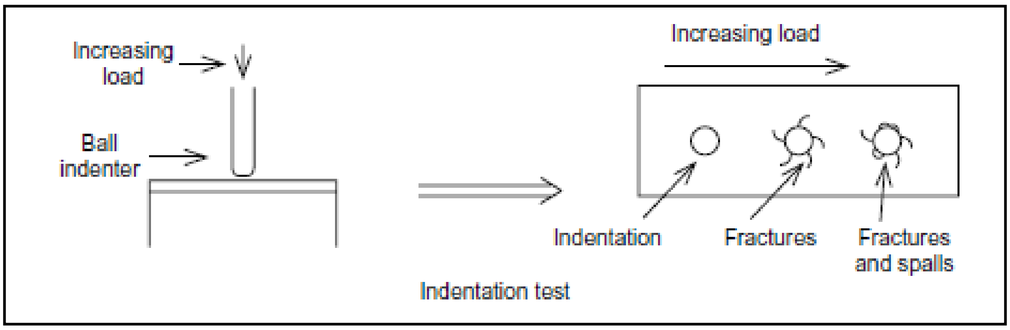

Figure 9: The functional principle of a (nano-) indentation test. [4]

Studies of the scratch as well as of the indentation test lead to discussions about the critical load and its correlation to the adhesion of the film to the substrate. It might happen that for applied stylus loadings above or even below the "critical load" only parts of the film are removed from the substrate. This leads to the development of the "Threshold Adhesion Failure" and it was assumed to be an operational criterion for measuring adhesion.

This "Threshold Adhesion Failure" is defined as: *"Threshold Adhesion Failure occurs if, within the boundaries of a scratch and over its 1 cm path, removal of the film from its* *substrate can be detected by transmitted light with a microscope (40 times magnification) at even one spot no matter how small."* [3]

Some issues that came up are that this threshold failure loads can only be measured relatively, if two styli of any material are used, they do not yield the same values for the threshold load, each stylus and each material has its own testing and scratching characteristics and thereby shows different test behaviours. Despite these criticisms this method can be used to survey and follow effects of deposition parameters and other variables. Such an indentation test is applied to examine aging effects, effects of surrounding conditions (weathering) or point-to-point variations like the uniformity of the film thickness. With this method one can even test areas which are far too small to be tested using other methods.

2.3.1.9 Blister Method

To execute this kind of adhesion test a gas or fluid is injected at the interface substrate-coating beneath the film until the coating starts to detach or peel off from the investigated substrate. In most of the cases this method has been used on relatively thick paint films (~25 µm), so little or even no reference is found in literature where the method of blistering is used for studying adhesive properties of thin films. Independent of which film – either thick or thin – is investigated, the determined values for the adhesion strength will strongly be influenced by brittleness, ductility and of course thickness of the film, as well as on the properties (e.g. viscosity) of the applied fluid.

2.3.2 Nucleation Methods [3]

For these methods the kinetics of thin film formation is observed and therefore are called and grouped as non-destructive methods. Though adhesion is defined as a mechanical property of the film or the film-substrate interface, on the atomistic scale removing the film resembles breaking the bonds between the single atoms of the film and the substrate. For this reason the macroscopic adhesion can be considered as the summation of all the acting atomic forces, so it should somehow be possible to relate the adsorption energy of an atom on the substrate surface to the totally acting adhesive force. The value for adhesion determined in such a way refers to the definition of the "basic adhesion", whereas only the adsorption forces should be considered.

For gaining results by using these methods one has to determine the nucleation rate, the island density, the critical island size and the residence time of the depositing atoms building up the film. For the quantitative determination of adhesion of thin films this method appears to be very useful and simple but on the other hand nucleation methods are quite complicated and the range of application is limited. A scanning electron microscope (SEM), a scanning tunnelling microscope (STM) or an atomic force microscope (AFM) will be necessary to count the island density.

It is also difficult and therefore not often found in literature, to compare values for adhesion measured with nucleation methods or with mechanical techniques, because mechanical methods not always give reliable quantitative results and the nucleation methods suffers from their limited applicability.

So, nucleation methods are testing methods that lead to the better understanding of the thin film formation process, rather than being suitable tests to measure the magnitude of adhesion as these techniques cannot be applied to completed films. In opposition to mechanical tests nucleation methods just provide the adsorption energies for single adatoms making up the whole film. One would have to use these adsorption energies for determining the adhesion per unit area.

2.3.3 Miscellaneous Techniques [3]

The several techniques discussed in this section cannot be named practical for testing films concerning their adhesive properties because some of the tests need to be further developed while offering great practicable potential. Others are of academic and scientific interest, but none of them were really used because no quantitative values for adhesion could be determined.

2.3.3.1 Thermal Method

This method obeys the following principle: whenever a film acting as a coating is chemically dissolved and removed from his substrate, the energy which is set free equals the heat of the solution of the film itself minus the adhesion energy between the film and the substrate. But this liberated amount of heat is such small a micro-calorimeter of today’s level of technology could not measure it.

2.3.3.2 X-Ray Method

This is a so called non-destructive method being an opportunity for determining the adhesion at the interface of a substrate and the film deposited on it. With this technique using X-ray topography one can obtain qualitative results for the adhesion of mono- or polycrystalline films, thus, only to be applied for epitaxial grown films on single crystalline substrates. The functional principle of this technique is based on the observation of contrasts in the x-ray diffraction caused by strains at the film-substrate interface and by “poor” adhesion, and therefore this method offers qualitative results about adhesion and strain at the interface. This method can only be applied in certain situations, must never be generalized and does not offer any numerical values for adhesion, not even for epitaxial films, but it can be used as a comparative way to characterize epitaxial films. Almost the same functional principle is used for the Electron Spin resonance method, but it is even less developed as the x-ray method.

2.3.3.3 Capacitance Method

To execute this method an elastic electrode is placed on a coated metal panel forming a new “bigger” electrode whose absolute capacitance is measured at very high and also at very low frequencies. The obtained difference of the capacitance for high and low frequencies, leads to a coefficient characteristic of the adhesion, being only an indirect measurement for the adhesion of the investigated film.

2.3.3.4 Cathodic Treatment Method

This method follows almost the same principle as the blister method, with the main difference, that hydrogen is used instead of the fluid to detach the film from the substrate at the interface. The coated part is handled as the cathode inside an electrochemical cell and the evolved and expanded hydrogen then starts to diffuse through the coating and accumulates at the interface until it causes blistering and peeling-off. Because of the functional principle of this method it gets obvious that this method is limited to metal substrates, only gives qualitative results and that the obtained results are influenced by interactions of the evolved hydrogen and the film material.

2.3.3.5 Pulsed Laser or Electron-Beam Method

For this quite interesting method used to measure the adhesion of especially thin films a stress wave – in terms of a compressive pressure wave – is generated in the solid specimen one is interested in. After being generated the wave transferred into a tensile wave by reflection and then stresses the interface which should be investigated. In such form these tests have been used to execute dynamic tensile tests.

Nowadays a pulsed laser or an electron beam, pulsed as well, is used to apply the energy necessary for generating the compressive stress wave. Before the actual testing procedure one has to prepare a substrate of convenient size and coat a desired area. The remaining uncoated area is then bombarded by using the electron or laser beam machine, generating a pressure wave that starts propagating through the sample and being reflected from the coated region of the surface. As soon as the compressive wave hits the free surface (free by the means of not being bombarded by the incident electron or laser beam) it gets reflected and inverted into a tensile wave of almost the same amplitude. The amplitude of the wave can be controlled by the energy of the initial electron or laser beam.

When using this method it won’t be easy to obtain some numerical values for adhesion of the investigated thin film, even because it is quite challenging and might be expensive under certain circumstances.

2.3.3.6 Scanning Thermal Microscopy (SThM) [4]

With this method it is possible to record the thermal pattern over a chosen surface of a film with a thermocouple junction positioned on the probe tip of the atomic force microscope (AFM). By sending thermal pulses through the substrate one can detect differences in the surface temperature what may indicate a poor adhesion at the interface because of the detected poor thermal contact.

2.3.4 Abrasion Method [4]

This method did not gain much popularity with respect to measure the adhesion, rather than the abrasion resistance and furthermore the durability of the film. The resistance against abrasion has been determined by rubbing the surface or the film with a rubber loaded with emery. As this method also involves buffing, polishing and stripping actions the obtained values for the adhesion of the film are strongly influenced by these additional side-processes. Though this method might offer some advantages for determining the abrasion resistance, it will not be used when one is interested in quantitative values for the adhesion of a certain film.

3. Thin Films

When talking about thin films one thinks about layers build up of a solid type of matter in the range of micrometers or even nanometers. Such thin films often offer certain physical properties a massive body built up of exactly the same material will never provide. That way properties can be achieved which will not be present otherwise, for which reason thin films are applied in fields of surface coating and finishing as well as in fields of microelectronics in the semiconductor industry. In many cases thin films can only be manufactured up to a certain thickness as they show high internal stresses that might result in bad adhesion to their substrate or subjacent layer, or they completely peel-off when a certain thickness is exceeded.

When the plural “thin films” is used in context of the fields of applications mentioned above one wants to especially point out the properties of peculiar thin films for various applications (optical filters, diffusion barriers, thin film devices and solar cells, passivation layers, etc.).

The importance of such thin films and also of thin film technology from the economic and industrial point of view results from the special properties accompanying with the low magnitude of film thickness, from the economics of the many different materials and from the steadily improving principles and operations applied in mass production. With the aid of thin film technologies microelectronic devices can be processed, applying a wide range of different procedures.

The greatest economical impact of thin film technology is in the fields of microelectronics and microelectronic devices like microprocessors, memory devices, hard discs, screen and so on.

Other important applications are electronic displays, like liquid crystal displays, organic light emitting diodes or photovoltaic devices (e.g. thin film solar cell). For this purposes almost every material is applied, ranging from metals used for conducting paths and electric contacts like copper, silver, aluminum or gold, typical semiconductor materials such as silicon, germanium, gallium arsenide, up to dielectric materials used as passivation layers like silicon oxide, silicon nitride, oxi-nitrides or amorphous carbon films.

Examples for a more conventional application of thin films in fields of electronics are spayed coatings deposited to act as insulating layer.

3.1 Dielectric Films

Dielectric thin films allow definitely more and further specialized applications compared to thin metal films, as one can control their level of optical reflection inside a wide range from 0% up to 100%. This can be done at least in narrow spectral region and there is the opportunity to affect the polarization of the reflected or transmitted light. Such properties of thin dielectric films and their adjustment for optical applications are mainly based on the interference of light within these layers. Therefore it strongly depends on the path covered by the light wave within the layer, the refractive index of the thin film and the wavelength of light whether an incident light beam is amplified (in case of constructive interference) or diminished (for destructive interference). The manufacturing process of such films has to be executed very carefully, taking into account that factors like reflectance or transmittance depend on the wavelength and the incident angle. Furthermore, the chosen material depends on the requested properties for each particular application. Even the level of surface contaminations can affect the expected properties.

Such dielectric films are also utilized as insulating layers, whereas the deposited films completely resist to the flow of electric charges and do net respond to prevailing electric fields. Though, according to practical applications the perfect insulating film does not exist, film materials with a very high dielectric constant are considered to be insulators. When assimilated in electric equipment and especially in fields of semiconductor devices, they manly act as separation to electrically conducting films without allowing any current passing through themselves. In many different microelectronic components such as integrated circuits and various designs of transistors silicon – originally being an insulator – acts as an electrical conductor because of the applied doping materials, but applying heat and using oxygen the silicon selectively can be turned into an insulator. Beside the thereby arising silicon oxide, also silicon nitride is a currently applied insulating film, though it has a higher dielectric constant as silicon oxide for which reason it is not applied between metallization layers.

Furthermore, dielectric films are also applied to act as passivation layers against environmental attacks, such as water or air, being the most severe ones. These factors might change the electrical and mechanical properties of the regarded material or even, in our context, entire film stacks and beyond that the functionality of the whole device could be affected. This passivizing effect, also to prevent abrasion, can be achieved by a thin film of various metal oxides, similar to a shell against corrosion or other environmental influences.

Some materials or substances that inhibit corrosion promote the formation of passivation layers on the particular surfaces to which they are applied, e.g. on metals. Other compound which can be dissolved in solutions form passivation films that are not reactive.

In microelectronics passivation requires certain special conditions as the applied oxides enhance and improve the performance of silicon. For photovoltaics passivizing the particular surface with silicon dioxide, silicon nitride, or titanium oxide is able to reduce the surface recombination being a loss mechanism that occurs in solar cells.

3.2 Physical Properties of Thin Films

Independent of the way the film has been deposited, it can be characterised by either its mechanical, electronic or its optical properties. Mechanical properties include the hardness of the film, the intrinsic stress and, whereupon most of the attention is paid to in this thesis, the adhesion of the film to its substrate, depending on the regarded process route or product type. As the electronic and optical properties of a film do not really affect the adhesive properties they will not be treated in this thesis. (compare [13])

3.2.1 Mechanical Properties of Thin Films

The mentioned mechanical properties of thin films – adhesion to the substrate, intrinsic stress and hardness – are strongly affected by the film structure, its chemical composition, the level of incorporated impurities, pre-treatments of the substrate the film is deposited on and different types of curing or finishing treatments.

3.2.1.1 Different Interfaces [14], [15]

The adhesion itself depends on the type of interface formed during the deposition or coating process. Therefore the nature of this interface determines the quality of adhesion of the deposited film. A distinction of the interface can be made in accordance to the differently formed microstructure between the substrate and the film. Generally one can distinguish between five different kinds of interfaces, shown in figure 10.

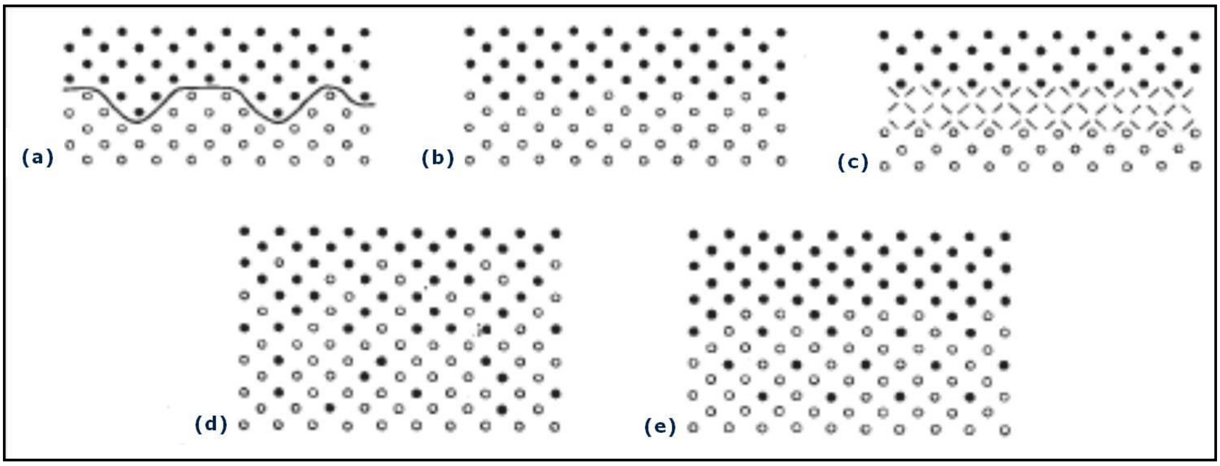

Figure 10: Schematic illustration of the interfacial region between substrate and coating.
a) mechanical interlocking, b) monolayer on monolayer, c) chemical bonding or compound interface, d) diffusion interface, e) pseudo-diffusion interface. After Heafer [14].

Mechanic Clamping Interface

This interface prevalently builds up on rough porous substrate surfaces, where the deposited film couples itself into the porosities and other suitable positions of the substrates surface as long as a sufficiently high wetting is pre-existing. This leads to a purely mechanic adhesion strength of the film on the substrate. The reached adhesive strength depends on the physical properties of the film as well as the substrate material. Mechanical clamping results in a relatively good adhesion.

Interface between two Single Monolayers

Typical for this kind of interface is the sudden changeover from the film towards the substrate whereas this changeover between the two materials occurs within some atomic layers (about 2-5 Å). Monolayer interfaces form if there is no diffusion and no or only few chemical bonds between the two types of matter. This occurs when there is no opposite solubility or when there are impurities on the substrate. Such an interface establishes on glazed plane surfaces which are chemically less active, most of the time leading to bad adhesive properties, except substrate and film consist of the same type of material and the surface is very clean and free of any contaminations.

Chemically Bonded or Compound Interface

Signalizing for this type of interface is a constant chemical composition stretching across many lattice planes of the materials. The construction of the interface is the result of chemical reactions between substrate and film material, whereas these reactions can be induced by different plasma gases during plasma treatment. In many of our applications an oxide (silicon oxide, undoped silicon glass, boron and/or phosphorous doped silicon glass) is formed. This sort of interface leads to the formation of a new compound between the substrate and the film material and therefore leads to very good adhesive properties.

Diffusion Interface

This interface is characterised by a floating crossover of the lattice structure and the composition of a mixed zone between film and substrate. Therefore partial solubility of the two composites with one another as well as an according heating of the substrate are required. Through diffusion a smooth crossover is formed between film and substrate material. Such diffusion films have special properties that enable using them as inter-layers between two different films to reduce thermal stresses resulting from thermal expansion or contraction of the film stack. The established diffusion layer is about 1 nm to 10 nm “thick” and often yields good adhesion between the substrate and the coating material.

Pseudo-Diffusion Interface

This type of interface originates from the implantation of particles of the film into the substrate material. These films have the same properties as diffusion films but they may also be produced from materials which do not build diffusion interfaces. Highly energetic ions or neutrons irrupt into the substrate according to the amount of their energy and remain there without diffusing through the substrate material. As this interface is created by sputtering or implantation, by processes applying high energies, so this interface adheres very well.

Real Interface

All the different types of interfaces just mentioned are idealized. Those interfaces occurring during practical exercise consist of a combination of the existing types of interfaces. The formation of such a real interface depends on many parameters such as the combining of surface and film material, the applied deposition process and the conditions during the actual deposition process. In case of vapour deposition processes, such as by implantation or sputtering, we talk about pseudo diffusion interfaces. With regard to their adhesive strength, these films are the best as they distribute their internal stresses throughout the whole volume of matter without reducing the stability and resistivity of the film.

3.2.1.2 Internal / Intrinsic Stress [16]

The term “mechanical stress”, represented by the symbol σ, arises from the strength theory and it is defined by force *F* per unit area *A*, acting in an imaginary cross sectional plane through a solid body, a liquid or even a gas.

$$\sigma = \frac{|F|}{A} \tag{17}$$

The mechanical stress has the same unit as the physical pressure, as this is also force per unit area.

When stresses are handled in the context of thin films and thin film technology they are induced by externally applied forces. Normally, if the applied load is removed, the stress is expected to disappear again, but not for thin films. They can even be stressed without any external forces being applied and thin films tend to feature residual stress.

It has been known since long time that stress in thin films manufactured by either chemical or physical vapour deposition do exist and, though it can be experimentally measured, it is still not certain where these stresses originate from.[16] Such residual stresses do not only appear in compound film-substrate systems but generally they can appear in almost every kind of homogeneous matter, being distinctive more strongly or weakly, always depending on the existing conditions. Residual stresses do not only arise in thin films, but also in casted components, welded or soldered parts or other machined or tempered materials, where they might be desired or not.

During the deposition process of thin films the appearing residual stresses, whose generation is schematically shown in figure 11, can either be compressive or tensile. [16]

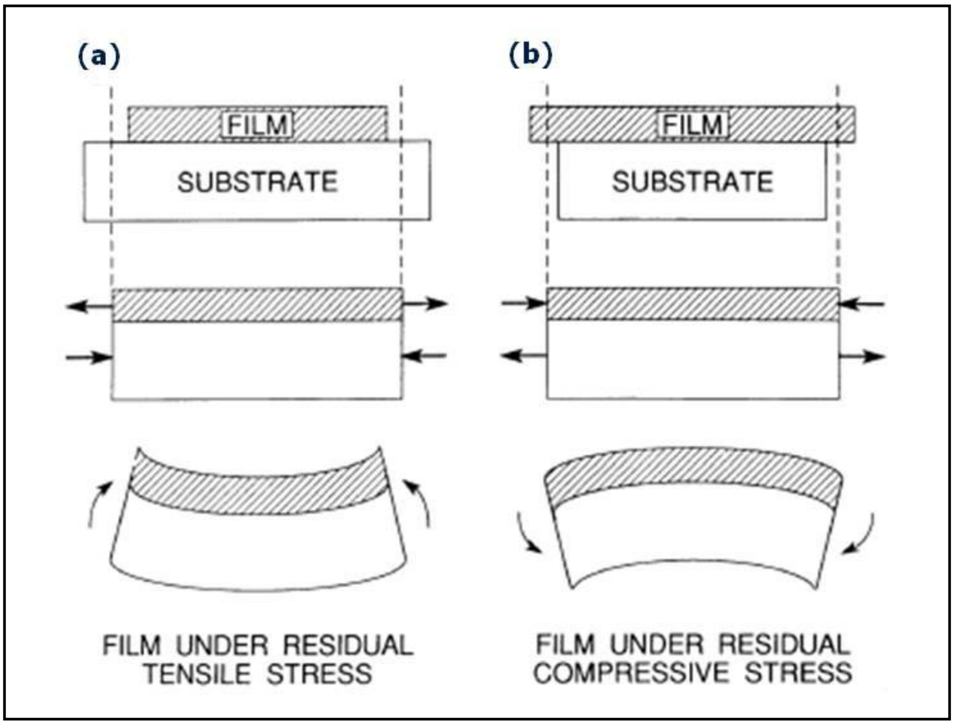
(a)
(b)
FILM
SUBSTRATE
FILM
SUBSTRATE
FILM UNDER RESIDUAL TENSILE STRESS
FILM UNDER RESIDUAL COMPRESSIVE STRESS

Figure 11: Sequence of events leading to (a) residual tensile stress in film; (b) residual compressive stress in film. After Ohring [16].

No matter which explicit distribution of the internal stresses predominate the film-substrate interface of interest, the stresses have to compensate each other. To ensure the mechanical equilibrium to be conserved, net force (*F*) and the acting bending momentum (*M*) has to vanish for every single cross section of the film-substrate interface.

$$F = \int \sigma \, dA = 0 \tag{18}$$

$$M = \int \sigma y \, dA = 0 \tag{19}$$

In both equations *A* is the cross sectional area and y in equation (19) is the arm length of the moment lever force. These two equations are used to derive the *Stoney formula* (compare [16] Ch. 12.3.3).

In figure 11 (a) the deposited film shrinks relatively to the substrate while cooling down after the deposition process, maybe because of surface tension forces. The compressive forces inside the substrate balance the tensile forces which develop in the film and as a result films with high tensile stresses will bend the substrate ending up in a bowl-like shape. In a similar way compressive stress is formed inside the thin film leading to an expansion of the film relative to the substrate as shown in figure 11 (b). The result is kind of a dome shape, caused by residual compressive stresses.

Is some cases the order of magnitude of tensile stresses is large enough to cause film fractures and, as the case may be, films with high compressive stresses start to wrinkle due to a local loss of adhesion. Both of these cases that should not, but might occur are illustrated in figure 12 below for a silver-lithium thin film.

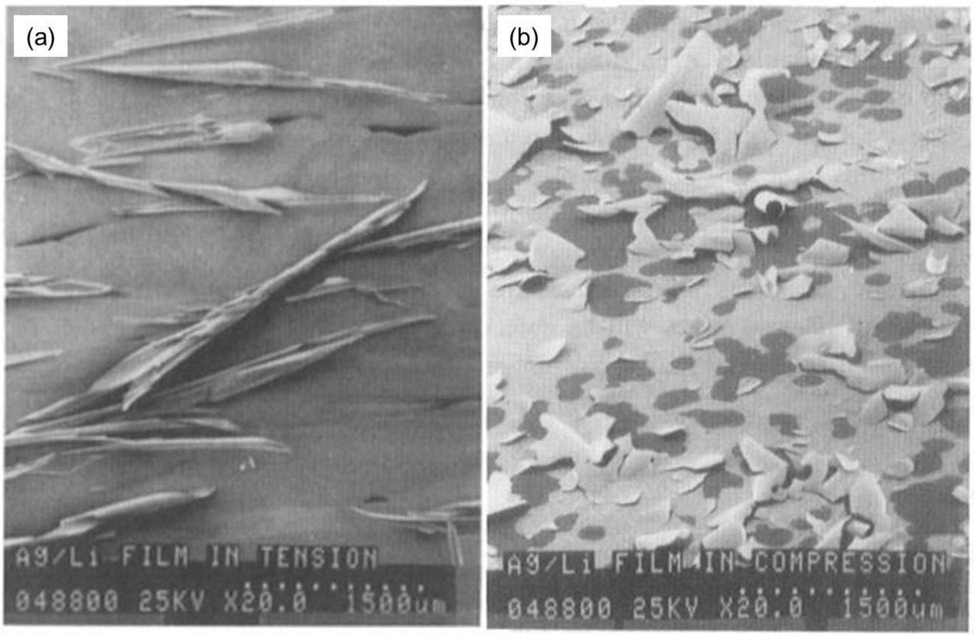

Figure 12: Stresses in silver-lithium thin films: (a) Tensile film failures during deposition; (b) compressive film failures during aging in Ar. After Ohring [16].

Similar to the silver-lithium film shown above the appearing stresses can result in cracks, rising or lifting of the film, peeling-off and even destruction of the substrate material (being possible in thin wafer technologies). The total stress inside a deposited film, depending on the film thickness and on the deposition parameters, consists of three main components: external stresses and strains due to aging effects of the substrate; internal stresses caused by the structure of the coating (e.g.: lattice constant, emplacement of voids and foreign atoms, grain boundaries, so everything affecting the microstructure of the film); thermal stresses induced by unequal expansion and/or contraction coefficients of the film and the substrate material either resulting in compressive or tensile stresses.

3.2.1.3 Hardness of Thin Films

The mechanical hardness of a deposited thin film is dictated by the acting inter-atomic forces, the incorporated defects and the films microstructure. This hardness is said to be the mechanical resistance of a material against any kind of penetration or indentation with a harder specimen. To obtain a quantitative value for the hardness of a thin film one measures the indentation depth of pointed diamond tips after a certain load has been applied. For hardness measurements the indentation depth of the tip into the coating should not exceed 10% of the original film thickness.

3.3 Thin Film Technologies

In fields of thin film technology the applied thin films are deposited by different procedures like physical vapour deposition (e.g. thermal evaporation, sputtering) or chemical vapour deposition to cover all over the substrate. In semiconductor industry silicon wafers and sometimes ceramic or glass wafers act as substrates. After the deposition process further treatments of the layers and films can occur including tempering, recrystallization or doping the deposited layer or well-directed erosion of film material. Especially, while manufacturing products for semiconductor industry like integrated circuits, thin film solar cells, microsystems technology, sensors and actuators, the films and layers have to be structured by means of a specific removal of the film material at certain sites. Creating such a structure procedures like photolithography followed by wet chemical or plasma etching, or treating the sample directly with laser or electron beams are applied.

3.4 Film Properties affecting Adhesion [4]

Concerning the adhesive strength or compound strength and adhesion failure, many properties of the film in the investigated interface between the deposited film and the substrate underneath are of great importance.

Residual Film Stress

A very important factor influencing the apparent adhesion is the residual film stress which can be either compressive or tensile. The reason for such stresses is the difference of the thermal coefficient determining expansion and relaxation of the substrate and especially the film, when deposited under high temperatures. Film parameters like material and film thickness strongly influence the total stress that can appear at the interface. Materials with a high Young’s modulus like chromium or tungsten, but also compound materials show the highest residual stresses. Whenever any kind of external stress is applied to an interface and, accordingly applied to the deposited film, this value has to be added to the predominating residual stress. In extreme cases high residual stresses can even lead to undesired spontaneous peeling off or de-adhesion of the film and might accelerate the process of corrosion.

Film Morphology, Density and Mechanical Properties

The ability of a material to transmit mechanical stresses or to sustain internal and residual stresses depends on the deformation of the film material, its microstructure and its morphology. For instance, if a film shows a regular morphology it might have a good adhesion as each of these columns will be separately bonded to the substrate material while the columns themselves are poorly bonded to one another, and therefore avoiding internal stresses to build up. On the other hand such columnar adhesion can also decrease the adhesive properties, especially over a long period of time. For this reason this columnar adhesion is not desired as it also causes the film to get porous allowing interfacial corrosion.
The distribution of film stresses is determined by the mechanical properties (which will be discussed later on). If the mechanical and physical properties of the substrate and the deposited film strongly differ from each other, it is recommended to classify these properties through the region around the interface. When grading the properties of the substrate and the film separately one will receive quite discontinuous values describing the properties.

Flaws or Voids

Other factors that determine adhesion are flaws near or even at the interface. The generation of such flaws usually needs more energy than flaw propagation through the compound material and present flaws decrease the materials fracture toughness. Flaws can also lead to local stress concentration where the magnitude of residual stresses becomes higher than usual. The reason for flaws coming up at the interface can be that there have already been flaws at the substrate surface, they can result from a poor or incomplete contact between the substrate and the film material or voids which have developed during film growth. If a film with a high compressive stress is deposited onto a substrate it will introduce a tensile stress to the substrate surface and may produce flaws, for which reason flaws tend to come up for deposited films with high internal stresses.

Lattice defects and incorporations

When a film grows during a deposition process, for instance, it may incorporate lattice defects (like Frenkel and Shottky defects) or mobile gas molecules leading to voids inside the compound. These voids tend to form at preferred sites such as grain boundaries, interfaces or surfaces of any matter, at all sort of dissimilar materials. In case they form at an interface between two materials they end up in a so-called plane of weakness that affects the whole interfacial region, weakens the interface and ends up in worse adhesion. This effect is even reinforced if the substrate surface has been treated and “contaminated” with hydrogen, applied during acid cleaning or by any other gas used for sputtering as a cleaning process.

Pinholes and Porosities

In case porous sites or pinholes are present at an interface, impurities and foreign particles can cause corrosion and weaken the interface, whereas the porosity of a thin film, or of films in general, is influenced by the process parameters. These process parameters, furthermore, affect the growth of the already mentioned columnar-like microstructures. A vacuum deposited (chemical vapour deposition – CVD) thin film for example can be porous up to a certain order, defined by the roughness of the substrate surface or the incidence angle of the flux of the atoms to be absorbed by the substrate.

Nodules or Nuggets

In deposited thin films such nodules or nuggets might be formed during the actual growth process by discontinuities and they establish on surface features like molten droplets from the vaporization source or very small particles, named particulates. These particulates and droplets can be already present on the surface of the substrate at the beginning of the deposition process or are deposited on the surface right while the film is growing. As nodules or nuggets are not well bonded to the substrate surface they can easily be removed, but resulting in pinholes.

3.4.1 Substrate Properties affecting Adhesion [4]

The adhesion is not only affected by the film properties we have already heard about, adhesion also depends on the properties of the substrate a coating or film is deposited onto. Therefore it is of great importance that the surface of the substrate and the substrate material located close to the surface shows high fracture toughness. Neither the surface nor the material of the immediate surrounding should contain any flaws or voids that might become part of the interfacial region. Another factor that could impinge the adhesive properties of the interface is the inclusion of gases into the substrate surface, for instance during sputter or acid cleaning processes. After the film is deposited on the substrate, gas molecules may accumulate at the interface, for example due to tempering processes, causing additional internal stresses and leading to poor adhesive properties.

4. CVD – Chemical Vapour Deposition [16], [17]

As the name already indicates CVD is a chemical process that is applied to fabricate solid films of high purity for high-performance applications. [16], [17] This process is often applied in semiconductor industry to deposit different variations of thin films. Some advantages of the CVD technology are the reproducibility of the process, the good uniformity of the deposited films and the degree of automation of the entire process. Though, this process must not be mixed up with another very popular method for the deposition of thin films, the Physical Vapour Deposition (PVD) as there are essential differences: in CVD technologies the deposition rate increases with rising temperatures as the on-going chemical reactions during the actual deposition process are benefited by higher temperatures. Furthermore, CVD offers some advantages compared to PVD: the film parameters can be controlled and adjusted quite well, CVD can be applied to all basic materials (metals, insulators, semiconductors, alloys). For PVD processes the deposition rate decreases with rising process temperatures as atoms or molecules are desorbed from a surface, but the technical design of PVD process kits is not as complex and extensive as for CVD processes.

4.1 General Process Principles [16]

During the CVD process a solid film is deposited on the heated surface of a substrate, for our purposes a silicon wafer, because of a chemical reaction out of the gas phase. One important condition is that volatile compounds of the film components do exist and that they deposit at a certain reaction temperature to deposit the expected film. The process of chemical vapor deposition is characterized by at least one chemical reaction at the surface of the substrate, including one gaseous starting compound and at least two reaction products, one of them being present in its solid state. To ensure the expected chemical reaction to occur at the surface of the substrate and not somewhere else such CVD processes are always operated at reduced pressure (typically 1 Pa – 1000 Pa ≡ $7{,}5 \cdot 10^{-3}$ Torr – 7,5 Torr). One very special property of this procedure is the good edge coverage of CVD films resulting in a conformal deposition of the film. Therefore on substrates which do not have a planar surface, even very small trenches and voids can completely be filled. Figure 13 shall illustrate the importance and the different grades of conformity. [18]

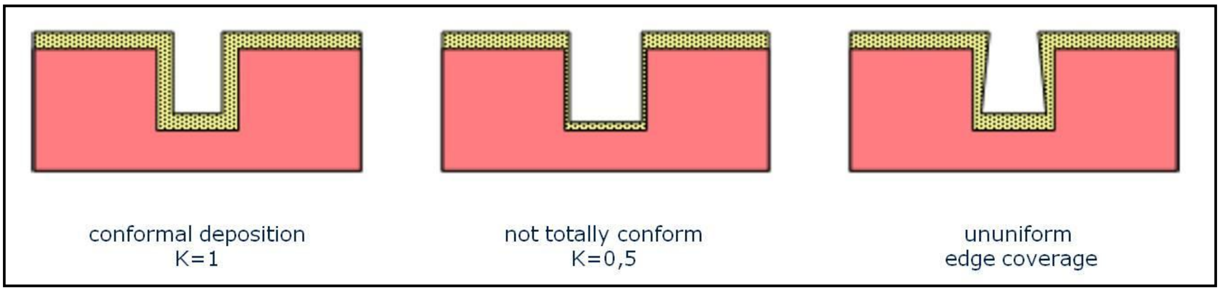
conformal deposition
K=1
not totally conform
K=0,5
ununiform
edge coverage

Figure 13: Possible profiles of conformity and edge coverage. [18]

Every single type of chemical vapor deposition passes the same fundamental process steps which are shown in figure 14 and briefly include: [16]

1. Convective and diffusive transport of reactants from the gas inlets to the reaction zone
2. Chemical reactions in the gas phase to produce new reactive species and by-products
3. Transport of the initial reactants and their products to the substrate surface
4. Adsorption (chemical and physical) and diffusion of these species on the substrate surface
5. Heterogeneous reactions catalyzed by the surface leading to film formation
6. Desorption of the volatile by-products of surface reactions
7. Convective and diffusive transport of the reaction by-products away from the reaction zone

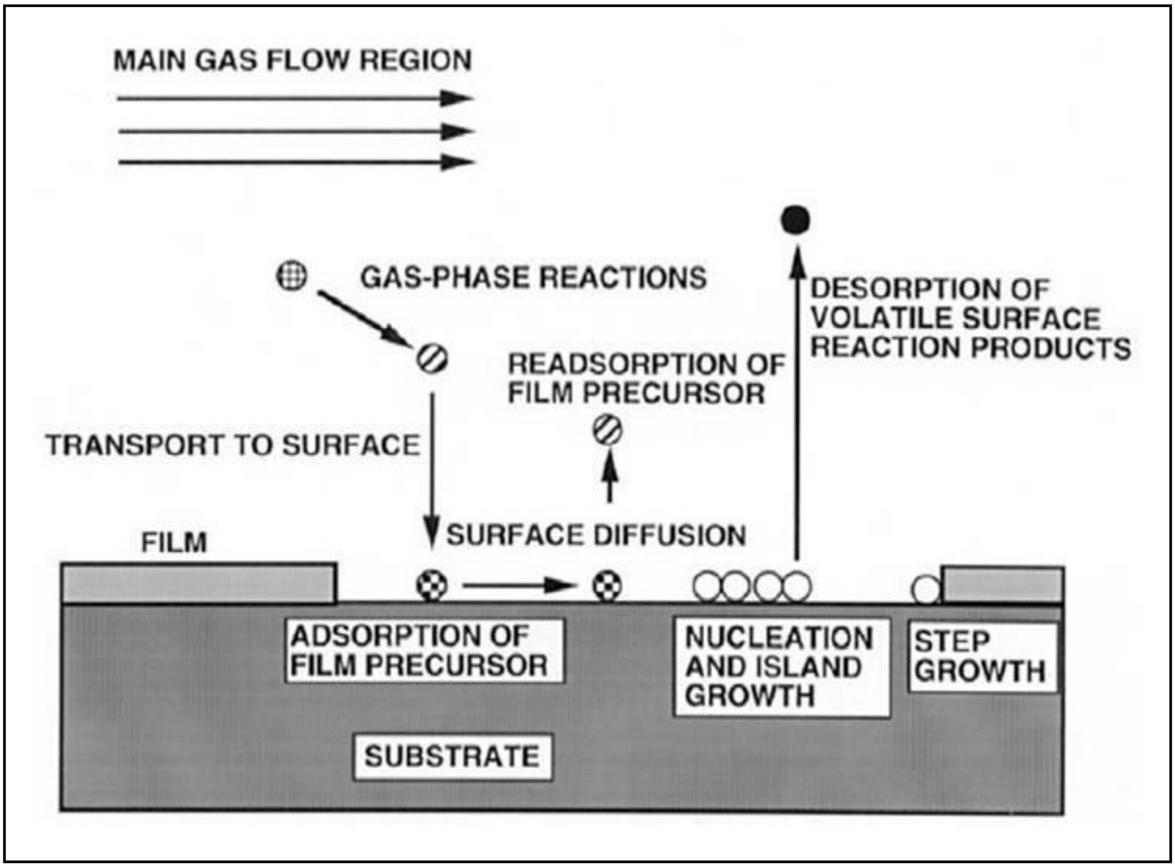
MAIN GAS FLOW REGION
GAS-PHASE REACTIONS
DESORPTION OF
VOLATILE SURFACE
REACTION PRODUCTS
READSORPTION OF
FILM PRECURSOR
TRANSPORT TO SURFACE
FILM
SURFACE DIFFUSION
ADSORPTION OF
FILM PRECURSOR
NUCLEATION
AND ISLAND
GROWTH
STEP
GROWTH
SUBSTRATE

Figure 14: Sequence of gas transport and reaction processes contributing to CVD film growth. [16]

These steps, especially the heterogeneous reactions leading to the film formation, depend on many factors and process parameters. These are the flow rate of the precursor gases and process gases involved in the chemical reaction, the geometry of the process chamber and the pressure inside. Also the correct spacing indicating the distance between the substrate surface and the so-called shower head from where the chemical substances are injected into the chamber is of enormous importance during the deposition process. But these are not the only influences that can affect the deposition process and the resulting film. One has to consider scientific aspects and engineering issues as well as practical concerns. All these aspects and other upcoming issues are summarized in figure 15. [16]

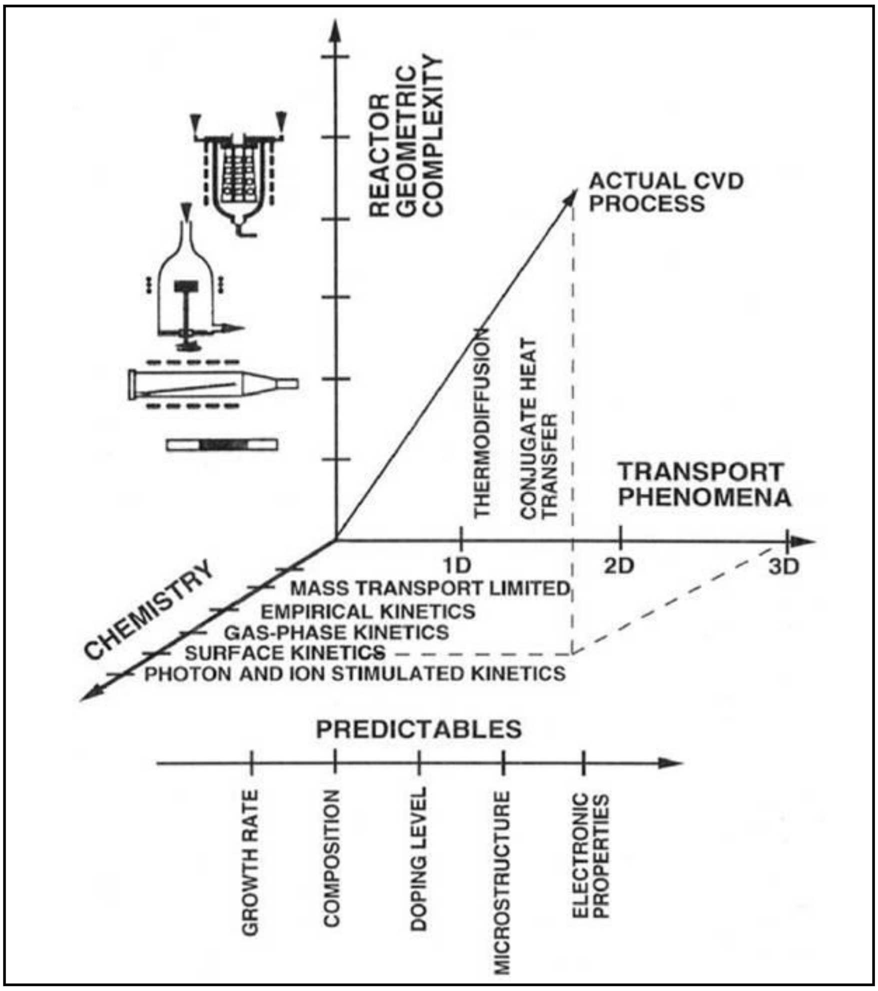
REACTOR GEOMETRIC COMPLEXITY
ACTUAL CVD PROCESS
THERMODIFFUSION
CONJUGATE HEAT TRANSFER
TRANSPORT PHENOMENA
1D
2D
3D
CHEMISTRY
MASS TRANSPORT LIMITED
EMPIRICAL KINETICS
GAS-PHASE KINETICS
SURFACE KINETICS
PHOTON AND ION STIMULATED KINETICS
PREDICTABLES
GROWTH RATE
COMPOSITION
DOPING LEVEL
MICROSTRUCTURE
ELECTRONIC PROPERTIES

Figure 15: Schematic diagram of the chemical, transport, and geometrical complexities involved in modelling CVD processes. [16]

The figure above demonstrates how many different parameters play an important role and have to be taken into consideration before one can start with the adjustment of the different unit processes that yield different types of films and coatings by changing the indicated variables.

Beside the parameters summarized in figure 15 one can say that the process parameters that are the most controlling ones and with can also be directly adapted and varied at the user interface of the CVD equipment are the following: [19]

- amount of substances
- process temperature
- pressure inside the CVD chamber
- spacing between wafer surface and showerhead
- RF-power driving the plasma in case of PE-CVD

For the amount of substances which are inserted into the reactor during the deposition process are given in three different units, depending on whether the process is based on silane or TEOS (Triethylorthosilicate) precursors or what type of CVD is regarded. For silane based processes the amount of gases is given in standard cubic centimeter per minute (sccm), for TEOS based processes the components (TEOS = TetraEthylOrthoSilikat, TEB = TriEthylBorate, TEPO = TriEthylPhosphate) are available as liquids, evaporated and diluted in He, leading to the unit milligrams per minute (mgm). In case the reactant and dilutent gases are used in a low-pressure CVD (LP-CVD) reactor they are given in standard liter per minute (mgm). For most of the CVD processes run inside a parallel plate reactor (see figure 18) the distance between the substrate and the showerhead, where the process substances are ejected from, is given in mils, whereas 1 mil resembles 25 µm. In case of plasma-enhanced CVD (PE-CVD) where the required energy for the process is provided by a RF-plasma (radio frequency plasma) at a frequency of 13.56 MHz, the RF-power driving and keeping the plasma upright is given in watts.

4.2 Methods of CVD

Following the same principle there exist a number of different types of chemical vapour deposition, which can be classified in some aspects, as they differ in the means by which the chemical reactions are actuated. Either the required gas and gas-solid reactions are activated by employing heat energy to the substrate or glow-discharge plasmas are applied within the deposition chamber to run the chemical reactions taking place simultaneously to the film deposition.

Some of these types are said to be the “classical” ones, including Atmospheric Pressure CVD (AP-CVD), Low Pressure CVD (LP-CVD) and Plasma-Enhanced CVD (PE-CVD) which are mainly applied in semiconductor technology, and hence for preparing the samples studied and discussed in this master thesis. Other processes classified as “more sophisticated" processes, which are not yet widely spread for industrial applications should just be mentioned. Such processes are Metal-Organic CVD (MO-CVD) and Laser-Enhanced CVD (LE-CVD) or Rapid Thermal CVD (RT-CVD) and Atomic Layer Deposition (ALD), as described in [17] more closely.

For our purposes it is essential and sufficient to focus on the three mentioned classical methods Atmospheric Pressure CVD (AP-CVD), Low Pressure CVD (LP-CVD) and especially Plasma-Enhanced CVD (PE-CVD).

Figure 16 gives a short overview of the pressure and temperature regimes – as applied at INFINEON [20] and differing from classifications found in literature, e.g. [16] – in which these types of CVD methods are operating. Other modifications include High Density Plasma (HDP) deposition processes or sub-atmospheric pressure processes (SA-CVD).

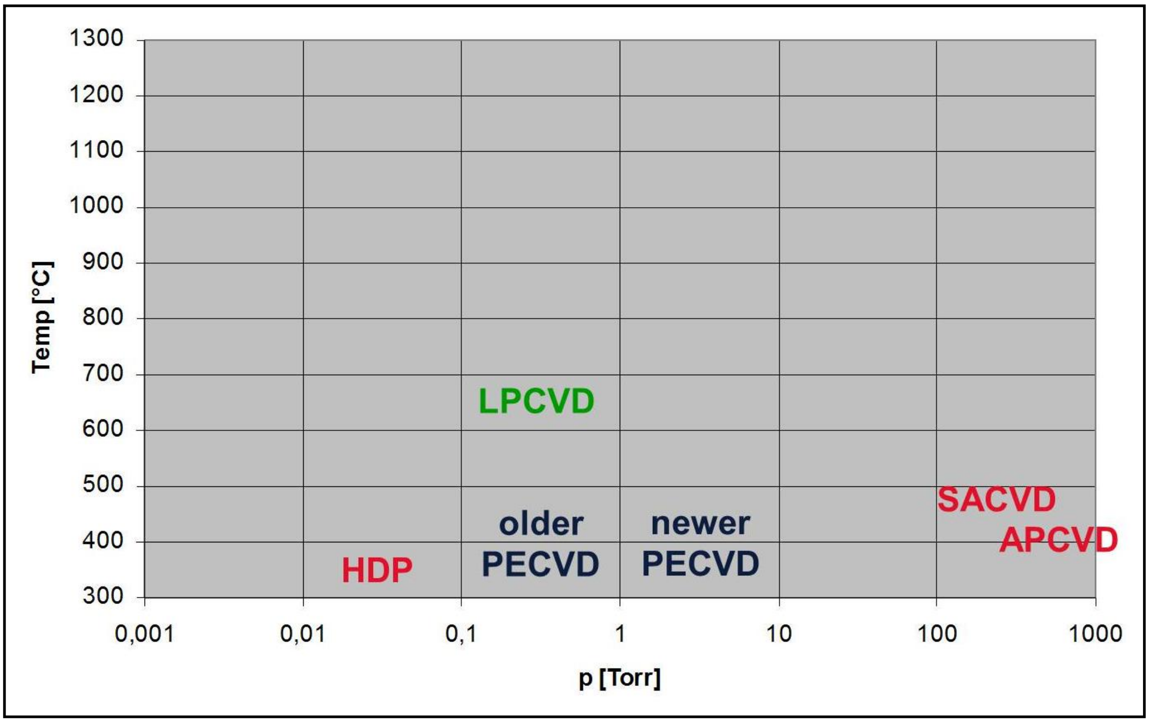

Figure 16: Pressure and temperature regimes of the most popular and well established processes in fields of Chemical Vapour Deposition as applied at INFINEON Technologies in Villach.

4.2.1 Thermal CVD [16]

Thermally activated CVD processes employ heat energy to activate the required reactions in the gas phase and at the surface, and in contrast to plasma-enhanced CVD processes, can be sectioned in atmospheric or low pressure processes, high or low temperature, hot or cold wall reactors, closed or open processes. Independent of the classification of the regarded CVD process the used process chamber must be capable of the following:

1. delivering and measuring the reactant and dilution gasses into the reactor chamber
2. supplying heat energy to the substrate so the reaction and deposition of the can proceed efficiently
3. removing the by-products and depleted gases

4.2.2 Atmospheric Pressure CVD (AP-CVD) [16]

This deposition method is often used to achieve high-quality, especially epitaxial thin films at relatively high temperatures, where the applied reactors are divided into cold-wall and hot-wall reactors. The most common three designs are schematically illustrated in figure 17 (a) – (c). [16]

Figure 16 (d) in addition shows another often used type of construction for AP-CVD reactors, denoted as gas-injection reactor that operates in a continuous mode. [21]

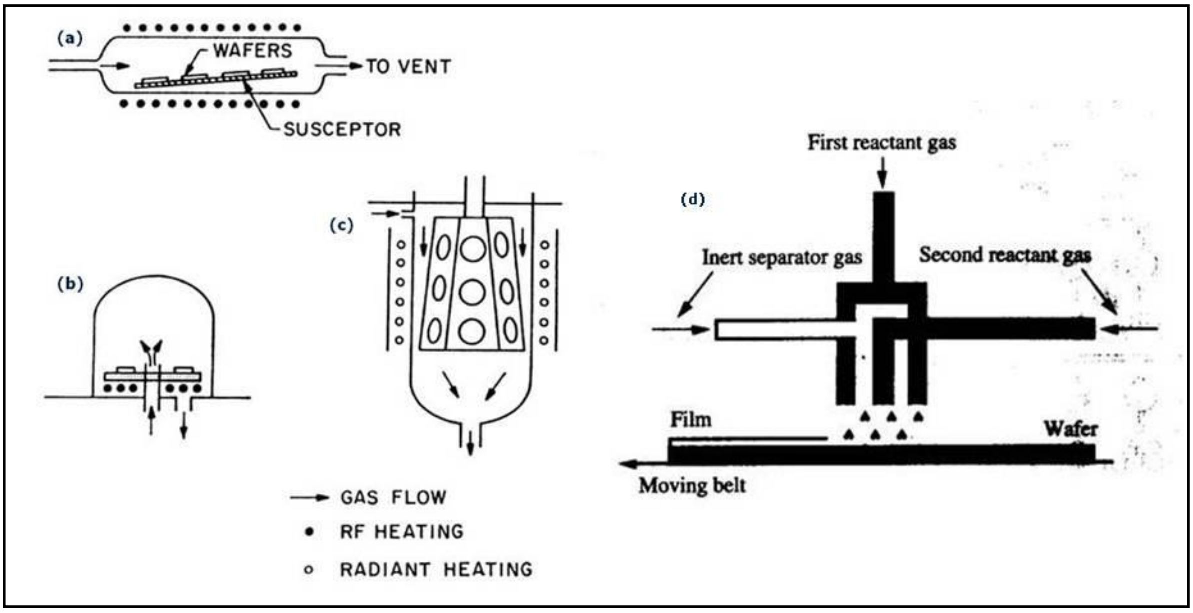

Figure 17: Schematic diagrams of AP-CVD reactors employed, among others, in epitaxial Si and CVD deposition processes. (a) Horizontal tube reactor; (b) pancake reactor; (c) barrel reactor; [16] and (d) gas-injection reactor, operating continuously. [21]

Atmospheric pressure CVD can be performed at three different temperature regimes divided into: high-temperature, T=1200°C–850°C; moderate temperature, T=850°C–700°C; and low-temperature T=700°C– 450°C.

High temperature AP-CVD processes are extensively utilized to process hard metalliferous coatings and films (coatings containing a high amount of metallic additives). One great advantage offered by this technique of thin film deposition is the large number of small tools, for our purposes a large number of silicon wafers, that can be batch coated at the same time. Hot-wall reactors for instance are capable of individual and/or sequential deposition of thin films by applying reactant gases like Al_2O_3, TiC or TiN.

Typical low-temperature AP-CVD reactors used for processing assorted thin films offering dielectric features like SiO_2 – either via oxidation of silane (450°C) or via decomposition of TEOS (700°C), BPSG (boron and phosphorous doped silicate glass) glasses or silicon nitrides are equipped with resistance-heated rotary chambers and a so-called close-space gas-nozzle. Despite their secure and reliable mode of operation AP-CVD methods have been step by step overrun and replaced by more effective and in some aspects more efficiently operating LP-CVD and PE-CVD methods.

One major disadvantage is that AP-CVD does not offer the advantage of greater lot sizes compared to LP-CVD processes run inside a furnace tube.

The widely applied SiO_2 films can either be deposited by oxidizing silane (SiH_4) or by decomposing TEOS ($Si(OC_2H_5)_4$, Tetraethyorthosilicate or Tetraethyloxisilane).

The intention to avoid using silane for processing SiO_2 – especially within AP-CVD processes – which is pyrophobic and therefore easily can ignite itself when it gets into contact with air, the way of gaining SiO_2 by decomposing TEOS, being existent as an inert liquid, lead to the advantage of better step and trench coverage during the deposition process.

Though AP-CVD using ozone (O_3) or TEOS, and LP-CVD have originally been employed to fabricate thin dielectric films, preferably SiO_2 and silicon nitride, the PE-CVD technology has been identified to be the novel and more prospective process, because these processes operate at lower pressures and much lower temperatures.

4.2.3 Low Pressure CVD (LP-CVD) [16]

Low pressure CVD processes run in reactors that operate at lower pressures than atmospheric processes, as the name already implies, and have been applied to fabricate many miscellaneous dielectric films, in particular SiO_2, silicate glasses and silicon oxi-nitrides. Since the mentioned films could also be deposited in AP-CVD reactors, the question arises, why one should use LP-CVD processes though the reactors required for LP-CVD are much more complex. The main reason is that the higher costs that have to be afforded can be reduced by the possibility of packing the wafers more densely into a LP-CVD reactor. Figure 18 illustrates two different designs of typical low-pressure CVD reactors arranged in furnace-tube-like manner. For the reactor shown in figure 18 (b) the closure head is permanently fixed to the “boat”, offering the advantage of faster feeding of the furnace tube. [21]

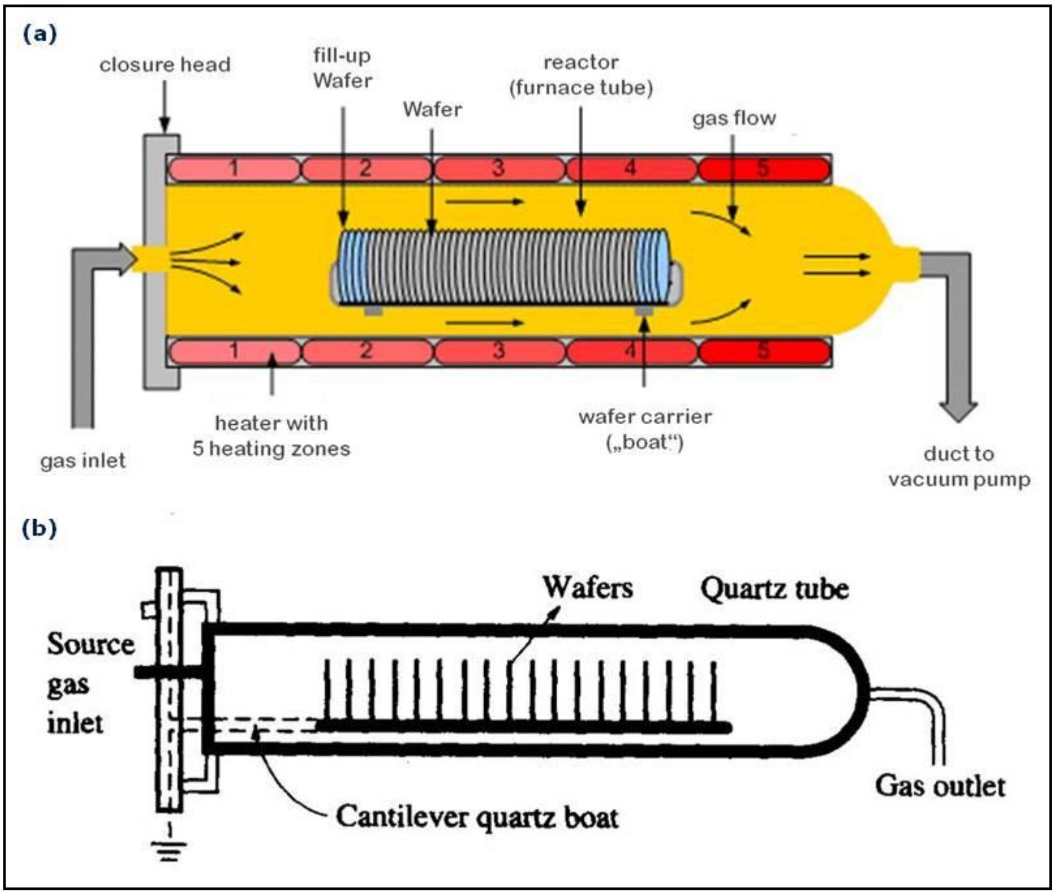
(a)
closure head
fill-up Wafer
Wafer
reactor (furnace tube)
gas flow
1
2
3
4
5
gas inlet
heater with 5 heating zones
wafer carrier („boat“)
duct to vacuum pump
(b)
Wafers
Quartz tube
Source gas inlet
Gas outlet
Cantilever quartz boat

Figure 18: Different design of typical hot-wall multiple wafer LP-CVD reactors with a separate closure head (a) or with a closure head which is permanently fixed to the wafer carrier “boat”. After [21].

The great advantage of processing a few hundred wafers at the time is combined with many outstanding benefits of the LP-CVD procedure compared to the former AP-CVD reactor applied for depositing the desired dielectric films. Some of these benefits are the high purity of the film, a high film uniformity across the whole wafer, a conformal step coverage and the high throughput. [21]

With LP-CVD one can further distinguish three different process regimes, depending on how much below atmospheric pressure (p=760 torr) the reactor is performing: between 100 tor – 1 torr one deals with reduced pressure CVD (RP-CVD); the real low pressure CVD process operates at 1–10 mtorr; whereas ultrahigh vacuum CVD (UHV-CVD) processes are executed at about 10^{-7} torr. To ensure similar deposition rates for LP-CVD processes as for CVD processes operating at atmospheric pressure regimes these lower pressures have to be compensated in some way. This is achieved by enriching the input concentration of the reactant and the dilutent gases, leading to a comparable partial pressure of the ongoing reactions and furthermore to even higher growth rates of LP-CVD films compared to films processed in “conventional” AP-CVD reactors.

In commercial LP-CVD systems horizontal hot-wall reactors are employed which are heated resistively. The main difference between LP-CVD and AP-CVD reactors is related to the amount of deposit of the film material on the inner walls of the reactor. In hot-walled LP-CVD reactors the agglomerated deposit is quite dense, hard and thick, whereas residues of the deposited film material that are formed during AP-CVD processes are less adherent to the reactor walls and are less minted. Concerning the quality of the fabricated film one always hast to handle and deal with the problem of incorporations of impurities or detachment of particulates during film deposition that might arise in AP-CVD systems where the wafers are positioned in a horizontal manner. For prevention LP-CVD reactors offer the opportunity to stack the wafers vertically before batch coating, which is a further advantage of this method of thin film deposition.

4.3 Plasma-Enhanced CVD (PE-CVD) [16]

In PE-CVD processes, as said already in the name, the process is promoted by a glow-discharge plasma which is generated and maintained inside the process chamber, whereas the chemical reactions from the vapor phase and the film deposition process take place simultaneously. Since the demands of semiconductor technology concerning product quality and process reproducibility become more and more challenging, advances not only for processes like plasma etching or sputtering but also for PE-CVD processes were demanded. In most of the industrially applied plasma-enhanced CVD processes the plasma is exited and maintained by an electrical RF field because the deposited dielectric films cannot be processed by using DC-discharge plasmas. The induced energetic discharge inside the excited plasmas is sufficiently high to decompose the reactant and dilutent gas molecules into ions, free radicals and atoms or molecules available in exited or ground states. These “free” particles start interacting with each other and thereby provoke the chemical reactions necessary for the deposition, to proceed at much lower temperatures than in AP-CVD or LP-CVD processes (lowest possible process temperatures: 500°C in AP-CVD and LP-CVD; 200°C in PE-CVD [21]). Certain chemical reactions cannot take place below a certain temperature. This displays a problem because some substrate materials are susceptible to thermal stresses induced by high temperatures. For this reason plasma-enhanced CVD processes have been chosen to activate such chemical reactions being essential for manufacturing a certain type of film or material (e.g. epitaxial silicon is decomposed from silane at $T \geq 900°C$ [19]).

PE-CVD also offers the opportunity to deposit a large variety of assorted materials such as carbon in terms of diamond-like or amorphous carbon, borides, metals, nitrides, oxides, and doped and undoped silica glasses.

Depending on whether the plasma of the considered PE-CVD process is excited by capacitive or inductive coupling, microwaves or RF, one distinguishes between several types and configurations of available PE-CVD reactors. Well-known construction forms are for instance the parallel plate reactor, the horizontal tube reactor and single and multiple wafer reactors, whereas the most common and widely applied type is perhaps the parallel-plate Reinberg form reactor, which is shown in figure 19. This or similar types of reactors are applied for conventional or, as it is called, direct PE-CVD processes and follows the operating principle of a single-wafer reactor. [16]

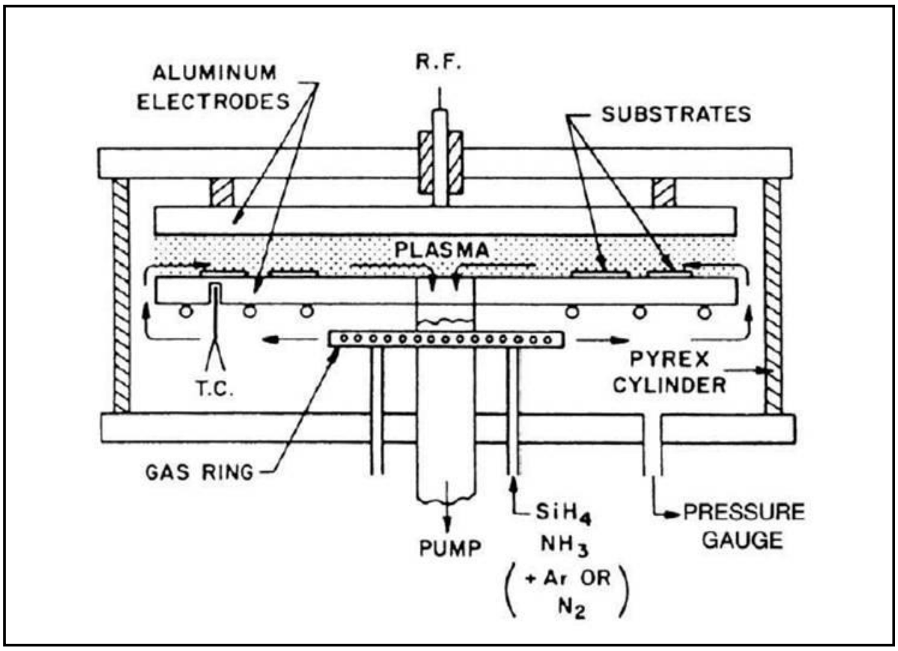

Figure 19: Reinberg-type cylindrical radial-flow plasma reactor for the deposition of – in this case – a silicon-nitride film. [16]

Some more reactor types, especially those applied to deposit the sample films which have been studied during this master thesis will be described in a proper chapter.

4.4 CVD Thin Films [16], [17]

For the better understanding of the several requests, standards and demands which are generally made on thin CVD films, especially with respect to properties and fields of applications, this section introduces typical functional film processes by CVD principles for silicon oxide, silicon nitride, amorphous carbon and, for the completeness, silicon oxinitride.

Silicon oxide and silicon nitride as typical insulating dielectric CVD films are treated a bit more detailed as they were the thin film materials which, in most instances, have been studied in this thesis and to introduce the several chemical reactions which constitute the growth of the particular film under miscellaneous conditions. Beside these two dielectric films also amorphous carbon was studied because it is applied for a new emerging technology, though it is no dielectric material.

For every single deposited film there is not only one single process or CVD method to be applied but multiple options. These various processes for the particular film mostly differ concerning the process parameters (temperature, RF power in case of PE-CVD, flow of reactant substances, etc.) properties of the deposited film (residual stress, chemical composition, adhesion to the subjacent material, etc. as well as the process properties themselves. Process properties are for instance the duration of the process and the associated consumption of reactant and dilutent gases or liquids, the criticality and the reproducibility of the process or the operational demands on the process chamber.

4.4.1 Silicon Dioxide [17]

Acting and being applied as a gap-filler between polysilicon and other functional layers (e.g. metal passivation layers) silicon dioxide (SiO_2) has been the mostly utilized materials in fields of semiconductor processing and semiconductor industry. The reason is some of its outstanding properties, such as the good adhesive properties to its underlayers, a high breakdown voltage and electrical resistance, and its high resistivity against chemical reactive, photoactive and thermal exposures. Silicon dioxide is either processed during oxidation under high temperatures provided by furnaces or by using precursors (silane or TEOS) containing silicon.

Because of the enormous importance of silicon dioxide in many fields of modern technologies various types of CVD reactors offering many different ways to produce SiO_2 have been developed, each of them used to deposit SiO_2 under certain conditions.

These conditions, influencing the whole deposition process and the on-going chemical reactions – especially pressure, and the type of the reaction – are summarized in table 2. [17]

Table 2: Pressure and temperature regimes in CVD Reactors applied for Silicon Oxide Deposition.

Reactor	***PE-CVD***	***AP-CVD***	***SA-CVD***	***LP-CVD***
Pressure (Torr)	max. 10	750	50-700	<10
Temperature (°C)	200-550	<500	<600	300-900
Reaction type	RF plasma	thermal	thermal	thermal
Reactor type	single wafer	continuous belt	single wafer	furnace

In comparison to thermal or PE-CVD oxide films, which tend to have compressive stress, CVD oxide films processed at low temperatures show tensile stresses after the deposition process.

SiO_2 films can also be achieved by depositing the film at high temperatures (T=500°C-1000°C) in multiple-wafer LP-CVD reactors from e.g. dichlorsilane reacting with nitrous oxide:

$$\mathrm{SiH_2Cl_2\ (g) + 2N_2O\ (g)\ \xrightarrow{T=900°C}\ SiO_2\ (s) + 2N_2\ (g) + 2HCl\ (g)}$$

Another option to deposit SiO_2, before the liquid precursor TEOS was invented the first time, was from silane-based reactions. For applications in semiconductor manufacturing this method is very popular to gain such a low-temperature oxide (LTO) from reacting silane and oxygen.

$$SiH_4\ (g) + O_2\ (g)\ \xrightarrow{T=300°C-450°C}\ SiO_2\ (s) + 2H_2\ (g)$$

In case dopants like boron and/or phosphorous are incorporated into the silicon oxide film the adding of PH_3 and/or B_2H_6 results in the (parallel) reactions giving PSG (phosphorous doped silicate glass) or BPSG (boron and phosphorous doped silicate glass):

$$4PH_3\ (g) + 5O_2\ (g)\ \xrightarrow{T=300°C-450°C}\ 2P_2O_5\ (s) + 6H_2\ (g)$$

$$2B_2H_6\ (g) + 3O_2\ (g)\ \xrightarrow{T=300°C-450°C}\ 2B_2O_3\ (s) + 6H_2\ (g)$$

In order to produce SiO_2 silane can also react with N_2O or O_2 within the RF plasma at less than 400°C:

$$\mathrm{SiH_4\ (g) + 2N_2O\ (g)} \xrightarrow{\mathrm{T=200°C-400°C,\ \ RF\ plasma}} \mathrm{SiO_2\ (s) + 2H_2\ (g) + 2N_2\ (g)}$$

The properties of the deposited oxide may be improved by impurities like hydrogen (H_2) or nitrogen (N_2) that often get incorporated during the PE-CVD process. Despite the convenience and simplicity of CVD processes applying silane as dominant component for the chemical reactions, being injected into the reactor as a gas, the resulting SiO_2 films suffer from bad conformity and relatively poor edge coverage. For this reason silane has been replaced by TEOS (Tetraethylorthosilicate, $Si(OC_2H_5)_4$) being on hand as a liquid which has to be evaporated before it is injected into the CVD reactor. During the deposition process executed in LP-CVD systems TEOS decomposes to form SiO_2 in the following manner:

$$\mathrm{Si(OC_2H_5)_4\ (vapor)} \xrightarrow{\mathrm{T>600°C}} \mathrm{SiO_2\ (s) + H_2O\ (g)} + 2C_2H_4\ (g)$$

The process temperature for decomposing TEOS to deposit the desired film can rigorously be reduced by “simply” adding ozone (O_3) or by choosing the plasma-enhanced way of CVD processing. This leads to the following reactions which are applicable for AP-CVD or PE-CVD processes and also for sub-atmospheric methods (SA-CVD):

$$\mathrm{Si(OC_2H_5)_4\ (vapor) + 8O_3\ (g)} \xrightarrow{\mathrm{T=400°C-600°C}} \mathrm{SiO_2\ (s) + 10H_2O\ (g)} + 8CO_2\ (g)$$

$$\mathrm{Si(OC_2H_5)_4\ (vapor) + 12O_2\ (g)} \xrightarrow{\mathrm{T=400°C,\ \ RF\ plasma}} \mathrm{SiO_2\ (s) + 10H_2O\ (g)} + 8CO_2\ \mathrm{(g)}$$

By adding so-called organo-dopant precursors to the mixture of reactant substances like TEB, Trimethylborate, or TEPO, Trimethylphosphate, which are also liquids, dopant materials can be added to the deposited film.

Processes using the silane reaction by applying the traditional hydrites B_2H_6 and/or PH_3 are not as stable as TEB or TEPO reactions. Therefore the application of TEB and/or TEPO facilitates the improving, even perfecting of the film properties tremendously.

4.4.2 Silicon Nitride [17]

Silicon nitride (Si_3N_4) is beside silicon oxide, another well-known and well explored material that is used for many different purposes for various applications in semiconductor industry. As such, Si_3N_4 is widely applied as a passivation layer because it is impermeable to many types of impurities, wherefore it is used to act as barrier layer preventing the diffusion of moisture or sodium, or it is applied to hinder oxygen to penetrate into subjacent silicon layers. Silicon nitride is, in some aspects, similar to silicon oxide being an amorphous material which can be gained from deposition processes including LP-CVD, PE-CVD and even high density plasma chemical vapor deposition (HDP-CVD) rather than from being grown inside a furnace at necessary temperatures of T=1000°C. Another possibility to produce silicon nitride, even in a stoichiometric composition is with an AP-CVD reactor according to the following reaction, with deposition rates varying from 1 nm/min (T=700°C) to 100-200 nm/min (T=900°C):

$$3\mathrm{SiH_4}\ (\mathrm{g}) + 4\mathrm{NH_3}\ (\mathrm{g})\ \xrightarrow{\mathrm{T=700°C-900°C}}\ \mathrm{Si_3N_4}\ (s) + 12\mathrm{H_2}\ (\mathrm{g})$$

From the practical point of view this atmospheric-pressure process is strongly limited by a bad control of the film thickness, especially by means of its uniformity because of the strong dependence on the relatively high process temperature. A further option to achieve silicon nitride films is the application of low-pressure CVD, but with much lower deposition rates (1.5 – 2 nm/min).

$$3\mathrm{SiH_2Cl_2}\ (\mathrm{g}) + 4\mathrm{NH_3}\ (\mathrm{g})\ \xrightarrow{\mathrm{T=700°C-800°C}}\ \mathrm{Si_3N_4}\ (\mathrm{s}) + 6\mathrm{HCl}\ (\mathrm{g}) + 6\mathrm{H_2}\ (\mathrm{g})$$

The temperature driving the chemical reaction to deposit Si_3N_4 films can be significantly reduced by PE-CVD, in comparison to AP-CVD or LP-CVD. Within a PE-CVD reactor the properties of the films deposited at rates of 10-30 nm/min depend on the predominating process conditions (pressure inside the reactor, RF power, spacing between the shower head and the substrate wafer, as well as the substrate temperature).

$$\mathrm{SiH_4}\ (\mathrm{g}) + \begin{cases}\mathrm{NH_3}\ (\mathrm{g}) \\ N_2\ (g)\end{cases}\ \xrightarrow{\mathrm{T=200°C-550°C,\ \ RF\ plasma}}\ \mathrm{Si_x}N_yH_z\ (s) + H_2\ (g)$$

4.4.3 Silicon Oxinitride [17]

Another quite interesting feature of films produced in PE-CVD reactors which is executed when necessary, is the possibility of adjusting and changing the composition of the deposited film from nitride to oxide in a continuous way. This can “easily” be managed by adding N_2O to the reactant SiH_4/NH_3 gas mixture and the properties of the film that gets processed are changed from “nitridic” to “oxidic” properties.

The silicon oxinitride films which are produced in such a manner offer advantageous properties like reduced incorporated hydrogen impurities, upgraded stability and better resistance against cracking due to lower film stresses. These films are applied to planarize multilevel interconnects in the form of a two-layered silicon oxinitride and silicon nitride film stacks. Furthermore, SiN_xO_y can be deposited acting as gate dielectric as it offers improved interface properties between the silicon and the silicon oxinitide (Si-SiO_xN_y). Despite the properties and advantages already mentioned, one can also tune the refractive index of SiO_xN_y to the desired value, which is suitable for the application as dielectric anti-reflexion coating (DARC), where they replace, for instance, organic ARC films fabricated by spin coating processes. Regardless of the application field of the film, the deposition process is always based upon the similar reaction combining SiO_2 and SiN ending up in silicon oxinitride.

$$\mathrm{SiH_4\ (g) + N_2O\ (g) + He\ (g)} \xrightarrow{\qquad} \mathrm{SiON\ (s)}$$

where helium is just used as dilutent component improving the films stability and uniformity.

4.4.4 Carbon Films [16], [22]

With some of the mentioned CVD methods one can also produce ultra-hard thin films, including carbon films that are, by far, the most important ones of this type of films, beside others like boron nitride or carbon nitride. Carbons that appear in an amorphous state usually contain a worth mentioning amount of hydrogen and therefore are identified as a-C:H materials. These diamond-like films produced either by RF or DC driven plasma CVD techniques contain an adjustable amount of hydrogen (H/C ratios from 0,2–0,8 and even higher) and can become even harder than SiC because of the enclosed sp^1, sp^2 and sp^3 hybridized bondings.

Amorphous carbon films (a-C), however, are produced with techniques like sputter-deposition or ion-beam assisted methods without presence of any hydrocarbons. During both processes bombardment of highly energetic ions leads to the deposition of the carbon film. Carbon films that are processed by thermal evaporation instead will show high conductivity though the films are soft and not as hard as diamond-like carbon layers. The impact energy of the “bombarding” ions seems to be or even is the critical and essential parameter influencing the structure and for this reason also the hardness of the deposited film. When the film is built up at lower ion-energies the properties then tend to be more graphitic.

The composition as well as the percentage of sp^2 and sp^3 hybridized bondings of the different, partially amorphous C-H alloys in their typical ternary phase diagram are summarized and displayed in figure 20. [22]

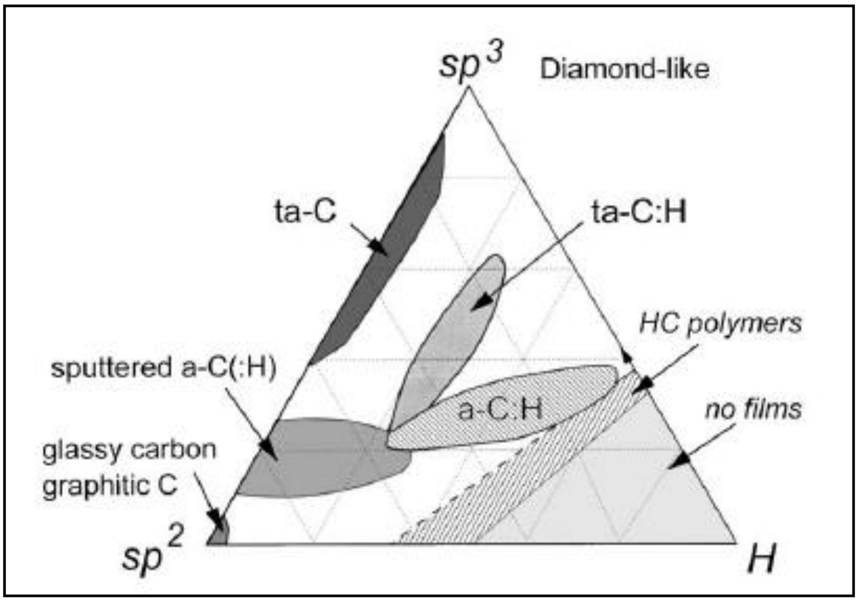

Figure 20: Ternary phase diagram of bonding in amorphous carbon hydrogen alloys.

4.5 Cleaning Process/Cleaning Chemistry [17]

During the deposition process of the thin films the process gases do not exclusively react on the substrate wafer but also on the inner walls and other components of the reactor, like sensor devices and even the gas inlet valves of the shower head, where they form solid material. This deposit load can lead to unrequested defects and up to particulates on the wafer surface. To ensure almost the same process conditions to every charge of processed wafers after the proceeded deposition the process chambers of PE-CVD reactors are cleaned with special cleaning processes being adapted for this special purpose.

Many of such film materials that are deposited in semiconductor industry like polysilicon, silicon in a doped or undoped mode, silicon nitride, or doped silicon oxides can be reacted or by proper means cleaned away and then pumped out of the process chamber as volatile products of the chemical cleaning processes that have taken place.

As the applied materials react with fluorine and therefore are forming very volatile silicon fluorides large numbers of fluoride radicals are generated when mixed with oxygen inside the RF plasma. In comparison to C_2F_6/O_2 which has been used for purposes of cleaning the interior of CVD reactors after the deposition processes, NF_3 plasmas enclose much more fluorine radicals resulting in much faster and higher cleaning rates, though the NF_3 plasma corrodes the process kit more aggressively. Especially parts consisting of quartz crystal and the heaters where the highest magnitudes of temperature are located are strongly affected, particularly aluminum heaters (denoted as DxZ heaters according to the nomenclature of Applied Materials, shortly AMAT), which are most frequently used in PE-CVD systems. Beside NF_3 chemicals like ClF_3 or HCl can be used depending on the material that has been deposited inside the reactor chamber to produce the desired film. HCl for example has been used predominantly to clean reactors where epitaxial silicon was grown because the high temperatures that prevail inside an epi-reactor ($T \approx 1000°C$) do not tolerate fluorine, as it would be too aggressive to the interior parts of the CVD device. ClF_3, therefore, offers another opportunity to provide fluorine that is necessary for the cleaning process, but this gas is by far not that aggressive as the fluorine radicals of NF_3, though it is much more reactive than fluorine in its molecular appearance.

5. CVD Reactors [17]

The design of CVD reactors is based upon the substrate that should be easily combined with individual ways of getting supplied with the required heat energy and with the essential gas delivery system for every individual application or chemistry. Such CVD systems basically consist of a reactor, a supply system for the reactant and dilutent gases and liquids, an exhausting plant, and a suitable system for the wafer handling. The current types of CVD reactors can be categorized among the following aspects:

- operative pressure: atmospheric or low pressure CVD, sub-atmospheric or reduced pressure
- way of reaction energy supply: thermal or plasma enhanced
- way of “heating” the substrate: induction heated, radiant heated (lamp heated), resistance heated
- wall temperature of the applied reactor: hot or cold wall reactor
- capacity of processed wafers: single wafer, multiple wafer, batch, or continuous batch

For applications in semiconductor processing technology the process controlling was more and more automatized and systems for wafer transfer were established to facilitate the controlling of film thickness, uniformity and number of enclosed defects. Automation of technical processes furthermore improved the reliability, the safety and the throughput of the system, which is not totally warranted for human operation.

Most of the CVD reactor systems which were used to fabricate the explored films and film stacks (Centura, P5000, Producer, Watkins Johnson) originate from a manufacturing company called *Applied Materials*, shortly *AMAT*, except the AP-CVD reactor from the homonymous manufacturer *Watkins Johnson*. Before these cluster tools are briefly described one should be familiar with the nomenclature established by AMAT. [23]

Cluster tools generally consist of a mainframe and an individual process chambers. The process chambers can typically be of various types.

- *Process Kit:* inner parts of a chamber which are in direct contact with the wafer or dominate the flow of process
- *Chamber Body:* outer casing of a chamber; often, one type of body can hold a couple of different process kits; one set of process kit can sometimes fit into various bodies as well
- *Mainframe:* central chassis for the multiple process chambers; it contains the robot and general features; has an influence on throughput, but not on process result.

In the following table 3 shall give a brief overview across the AMAT equipment hardware and the appearing possibilities of the configuration concerning process kit with the different heaters and susceptors, the wafer hold capacity of the process chamber, and the individual mainframe.

Table 3: Overview across the Applied Materials equipment hardware.

DxZ . . . Aluminum Heater, Zero consumables
CxZ . . . Ceramic Heater, Zero consumables

Process Kit	Chamber Body	Mainframe
Lamp Heated various susceptors possible	Universal Chamber	P5000 or Centura
DxZ aluminum heater, cover plate	Resistive Heated Singel Chamber	P5000 or Centura
CxZ ceramic heater, no cover plate	Resistive Heated Singel Chamber	P5000 or Centura
DxZ aluminum heater, cover plate	Resistive Heated Twin Chamber	Producer
CxZ ceramic heater, no cover plate	Resistive Heated Twin Chamber	Producer

In this context the shortcut D in DxZ indicating an aluminum heater refers to earlier periods of CVD technology where aluminum heaters have been used for processing dielectric films. That’s where the “D” originates from. It is quite similar with the expression “zero consumables” by means of wear parts, as before cleaning processes applying fluorine in combination with plasma, the installed heaters have not been that heavily affected by the cleaning process.

Beside the three mentioned CVD reactors of AMAT, another equipment was used for the preparation of some wafers, namely *Watkins Johnson*, a tool that deposits CVD films under atmospheric conditions, following the principle explained in section 4.3.2.

5.1 P5000

The equipment of the type P5000 by Applied Materials is the most frequently applied equipment to process CVD films at INFINEON Villach, mainly differing in the applied precursors (TEOS or silane). Therefore the process chambers of the applied equipment will be explained on the basis of a P5000 chamber as it is quite similar to those assembled into other mainframes.

In a P5000 equipment four process chambers are aligned around the load lock chamber as shown in figure 21. The load lock chamber is situated in the centre of the mainframe containing the automatically operating wafer handler, which distributes the wafer from and to the storage elevator before and after every single deposition process. [24]

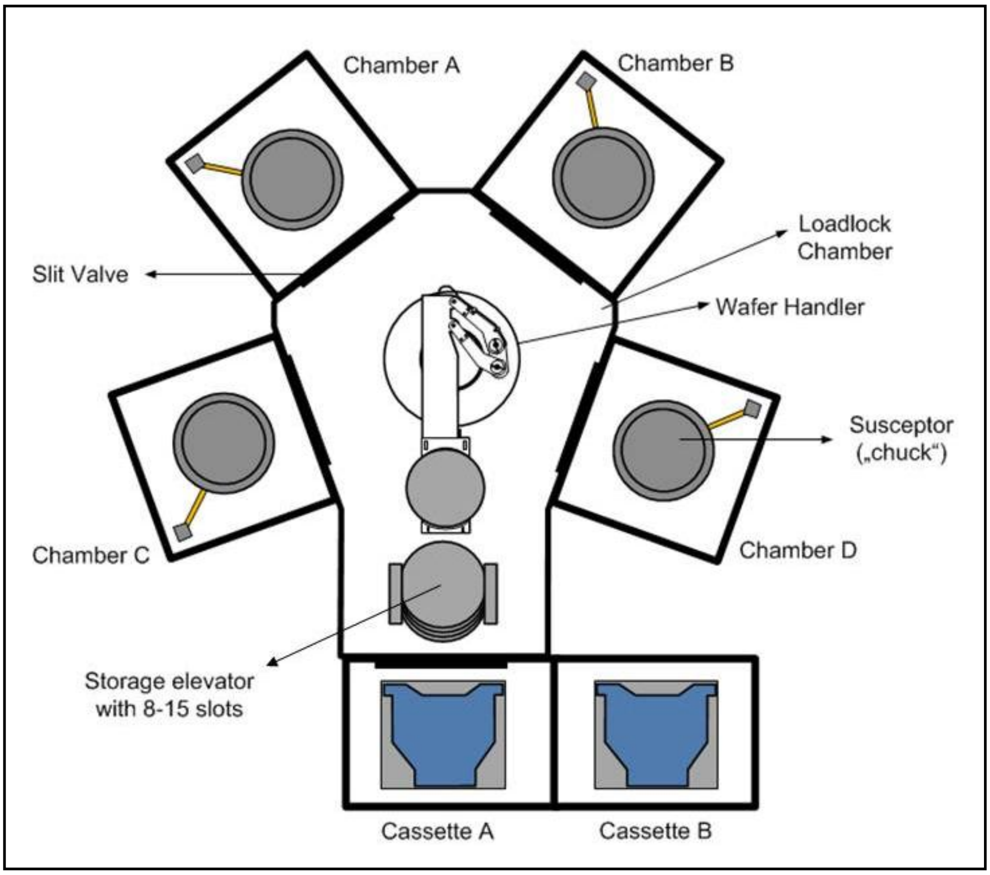
Chamber A
Chamber B
Loadlock Chamber
Slit Valve
Wafer Handler
Susceptor („chuck“)
Chamber C
Chamber D
Storage elevator with 8-15 slots
Cassette A
Cassette B

Figure 21: Schematic image of the P5000 mainframe showing the arrangement of the process chambers around the load lock chamber in the centre.

The susceptors or „chucks“, as they are called by the maintenance crew, are either lamp heated or resistive heated. For lamp heated process chambers the lamp module is aligned underneath and separated from the actual process chamber by a quartz window being permeable to heat radiation. Such a process chamber, in this case used for plasma-enhanced CVD, is shown and described in figure 22. [24]

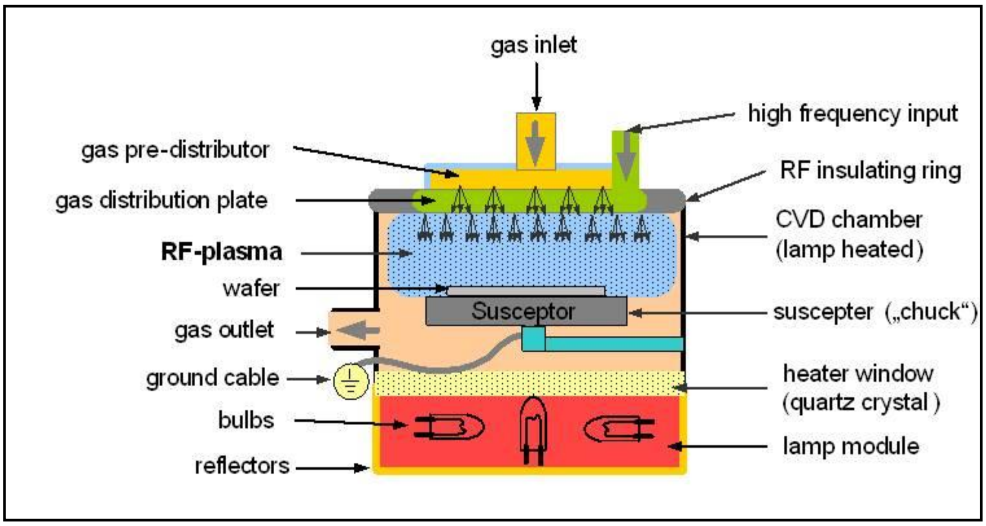
gas inlet
high frequency input
gas pre-distributor
RF insulating ring
gas distribution plate
CVD chamber
(lamp heated)
RF-plasma
wafer
Susceptor
suscepter („chuck“)
gas outlet
ground cable
heater window
(quartz crystal)
bulbs
lamp module
reflectors

Figure 22: Schematic image of a P5000 process chamber. In this case the “chuck” is lamp heated and used for plasma-enhanced CVD, indicated by the blue RF-plasma cloud.

The susceptor is heated with fourteen lamps from the lamp module, whereas each lamp has a power of 1000 W, radiating through the quartz window to provide a process temperature of 430-480°C required for plasma-enhanced CVD. The gas supply is situated at the top of the chambers lid. To achieve the highest possible uniformity with respect to the film thickness the reactant and dilutent gases are equally distributed across the chamber with a so-called blocker plate and a shower head. Both of these pre-distributor plates are electrically conducting and are arranged isolated from the chamber with an insulating ring. As the susceptor is electrically connected to earth and the showerhead to radio-frequency, so the RF-plasma can be discharged by correct magnitudes of pressure and concentration of gases, at a frequency of 13.56 MHz and a driving power, typically ranging from 600 W to 1000 W.

As mentioned in the section about cleaning processes and cleaning chemistry some cleaning processes apply chemicals containing fluorine, like C_2F_6/O_2, or ClF_3, especially in case of PE-CVD NF_3 plasma is used. The fluorine radicals, which arise during the cleaning process are quite aggressive and corrode the quartz window and the susceptor, in case it consists of aluminum (DxZ).

For this reason it is advisable to reconfigure the process chambers applied for PE-CVD processes with ceramic “chucks” (CxZ) combined with resistive heaters like it is depicted in figure 23. [24]

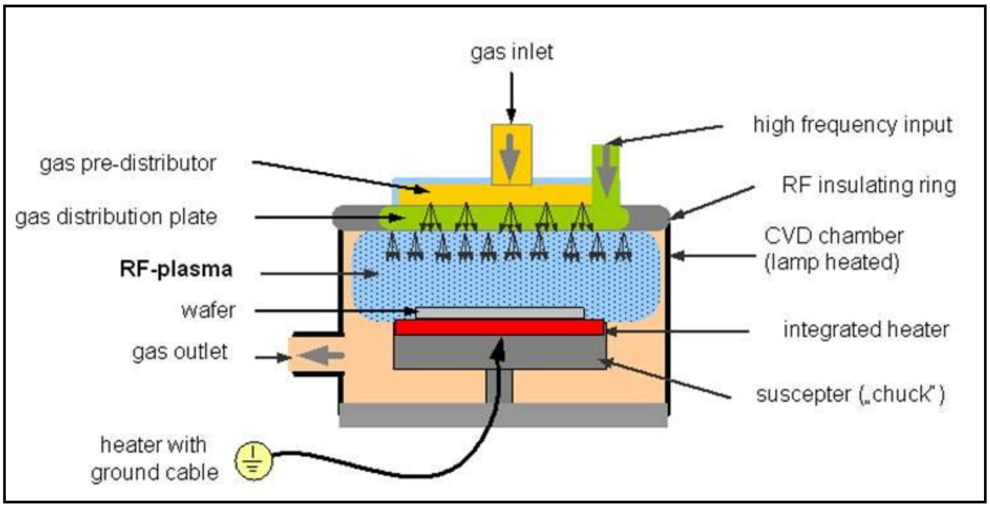
gas inlet
high frequency input
gas pre-distributor
RF insulating ring
gas distribution plate
CVD chamber (lamp heated)
RF-plasma
wafer
integrated heater
gas outlet
suscepter („chuck“)
heater with ground cable

Figure 23: Schematic image of a P5000 process chamber. In this case the “chuck” is resistive heated and again used for plasma-enhanced CVD, indicated by the blue RF-plasma cloud.

5.2 Producer

The setup of the process chambers inside the mainframe of a Producer equipment is similar to that of a P5000 with one major and significant difference: the mainframe consists of three twin chambers arranged around the loadlock chamber, as shown in figure 24. [24]

These twin chambers resemble a single wafer chamber of a P5000 with respect to the setup, but there are two susceptors each with its own gas or liquid supply, its own distribution plate and shower head.

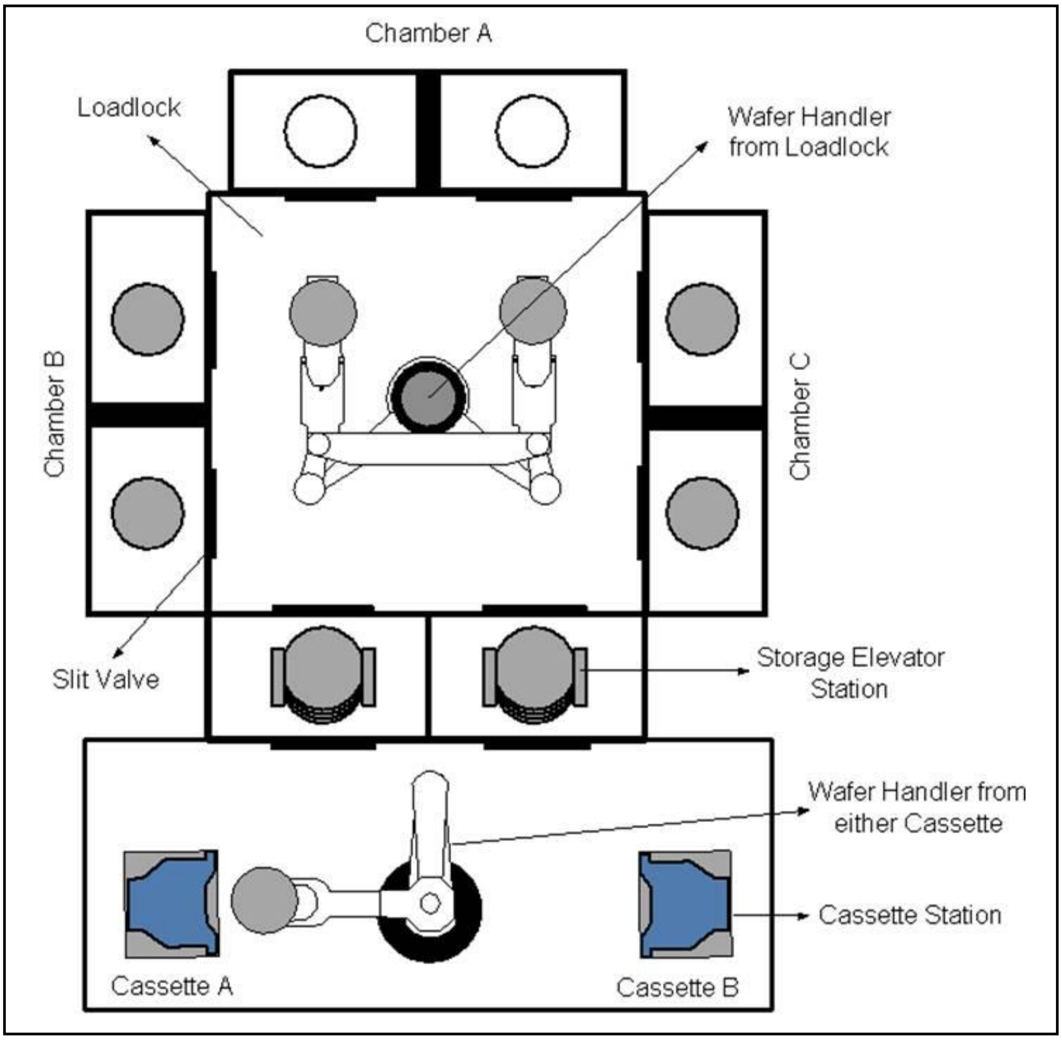
Chamber A
Loadlock
Wafer Handler from Loadlock
Chamber B
Chamber C
Slit Valve
Storage Elevator Station
Wafer Handler from either Cassette
Cassette Station
Cassette A
Cassette B

Figure 24: Schematic image of Producer mainframe with its three individual twin chambers arranged around the loadlock chamber.

Like for the P5000 the wafer handler equally fills the storage elevator stations from where the double-armed wafer handler inside the load lock chamber distributes the wafers from the load lock, containing the two wafer cassettes, to the individual process chambers: “individual” just because every single twin chamber of the Producer equipment can be accounted for different CVD processes, completely independent from one another. Therefore one sole Producer equipment can contain up to three different CVD reactors applying different CVD methods. The actual deposition process, however, elapses the same way as for a P5000 single wafer chamber, described in section 5.1.

5.3 Centura

Another frequently applied equipment to deposit a large variety of films is the equipment of type Centura. This CVD equipment shows different modifications of the main frame, in comparison to the P5000 and the Producer, depending on the intended field of application.

In a Centura used for CVD processes, as shown in figure 25, [24] the load lock chamber including the wafer handler is surrounded by four single wafer process chambers directly across from the load lock with the wafer cassettes. Additionally, the CVD Centura is equipped with an orienter chamber and a separate cool down chamber, whereas every single chamber is evacuated separately while the deposition process is running. Inside the depicted orienter chamber F the wafer gets aligned correctly with the help of the notch (for 12 or 8 inch wafers) or the flat (for 6 inch wafers). After the deposition process the wafer is placed into the cool down chamber to get rid of the high process temperatures before the completely processed wafer is returned to the same position of either cassette where it has been extracted.

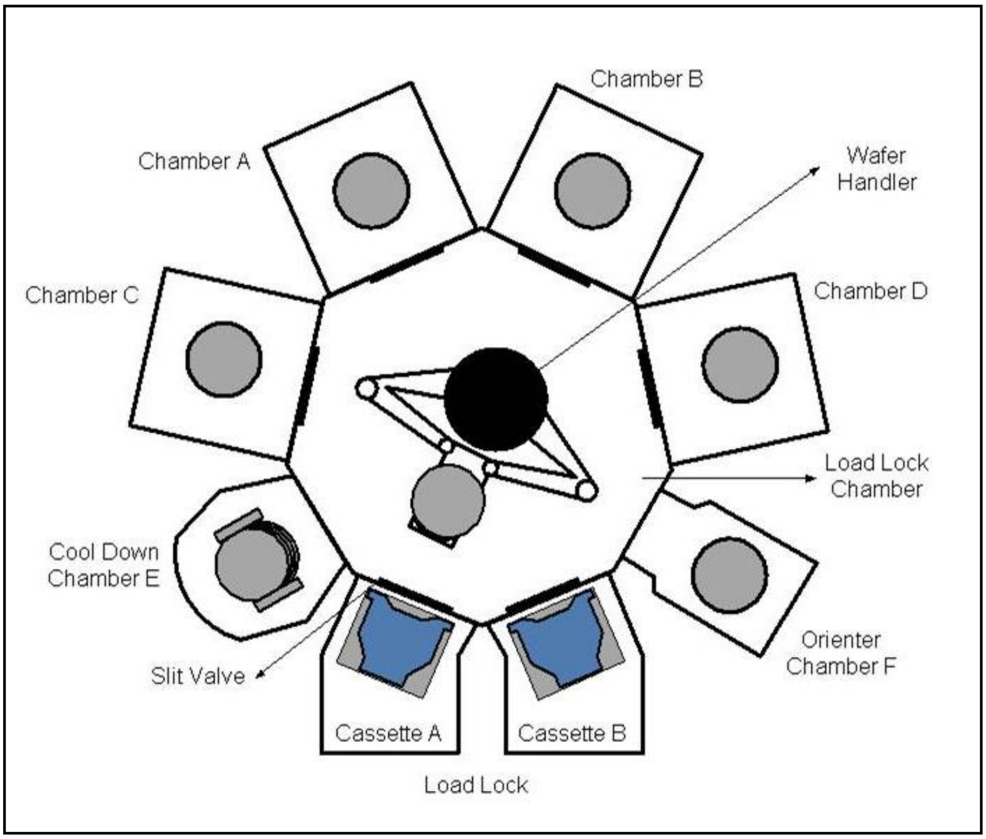
Chamber B
Chamber A
Wafer Handler
Chamber C
Chamber D
Load Lock Chamber
Cool Down Chamber E
Orienter Chamber F
Slit Valve
Cassette A
Cassette B
Load Lock

Figure 25: Schematic image of CVD Centura mainframe including the process chambers, the orienter chamber and the cool down chamber, as well as the load lock station.

The setup and the arrangement of the chambers in the mainframe of a Centura equipment executing HDP processes is very similar to the CVD Centura, as one can see in figure 26. [24] In the mainframe of a HDP Centura there is no chamber D, and the process chambers C and A are additionally equipped with a better vacuum pump to ensure that the film is not only deposited on plane surfaces but also in the deep and narrow trenches of the arising semiconductor device.

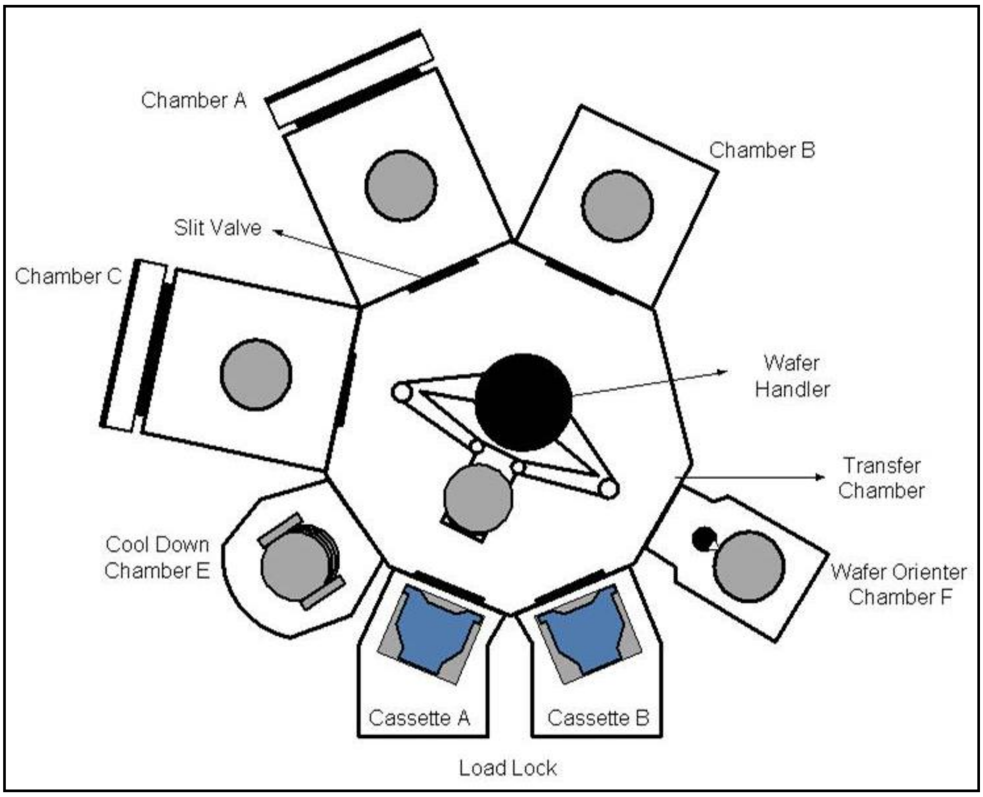
Chamber A
Chamber B
Slit Valve
Chamber C
Wafer Handler
Transfer Chamber
Cool Down Chamber E
Wafer Orienter Chamber F
Cassette A
Cassette B
Load Lock

Figure 26: Schematic image of HDP Centura mainframe. Process chamber D is completely missing, and chambers C and A are equipped with a special type of vacuum pump required for HDP deposition processes.

5.4 Watkins Johnson

Within a Watkins Johnson equipment the CVD process is driven at atmospheric pressure and it is preferably applied to process doped and undoped oxide films, USG, PSG or BPSG. Inside the process chamber, called “process muffle” silane diluted in N_2, and O_2 get thermally decomposed at about 400°C, the media react with each other and the emerging SiO_2 deposits on the wafer surface. This oxide layer has a low density and a moderate edge coverage due to the low temperature.

The “process muffle”, as depicted in figure 27 [24], consists of a heater source with 11 separate heating zones providing the required heat energy during the deposition process and is situated below the injectors. The shown N_2 shields are kind of N_2-curtains and they act as protective barrier outwards, otherwise the silane would uncontrollably react with the surrounding oxygen. The injectors distribute the reactant and dilutent gases (silane, O_2 and N_2), and the mentioned N_2-curtains separate the silane and the O_2.

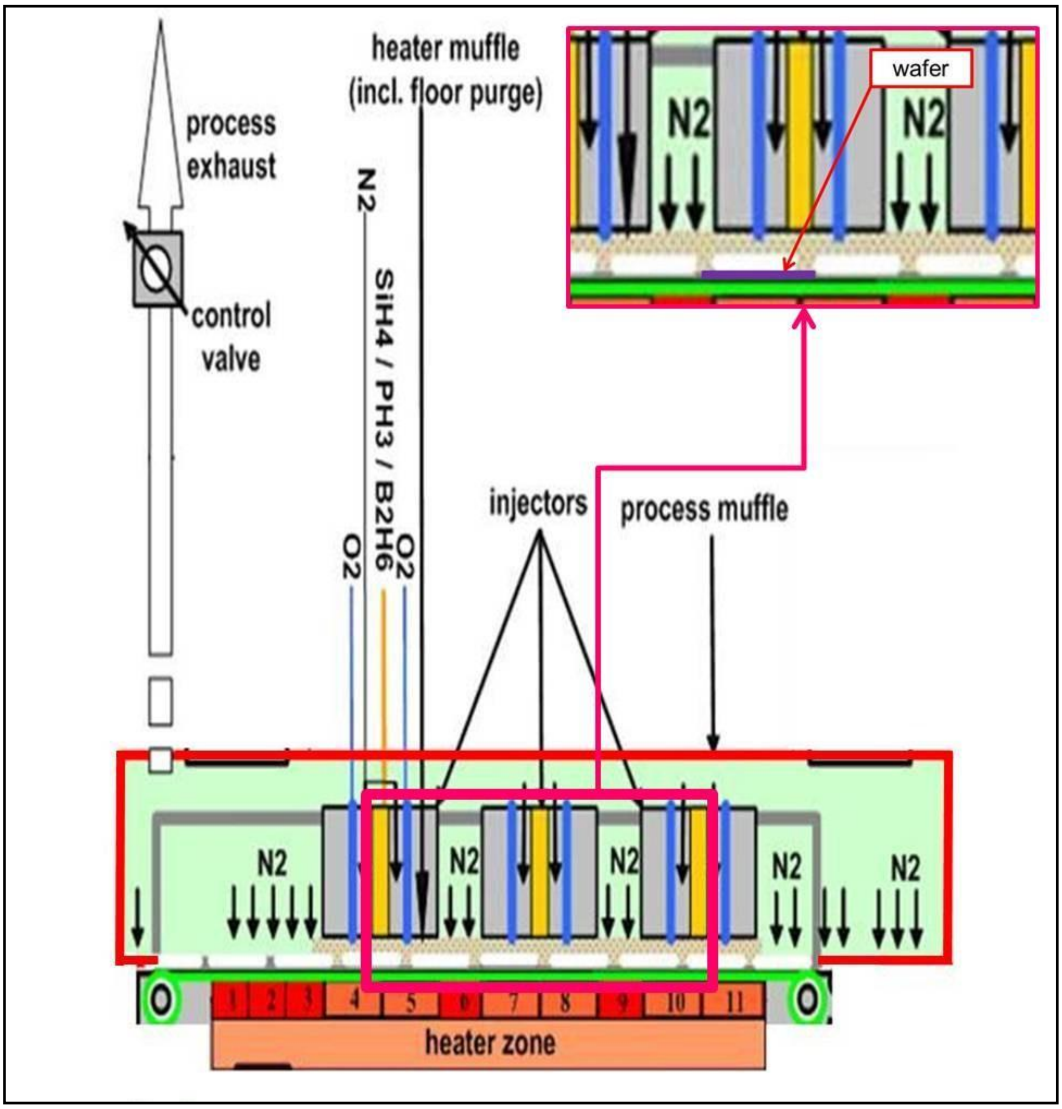
heater muffle
(incl. floor purge)
process
exhaust
control
valve
N2
SiH4 / PH3 / B2H6
O2
O2
wafer
N2
N2
injectors
process muffle
N2
N2
N2
N2
N2
N2
1
2
3
4
5
6
7
8
9
10
11
heater zone

Figure 27: Schematic image of the “process muffle” of a Watkins Johnson applied for AP-CVD processes.

During processing the wafer runs into the process muffle while being placed on the process belt. The wafer is preheated by the heater source (zone 1, 2, 3) whilst it is purged and shielded against the atmosphere by the N_2-curtain. The injectors have three exhalation chambers or zones: in the middle zone streams the mixture of process gases, SiH_4 with PH_3 and B_2H_6, both diluted in N_2, while the O_2 is streaming in the outer zones.

In order to achieve an ideal surface coating that is free of particles, the concentration of the reactant and dilutent gases, the O_2/silane ratio, the N_2-curtains as well as the extraction system have to be keenly adjusted.

6. Investigated CVD Films

The INFINEON Company Villach produces and provides large offer of various chips and devices based on several different technologies, all of them involving a large number of processes, also within the range of CVD. For this reason, only some selected sample lots have been studied during this master thesis, with respect to the adhesive properties and adhesion quality of the chosen thin films.

While choosing the sample lots, great attention was payed to explore process steps being essential for most, or at least many manufactured products, on the one hand, and on the other hand to explore fundamental physical as well as chemical phenomena that could affect adhesion, which possibly might occur during the particular process flow.

These aspects finally lead to the four sample batches covering several process groups, as well as product types:

- Boron and phosphorous doped silicon glass (BPSG) on silicon processed on different machinery
- Copper-nitride interface (CuNIT) on a product-specific substrate with varying roughness of the copper surface
- Silicon nitride (SNIT) films on assorted product-related oxide substrates
- Amorphous hydrogenated nitrogen-doped Carbon (a-C:H:N) affected by the substrate and the pre-deposition plasma treatment

6.1 Boron and Phosphorous doped Silicon Glass (BPSG) on Silicon processed on different Machinery

The purpose of this lot is to find a suitable alternative to the Watkins Johnson, applying AP-CVD, for depositing BPSG films at low doping levels. In the past such low-dopant films processed on a Centura at sub-atmospheric conditions (SA-CVD) have shown cracks as a certain film thickness was exceeded. Therefore people were interested in whether the susceptibility to cracks is influenced by the adhesion of the film to the substrate, and if any differences in adhesion arise for films deposited on a Centura or for those from a Watkins Johnson.

For this lot BPSG films have been deposited directly onto bare 6’’ silicon wafers. This film stack is schematically depicted in figure 28.

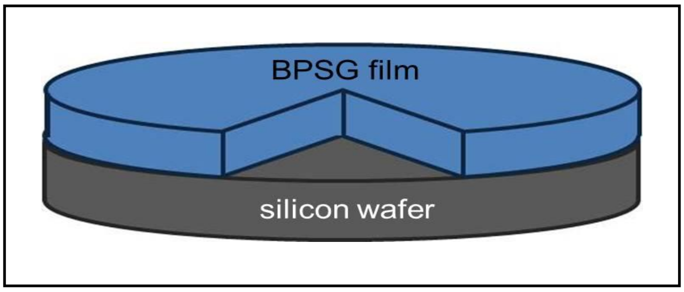

Figure 28: Film stack of boron and phosphorous doped silicon oxide on a bare silicon wafer.

Moreover, the BPSG films have been processed with different CVD equipments, applying different types of CVD, with the same film thickness, but with different doping levels of boron and phosphor. After the deposition process some wafers have been annealed in the furnace at 975°C for 20 min, in a N_2+O_2 atmosphere. The sample specifications are summarized in table 4.

Table 4: Sample specifications – BPSG on different equipments.

Cent . . . Centura
WJ . . . Watkins Johnson
ToD . . . Type of Deposition
SA-CVD . . . Sub-Atmospheric CVD
AP-CVD . . . Atmospheric Pressure CVD

dop. lev. . . . doping level [%]
B . . . boron
P . . . phosphor
film th. . . . film thickness [nm]

equipment	**ToD**	**dop. Level**		**film th.**
		B	*P*	
Cent	SA-CVD	1,0	2,7	1800
Cent	SA-CVD	2,3	2,7	1800
WJ	AP-CVD	1,0	2,7	1800

6.2 Copper-Nitride Interface (CuNIT) on a product specific substrate with varying roughness of the copper surface

The purpose of investigating this film stack, as shown in figure 29, was to analyse the adhesion of a PE-CVD silicon nitride film on a copper substrate, which has been processed under different sputter-powers leading to a different surface structure and also different magnitudes of film stresses – the higher the power, the higher the film stress.

At the beginning of the in-situ sputter process (TiW film and Cu film) the surface of the bare 8'' silicon wafer was sputtered and thereby cleaned with Ar-atoms. Afterwards a 100 nm TiW film and the 500 nm Cu film, processed at different powers ranging from 2 kW to 6 kW, always increasing by 1 kW, were deposited. Finally the 800 nm silicon nitride film was deposited during a PE-CVD process.

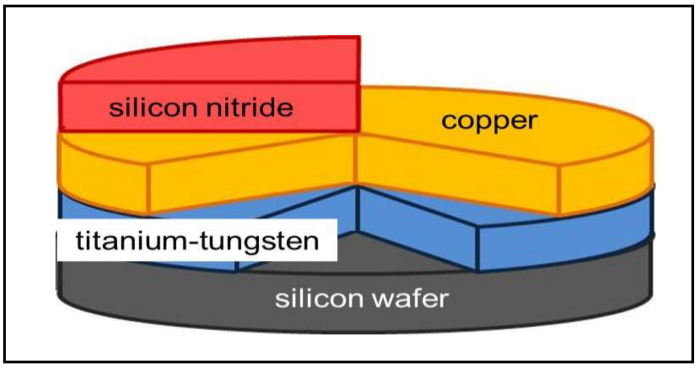

Figure 29: Film stack of the Copper Nitride showing the thickness of each deposited film.

The great intention in semiconductor industry is to use copper instead of aluminium for upcoming technologies and new high power devices, as copper has by far the better electrical properties, especially the high electric conductance makes this material that interesting.

With the help of this sample lot the results gained with the pull-off test and the tape test should be compared to each other to find out if there is any agreement between them.

6.3 Silicon Nitride (SNIT) Films on assorted product-related Oxide Substrates

The main reason for processing and investigating this sample lot was a task force on the high-holtage IGBT (insulated gate bipolar transistor) where problems concerning the adhesion of PE-CVD silicon nitride on DLC films (diamond-like carbon) and on various oxide films have come up. Therefore this series of experiments was aspired to study the adhesion of SNIT on various substrates, as they appear in recent product types, with respect to the influences of the atmosphere predominating inside a typical cleanroom at INFINEON Villach.

For this lot the SNIT film (1800 nm, PE-CVD) has been deposited on the following substrates:

- bare 8'' silicon wafer
- 850 nm EOX film
- another 1800 nm SNIT film
- 1400 nm USG
- 1600 nm PSG
- 910 nm BPSG – annealed
- 1350 nm BPSG – annealed
- 850 nm BPSG – annealed

Figure 30 shows the film stack of the samples, where the SNIT film has been deposited on an oxide-film, which has been deposited on a bare silicon wafer beforehand.

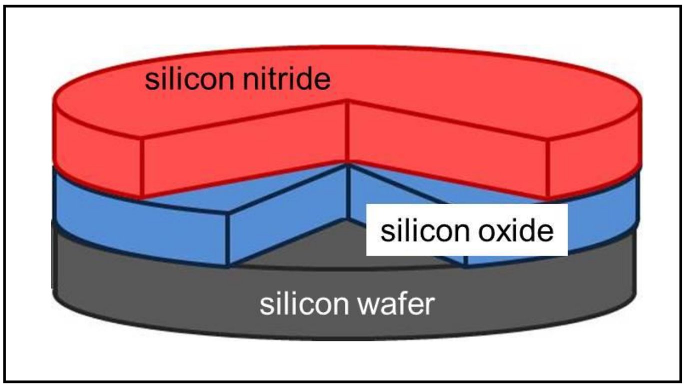

Figure 30: Film stack of Silicon Nitride on the subjacent oxide film.

All the specifications of the films processed and treated for this lot are shown in table 5 on the following page.

Table 5: Specifications of the substrate material and substrate films of Silicon Nitride.

sub . . . substrate
ToD . . . Type of Deposition
dop. lev. . . . doping level [%
B . . . boron
P . . . phosphor
film th. . . . film thickness [nm]
spec. treat. . . . specific treatment of the substrate film before the topmost SNT film was deposited

sub	equipment	ToD	dop. level		film th.	spec. treat.
			B	*P*		
silicon wafer	as received, ~700 µm					stored 3 weeks in cleanroom
silicon wafer	as received, ~700 µm					none
EOX	vertical furnace	LP-CVD			850	stored 3 weeks in cleanroom
EOX	vertical furnace	LP-CVD			850	none
SNIT	P5000	PE-CVD, silane			1600	stored 3 weeks in cleanroom
SNIT	P5000	PE-CVD, silane			1600	none
USG	P5000	PE-CVD, TEOS			1400	none
PSG	P5000	PE-CVD, TEOS		4,5	1600	none
BPSG	Producer	SA-CVD	4,0	4,9	910	annealed, 900°C, 30 min
BPSG	Producer	SA-CVD	1,8	2,7	1350	annealed, 975°C, N_2+O_2 20 min
BPSG	Producer	SA-CVD	1,8	2,7	850	annealed, 890°C + 1000°C, 40 min + 10 min

6.4 Amorphous hydrogenated nitrogen-doped Carbon (a-C:H:N) affected by substrate and pre-deposition plasma treatment

Though this fourth and last sample lot is not really a dielectric film, an a-C:H:N film shows a similar low electrical dynamic conductance as typical dielectric films but these a-C:H:N films establish electrostatic discharges ending up in electrostatic space-charge regions.

For technological aspects a-C:H:N films are that important because they are used as gap-definition layers required for the D-Sound technology being the basic concept for a small microphone. This tiny microphone is the, by far smaller follower of the piezo microphone and it is fabricated on silicon wafers applying current methods of semiconductor technology and semiconductor manufacturing processes. Figure 31 schematically depicts the brief setup of such a microphone processed according to the mentioned D-Sound technology. [25]

It has to be mentioned that the detailed setup and components of the D-Sound are parts of a confidential, company-internal project so no further information could have been provided to be included in this thesis.

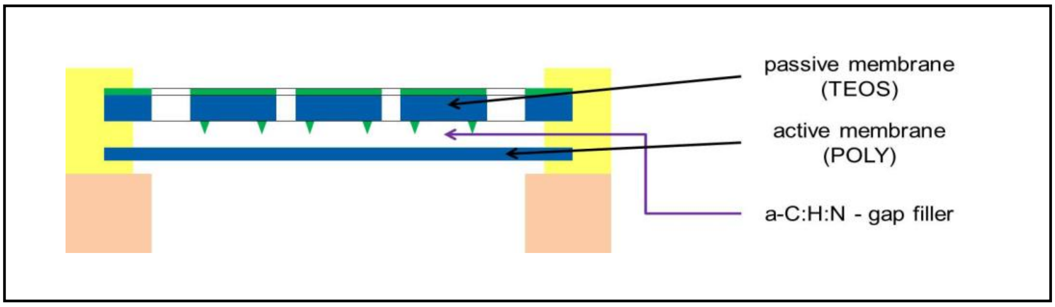

Figure 31: Schematic depiction of the D-Sound microphone, including the active and passive parts. The purple arrow indicates the gap, where the a-C:H:N film has been removed.

For this microphone the substrate is made up of poly-silicon processed inside a furnace tube (short: POLY) and the active and non-active membranes are TEOS. Colleagues from the department of Technology Development came across a problem that has been verified during processing: the a-C:H:N film did not adhere to the subjacent POLY film that well. For this reason one thought about a split plan for exploring the adhesion a-C:H:N, as-deposited or tempered, on two different substrates, POLY and TEOS deposited inside a furnace tube, including different plasma treatments. [26] The split plan with all specifications and film treatments is shown in table 6.

Table 6: Split plan for the a-C:H:N film on POLY or TEOS including different plasma pre-treatments and different post-deposition treatments.

sub . . . substrate of a-C:H:N film	p-treat pre dep . . . plasma treatment before deposition of a-C:H:N film
bg treat . . . post-treatment of the substrate	post treat . . . treatment of the completely processed a-C:H:N film

test	wafer	sub	bg treat	plasma treat pre dep			a-C:H:N dep	post treat
					plasma stop			
				no plasma	N_2O	NH_3		
pull-off test	1	POLY	annealing 700°C inert	**x**			**deposition of the a-C:H:N film target thickness ~ 1 µm**	**as-deposited**
	2				**x**			
	3					**x**		
	4	TEOS	annealing 900° inert 30 min gentle	**x**				
	5				**x**			
	6					**x**		
	7	POLY	annealing 700°C inert	**x**				**leveling at 700°C annealing at 780°C**
	8				**x**			
	9					**x**		
	10	TEOS	annealing 900° inert 30 min gentle	**x**				
	11				**x**			
	12					**x**		
tape test	13	POLY	annealing 700°C inert	**x**				**as-deposited**
	14				**x**			
	15					**x**		
	16	TEOS	annealing 900° inert 30 min gentle	**x**				
	17				**x**			
	18					**x**		
	19	POLY	annealing 700°C inert	**x**				**leveling at 700°C annealing at 780°C**
	20				**x**			
	21					**x**		
	22	TEOS	annealing 900° inert 30 min gentle	**x**				
	23				**x**			
	24					**x**		

Another intention of these experiments was to find an ideal plasma pre-treatment for the a-C:H:N film on POLY and on TEOS. The expectations of a colleague should have been verified as he stated the following: *if there is any oxygen at the interface between the substrate and the a-C:H:N film, the following annealing process leads to problems with adhesion due to enhanced chemical reactions of the oxygen with the carbon.* [27]

Originally it was expected to study more plasma pre-treatments, but as the adhesion should have been proven with the Pull-Off test as well as with the Tape-Test one would, according to all other split variations, finally end up with 8 additional wafers for every single plasma treatment.

As this would definitely have exceeded the feasible range, we left the split plan at the depicted state, whereas every sample shows a similar sequence of deposited films, depicted in figure 32 below.

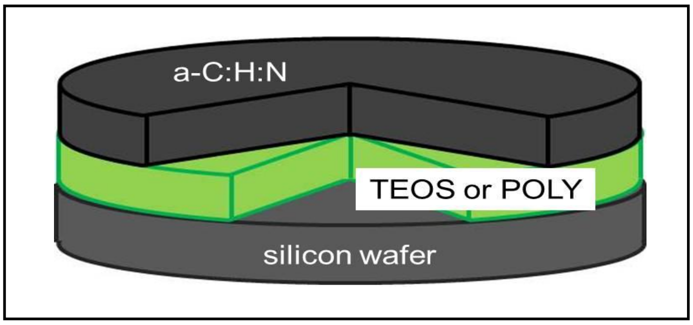

Figure 32: Film stack of a-C:H:N on either furnace POLY or furnace TEOS.

7. In-line Measurements and Processes

The determination of the several properties of the various deposited films - film thickness, uniformity of the film, film stress and, in case of doped silicon oxides, the doping level of boron and phosphor – require multiple measurements and measuring devices, before the samples were tested with respect to the adhesion of the applied thin films. The continuous investigation of the film parameters should also serve as inspection and survey to be sure whether the parameters of the deposited films agree with the corresponding process programs, which were run to fabricate or to aftertreat the films of interest.

But not only a further deposition process can influence or even change the properties of the already deposited substrate film, these parameters can strongly be influenced by annealing processes, which have been applied to several of the investigated film stacks.

Therefore this chapter shall briefly describe the functional principle of the applied measuring apparatus, as well as the basic principle of a typical annealing process.

7.1 Opti-Probe: Film Thickness Measurements [28]

The Opti-Probe 3290 is a fundamental and likewise important measuring device used for characterizing thin films by measuring the film thickness and also the uniformity of the film. The film thickness is required for further measurements like for determining the film stress or when one is interested in the magnitude of the boron or phosphor content in the doped film. In order to measure the required film parameters that precisely this tool applies three different techniques: the Beam Profile Reflectometry (BPR), where the reflectivity is dependent on the incident angle; simple Spectrometry, where the reflectivity depends on the wavelength of the incident beam of linearly polarized light; and Ellipsometry, detecting changes in the state of polarization.

Beam Profile Reflectometry is the core technology of an Opti-Probe as it affords to gain more information about the investigated sample from a transparent film stack, compared to ellipsometry or spectrometry alone. For ellipsometry linearly polarized monochromatic light irradiates onto the wafer at a given angle. The beam of light gets elliptically polarized by the thin film or film stack, is reflected and subsequently analysed by a detector, whereas for spectrometry the reflectivity of the film or film stack is measured at constant wavelengths of the incident light. On fully equipped Opti-Probes the system can use all three of the mentioned technologies to obtain reproducible results for film thickness, the average, the range and the uniformity of the film thickness, whose valid range is determined by the particular process program files, and furthermore the Goodness of Fit (GOF), from the executed measurements.

The measuring device uses a loading system for wafers with a diameter of either six or eight inches, placing the wafers from either cassette to the test site with a robot arm. To ensure that the measuring inaccuracy stays as low as possible, certain monitoring programs where introduced, depending on the material under investigation, being adapted to the particular film. During the actual measurement 9 points on the wafer, arranged in a Z-shaped pattern are measured, using the obtained values to calculate: the mean value (*equation 20)*, the range (*equation 21*), the uniformity (*equation 22*), resembling the maximum percental deviation of the measured values from the mean value, if required the refractive index, and the Goodness of Fit (GOF).

$$Mean = \frac{1}{9}\sum_{i=1}^{9} x_i = \frac{x_1 + x_2 + ... + x_9}{9} \tag{20}$$

$$Ran = x_{max} - x_{min} \tag{21}$$

$$Unif = \frac{Ran * 100}{2 * Mean} \tag{22}$$

The GOF is a measure of the fit between the measured value and a calculated parameter, and it is preferable to be closer to 1.0 but it may depend on either the quality of the film layers, the surface quality and cleanliness and/or on the inhomogeneous bulk material.

7.2 MX 204: Film Stress Measurements [29]

The Eichhorn+Hausmann measurement device for stress measurements is suitable for wafers with a diameter of 6 or 8 inch, whereas the device is equipped with a particular mounting, adapted to the wafer size, where the wafer is placed and moved into the device.

In front of the wafer geometry station there is a wafer centring station (both depicted in figure 33), on which the operator lays down the wafer he wants to measure. Four posts with conical ends centre and support the wafer. When the operator has pressed the button on the front panel of the instrument to start the measurement, these posts retract and lay down the wafer on the vacuum chuck bars of the drawer. Provided the chuck has clamped the wafer, an electric motor pulls the tray into the geometry station and lowers it there in order to lay down the wafer on the lower probe plate. [30]

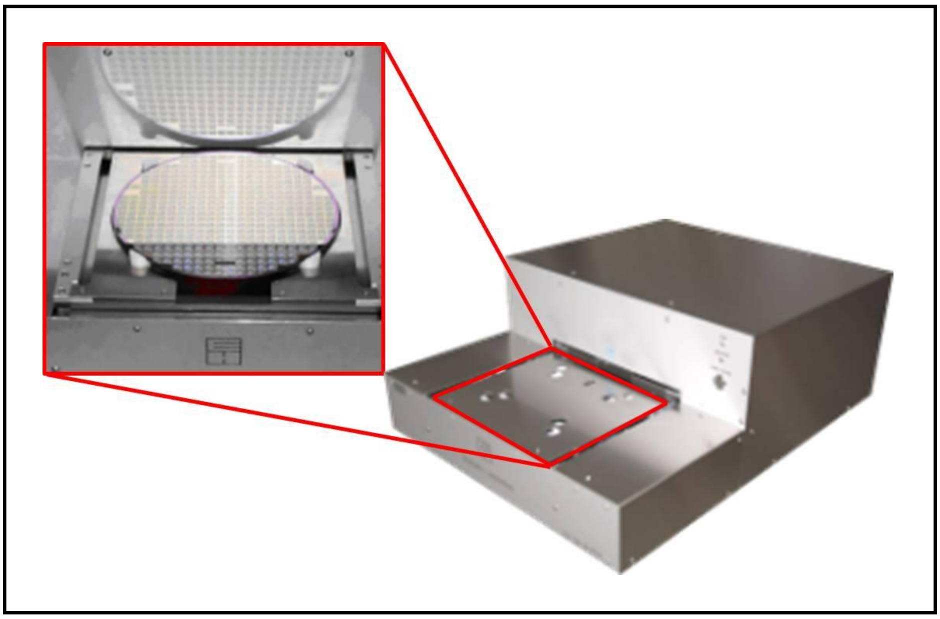

Figure 33: Wafer geometry and wafer centring station of the E+H MX204 measuring device, determining bow, stress and warp. After [30]

For more specific applications this instrument is equipped with a special geometry program evaluating the stress using the wafer bow. The obtained results for the wafer bow, determined before and after a film deposition process which induces the stress, lead to a global stress information. By using all the received local values for warp and thickness (obtained by using the Opti-Probe) the special program is able to compute all the local stress information – centre stress, maximum stress and average stress.

The bow itself is determined by capacitive sensors being suitable for conducting materials only. Every single measurement point in a MX-204 is made up of a pair of such capacitive sensors measuring an upper and a lower distance to the focus point. This focus point halves the distance between the upper and the lower sensor which always stays constant without a wafer. When a measurement is recorded with a plane wafer the upper and the lower distance between the wafer and the upper and the lower sensor won't be constant any longer. So an average plane between all measurement points will be interpolated and then being used as reference for following measurements.

Actually stress is not the result from just one single measurement rather than the result of two comparative measurements performed before and after the deposition process. To determine the wafers stress characteristics the E+H device employs similar evaluation procedures:

1. Two local warp values determined at the same sensor position before and after the deposition process inducing the stress, lead to one “delta warp value”
2. For this procedure a delta warp value triplet is used to determine the curvature radius of the wafer

The example in figure 34 shows such a triplet of local delta warp points which are used to determine the curvature radius R, whereas the depicted distances d_1 and d_2 might differ in size. [31]

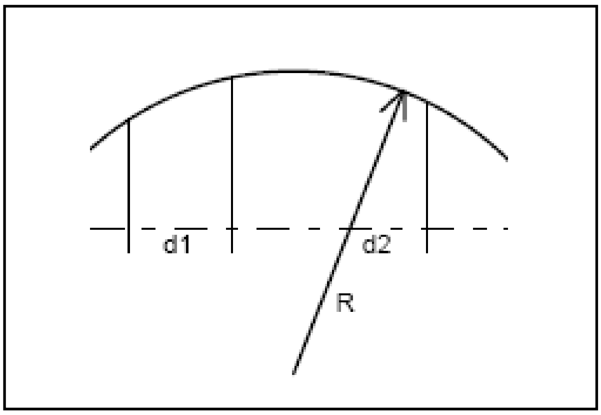

Figure 34: Triplet of local delta warp points used to determine the film stress.

The stress with the E+H gauge is then calculated by using a global stress formula:

$$\sigma_f = \frac{1}{6 * R} * \frac{E}{(1-\nu)} * \frac{t_s^2}{t_f} \tag{23}$$

where σ_f is the film stress [MPa], R is the radius of curvature, t_s is the substrate thickness, t_f is the film thickness and $E/(1-\nu)$ is the substrate elastic constant. Within the last expression ν is the Poisson ratio being the negative ratio of transverse to axial strain and E being the Young’s modulus.

7.3 RFA-2: Doping Level

For determining the doping level of boron and/or phosphor in PSG or BPSG a measurement device operating according to the principle of X-ray fluorescence spectroscopy (XRF spectroscopy) is applied, whereas just surface-near ranges of the investigated film are considered. The basic principle of this type of analysis is to shoot X-rays on a wafer so that it reacts by emitting X-rays (in an atom, the excited electrons emit X rays by going back to a lower electron level). These X-rays are oriented with a collimator and reflected on a OVO-B crystal (Mo-B_4C) suitable to detect boron and phosphor. The reflection angle depends on the wavelength of the X-ray, so consequently from the nature of the atom emitting it. For these measurements the complete system has to be under vacuum.

The hardware components of the RFA-device, as well as the optical path of the X-rays are shown in figure 35. [32]

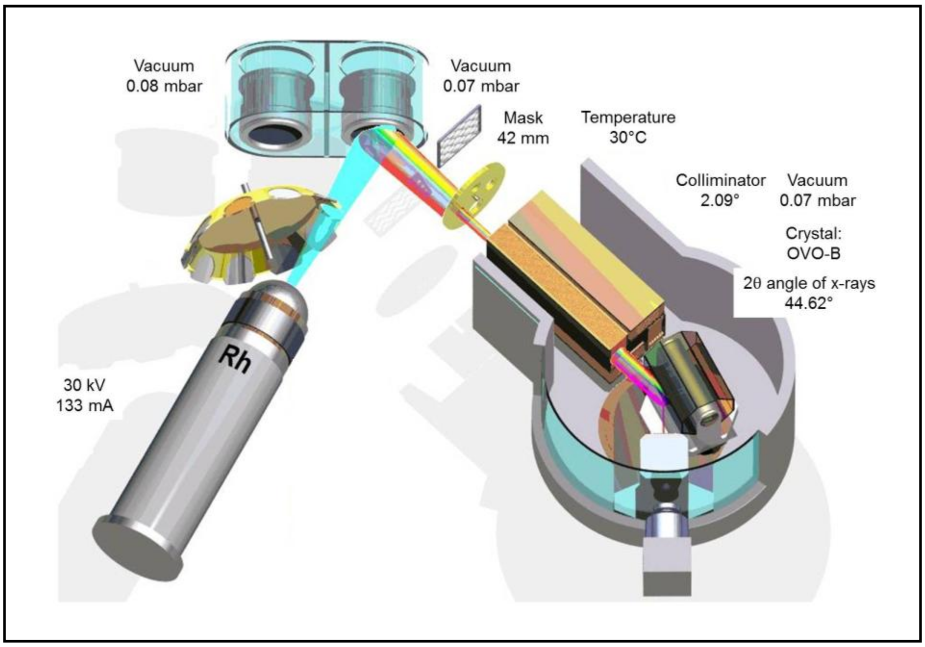
Vacuum
0.08 mbar
Vacuum
0.07 mbar
Mask
42 mm
Temperature
30°C
Colliminator
2.09°
Vacuum
0.07 mbar
Crystal:
OVO-B
2θ angle of x-rays
44.62°
Rh
30 kV
133 mA

Figure 35: RFA hardware components including the optical path of the X-rays. [32]

7.4 Annealing and Furnace Processes

After a multiplicity of deposition processes the deposited films are subjected to annealing processes executed in furnaces designated for certain purposes. The intention of such annealing processes is to increase the density of the deposited films resulting in a slight decrease in film thickness, the reduction of thermal stresses induced by the deposition process itself, eliminating defects, and to bake out undesired compounds from the film which have arisen during deposition. Therefore the wafers are treated inside the furnace at appointed temperatures, typically at 600°C to 900°C for a defined period of time, whereupon the dominating atmosphere inside the furnace strongly depends on the material to be annealed. Another effect that can be monitored after an annealing process is a change of the doping level of boron and/or phosphor detected with the RFA gauge. Annealing processes are furthermore applied to doped silicon substrates, where the silicon is furnished with dopant materials during a preceding process step. The doped atoms are implanted at interstitial sites inside the lattice of the silicon substrate. To achieve an improved electrical conductance of the silicon substrate it is annealed. During this process step the lattice defects which have been induced during the implantation process, are reduced.

In this context one has to insure a carefully controlled environment to avoid the dissociation and decomposition of the annealed semiconductor material, what might occur when heated above certain risen temperatures. This can be achieved by either controlling the pressure of the vapour that surrounds the semiconductor material, inducing an equilibrating environment at the surface of the treated material, or by encapsulating the material by an interface barrier. (compare [33])

8. Applied Testing Methods

Based on the knowledge about the basic principles of the current and well established mechanical methods, which are applied to investigate the adhesion of a deposited film to the substrate or the subjacent film, this chapter will specify the two testing methods, which have been applied during this thesis. Beside the used apparatus also the procedure of preparing the samples and executing or improving the particular test will be discussed.

8.1 Adhesion Pull-Off Test

The apparatus used for executing the pull-off tests, resembling a quantitative testing method, the PosiTest AT-M Manual is a simple, durable and versatile device which offers several advantages: the pull rate indicator allows the operator to easily monitor and adjust the pulling rate according to international test methods, the tester automatically calculates pressure based on the dolly size, which can simply be selected directly at the device and the calibrated, industrial pressure sensor ensures continued and certified accuracy (± 1%), just to mention some. In figure 36 the adhesion tester and its most important components during application are shown, including the LCD display (1), the pump handle (2), the actuator handle (3) and actuator assembly (4), and the quick-coupling (5). [34]

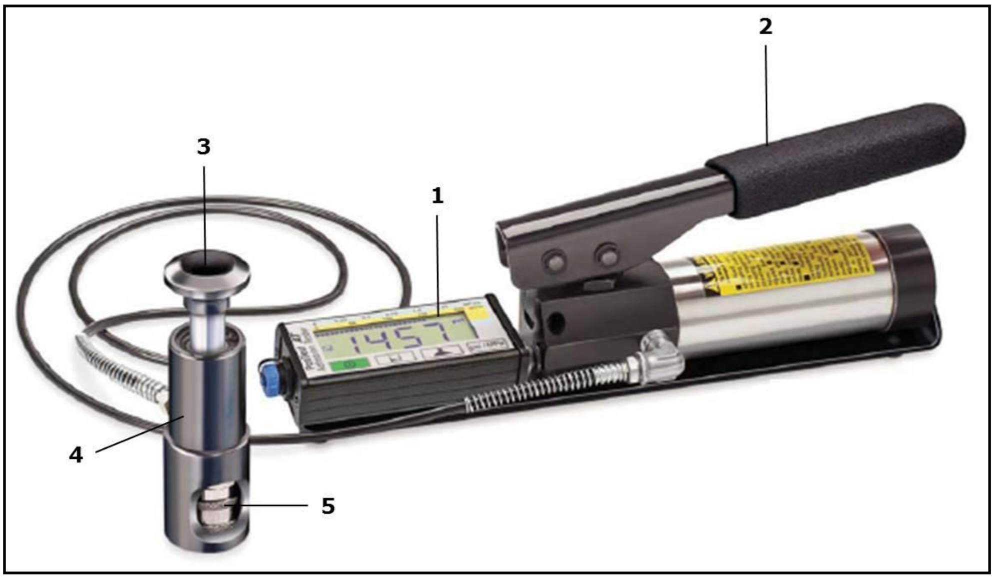

Figure 36: Image of the PosiTest AT-M Manual adhesion tester.

The most essential feature, simultaneously being greatest the advantage of the PosiTest adhesion tester with respect to the operation and execution of the test is its self-alignment feature. During testing an unequal pulling force due to uneven adhesive bond lines and coating surfaces or non-uniformly applied adhesive or glue can result in unexplainable and random results. In order to obtain more repeatable and meaningful values characterizing the adhesion of the film towards the substrate, a pulling force being applied uniformly across the surface being tested is compulsory. Therefore the self-aligning, quick-coupling actuator and spherical articulating dolly head, shown in figure 37, [34] enables the desired uniform distribution of the pulling force over the surface being tested, preventing a one-sided pull-off, while executing the test.

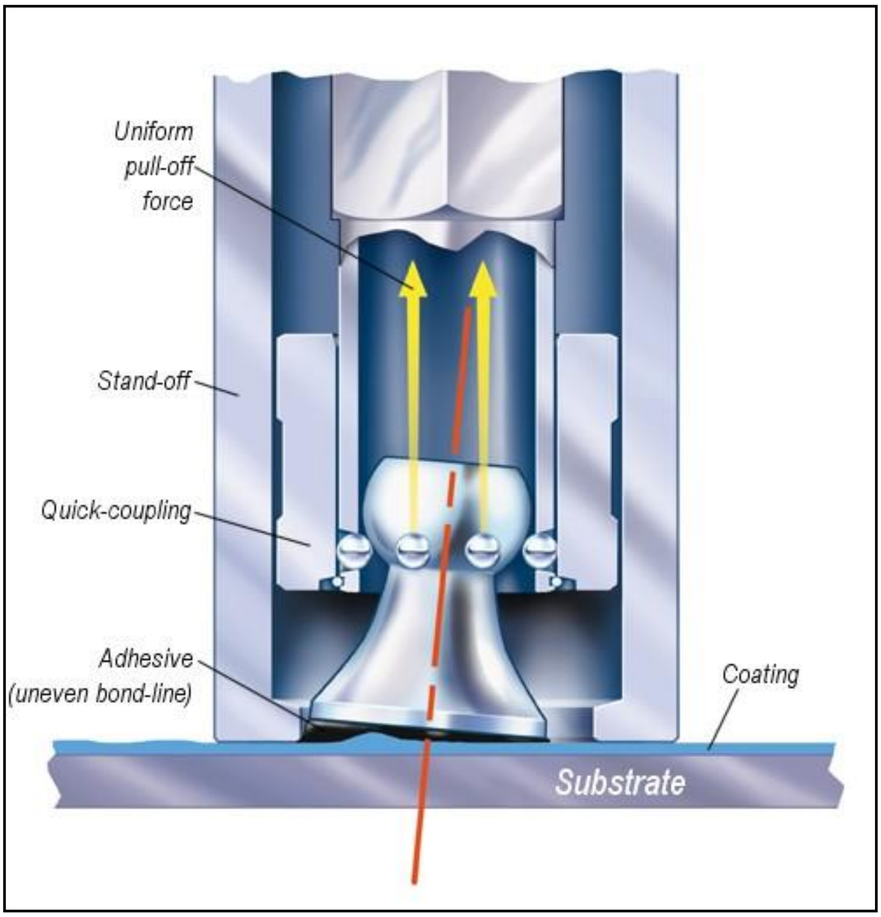

Figure 37: Image of the quick-coupling system of the PosiTest showing the main feature of the self-alignment system.

To get sure that the obtained results from the PosiTest are meaningful and reproducible the samples to be tested have to be prepared properly according to a certain procedure. [35]

- An aluminum plate (AlMgSi) with given dimensions (250*250*5 mm) whose surfaces were blasted with corundum (graining ~70 µm) was heated up to 80°C by using a heating plate (yellow line, yellow MAG HP 10, temperature range: 50-500°C, 260*260 mm heating plate, compare figure 38)
- preparing the adhesive, ARALDITE 2011 – a 2-component glue based on epoxy resin; mixing the resin and the hardener in a 1:1-ratio
- preparing the wafers
    - scarifying the wafer with a diamond cone and breaking it into 30*30 mm big samples
    - blowing the splitters away with compressed air
    - cleaning the upper and bottom surface with acetone or isopropanol using a cleanroom cloth
- preparing the dollies
    - roughening the rear side of the dolly with ordinary sand paper
    - cleaning the rear side with acetone or isopropanol
    - drying the rear side by placing it on a dry cloth or on the heated aluminum plate
- cementing the sample pieces onto the aluminium plate
    - adjusting the prepared glue onto the rear side of the sample with a wooden spatula
    - placing the sample on the aluminium plate
- cementing the dolly onto the sample piece
    - adjusting the glue onto the roughed rear side of the dolly as uniformly as possible
    - placing the dolly in the middle of the sample piece
- curing the glue for 2 hours at the pre-adjusted 80°C
- after the cure time has elapsed, switching off the plate and awaiting until the prepared samples have cooled down to room temperature

The completely prepared sample stack placed on the heating plate resembles the schematic drawing depicted in figure 38.

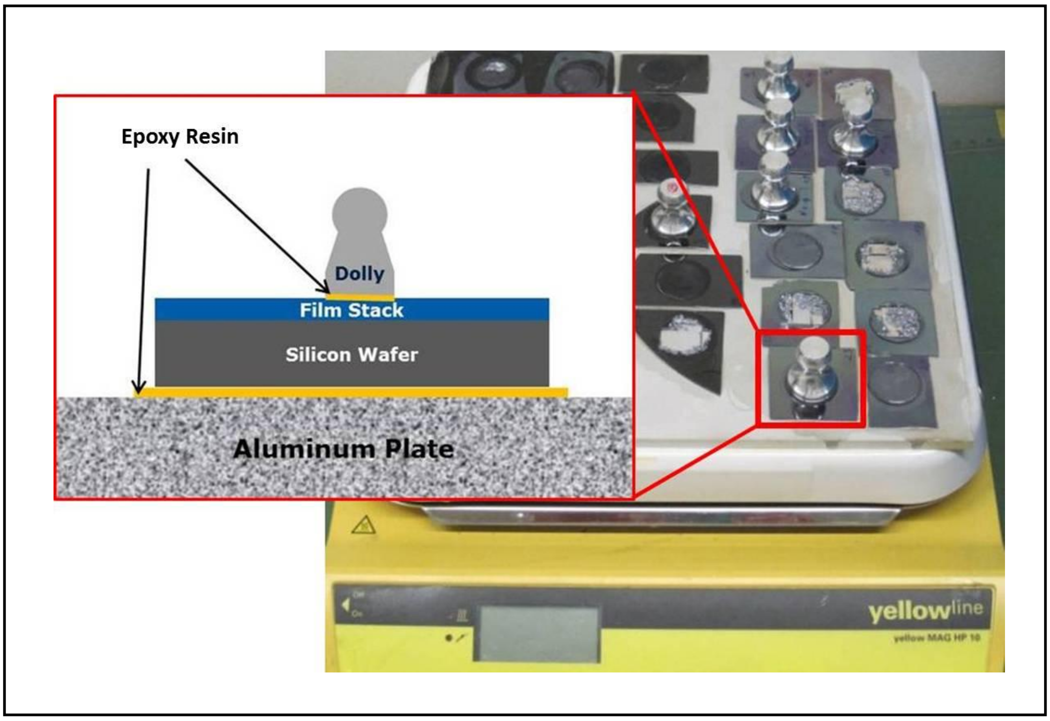

Figure 38: Schematic drawing of the completely prepared sample stack placed on the heating plate.

While preparing the samples for the pull-off test one has to mind that the glue gets thin fluidic when heated up so the whole sample setup might float across the aluminium plate or the dolly moves around or even off the piece of wafer. Another very important thing is the thickness of the glue when it is adjusted to the rear surface of the wafer piece or the doll as, according to the specifications sheet of the resin the greatest lap shear strength is achieved for a glue layer being 0.05-0.10 mm thick. For the applied cure time the glue should withstand a lap shear strength ranging from 24 MPa to 28 MPa. [36]

Unfortunately the recommended glue layer thickness could hardly be achieved as the glue was adjusted to the rear side of the dollies manually. By using a micrometre calliper the effective thickness of the glue film was found to range at 0.03 ± 0.01 mm. But this thickness is an estimated value because during measuring the thickness of the glue one is dependent on sites on the rear side of the dolly where there are glue residues. And, furthermore, the deviation of the determined values corresponds to the measurement inaccuracy of the calliper.

To execute the pull-off test with the prepared samples which have cooled down to room temperature one has to proceed and handle the adhesion tester in the manner explained in the user manual including the following steps: [37]

- Ensure the pressure release valve on the pump is completely open
- Push the actuator handle completely down into the actuator assembly. Place the actuator assembly over the dolly head and attach the quick-coupling to the dolly by reaching through the holes of the actuator assembly and lifting the quick-coupling.
- Close the pressure release valve on the pump completely
- As required, verify and adjust the dolly size by pushing the “dolly-button”. Select the pressure units by pressing the “psi/MPa-button”. The instrument then will maintain these adjustments after the “on/off-button” has been pressed.
- It is very important to zero the instrument BEFORE pumping and pressing the “on/off-button”. This prepares the instrument for the next reading by clearing the display and zeroing the instrument.
- Prime the pump slowly until the displayer reading approaches the priming pressure, which is dependent on the size of the used dolly. This priming pressure is the point that the instrument starts calculating and displaying the applied pull rate. This is also the pressure at which the ability to store certain readings is enabled.
- For optimum results, prior to exceeding the prime pressure, return the pump handle to its full upright position and then complete a single stroke at the desired pull rate until the actuator separates the dolly from the coating.
- As desired, readings may be stored by pressing the “disc-button”.
- Open the pressure relief valve and remove the dolly from the actuator.

This procedure was then repeated to execute all the many measurements, whereas the priming pressures for the applied dolly sizes are shortly summarized in table 7,[37] also including the maximum pull rates for every particular dolly size.

Table 7: Priming pressures and maximum pull rates according to the dolly diameter.

dolly size	**priming pessure**		**max. pull rate**	
	psi	MPa	psi	MPa
10 mm	400	2.8	10000	70
14 mm	200	1.4	6000	40
20 mm	100	0.7	3000	20

8.2 Tape Test

The tape test which has been applied during this master thesis, denoted to being a more qualitative or even comparative testing method compared to the pull-off test, was executed and graded according to a standardized procedure of the American Society of Testing Materials.
For this testing method, according to the ASTM International, Method Type B,[38] a lattice pattern with a well-defined number of cuts in each direction has to be made in the film to the substrate, a pressure sensitive tape is applied over this lattice and then removed. The adhesion is evaluated by comparison with descriptions and illustrations.

In detail, the preparation of the sample for this testing method is executed in the following way:

- Prepare a lattice pattern with six or eleven cuts with a spacing ranging from 1 mm to 5 mm depending on the thickness of the coating
- Inspect the lattice pattern and the cutting edges, brush away any flakes or ribbons
- Remove two complete laps of the utilized tape, then remove a piece of tape at a length of about 75 mm
- Place the centre of the tape over the prepared and clean grid, smooth it into place by hand and then rub it firmly with the eraser on the tip of a pencil
- Within ~90 sec rapidly (not jerked) remove the tape back upon itself at an angle as close to 180° as possible
- Inspect the grid area for removal of the coating from the substrate and rate the adhesion in accordance to the scale illustrated in table 8. For the evaluation one has to consider the smaller areas to be more heavily affected by delamination as the larger ones because of the different area-to-edge ratio.
- Afterward repeat the test in two other locations on each test panel

Concerning the reproducibility of the tape test two results obtained either at different locations on the sample panel or by different operators should be considered suspect and not significant if they differ by more than two rating units. For rating the adhesion a light microscope – Nikkon ECLIPSE L200 – combined with a camera has been used.

Table 8: Classification of the adhesion test results.

P.A.R . . . percentage area removed

cross-cut area . . . surface of cross-cut area from which flaking has occurred for the defined number of cuts and adhesion range by percentage

classification	P.A.R	Cross-Cut area
5B	0% none	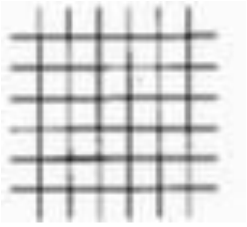
4B	less than 5%	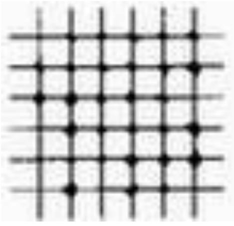
3B	5 - 15%	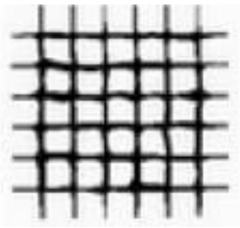
2B	15 - 35%	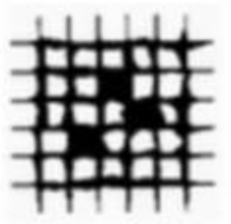
1B	35 - 65%	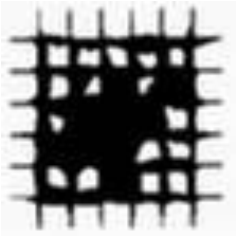
0B	greater than 65%	

Referring to the classifications from table 8, they can be also rephrased in words.

5B The edges of the cuts are completely smooth; none of the squares of the lattice is detached.
4B Small flakes of the coating are detached at the intersections; less than 5% of the area is affected.
3B Small flakes of the coating are detached along the edges and at the intersections of the cuts. The area affected is 5 to 15% of the whole lattice.
2B The coating has flaked along the edges and on parts of the squares. The area affected is 15 to 35% of the whole lattice.
1B The coating has flaked along the edges of the cuts in large ribbons and whole squares have detached. The area affected is 35 to 65% of the whole lattice.
0B Flaking and detaching is even worse than grade 1B.

Basically this test is most suitable to grade the adhesion of coating films on metallic substrates, when executed exactly in the described manner. For this purposes the number of cuts and especially the spacing in between is adjusted to the thickness of the tested coating. For coatings having a film thickness up to and including 50 µm the cuts should be spaced 1 mm apart, in case the coating thickness ranges from 50 µm to 125 µm the cuts have to be spaced 2 mm apart, and for all coatings whose thickness exceeds the 125 µm Method A, named X cut tape test is recommended.

To adapt this tape test to be suitable for our instant purposes of testing thin CVD films or stacks of such films, another type of lattice pattern had to be found, as well as a suitable way of cutting this pattern through the coating and slightly into the wafer. This intended purpose could then be accomplished by using a sawing pattern (figure 39), which has been successfully applied for such tests. Originally this sawing pattern has been invented for Transition Line Measurements (TLM) that are used to determine the electrical film resistance of back side metallisation films. For this sawing pattern, arranged on the particular wafer as depicted in figure 39, the lattice consist of 20 traces which are about 35 µm broad, 20 µm deep and are spaced apart as shown in the appropriate figure. [39]

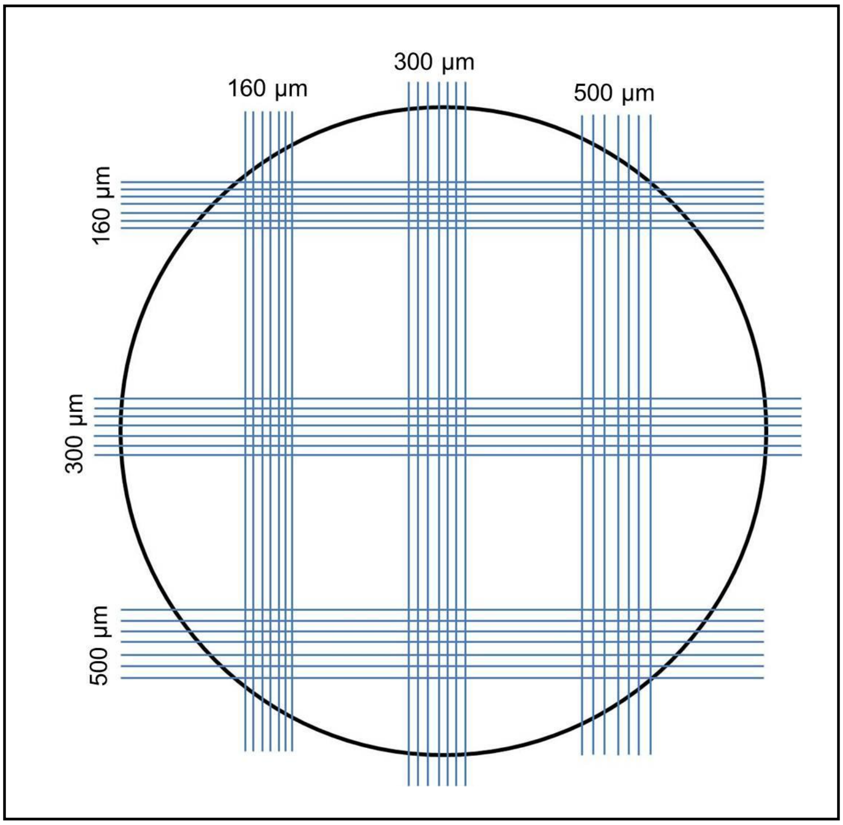

Figure 39: Illustration of the sawing pattern that has been used for the Tape Test showing the width of the single trace respectively.

8.3 Adjusting the Adhesion Pull-Off Test

In contrary to the tape-test, the results obtained from the pull-of test were not as satisfying as initially expected. The reason was the maximum shear strength or, in our instant case, the maximum strain to be applied with the adhesion pull-off tester, which has been tremendously limited by the utilized epoxy resin. For almost every sample the compound failed at the interface between the resin and the rear side of the dolly, which has just been roughed with sand paper.

So there have been two approaches for improving or adjusting this testing method by the following means:

- Looking for a new and better opportunity to roughen the rear side of the dolly and thereby increasing the essential bond area
- Altering and raising the maximum strength of the glue

Though it is recommended by the manufacturer of the PosiTest to use every dolly only once, a procedure had to be found to clean the rear surface by means of removing the completely hardened resin. In combination with the intention to roughen and increase the bond area of the dolly's rear side, the idea of blasting the lower surface either with corundum or with glass beads was considered by using different granulations: 70 µm for corundum, 70-100 µm for the glass beads.

In the face of improving the strength of the glue utilized up to now some research was engaged trying to find another adhesive being more suitable for our purposes or looking for a new way to preparing the samples for the pull-off test. As none of the considered glues has offered a higher strength as the present one, according to their specifications, a satisfying opportunity was discovered, namely changing the sample preparation by varying the procedure of curing the actual epoxy resin.

For this intended purpose the sample preparation has been preceded exactly as before, but from now on the resin was cured at 130-140°C for 35 minutes resulting in a guaranteed lap shear force of 30 MPa. Furthermore, the dollies which have been already used once, as well as some of unused dollies have been blasted with corundum and with glass beads to compare the obtained results during the following pull-off test. The first noticeable improvement was the improved shear strength of the epoxy resin, confirmed by the fact that the dollies with a rear side diameter of 20 mm could not be separated from the sample stack with the actuator anymore. The maximum displayed value for the applied pulling rate has been 23 MPa, being the limit for this dolly size. Thus, smaller dollies (14 mm and 10 mm lower surface diameter) have been utilized while preparing the test, also blasted with corundum or glass beads. A comparison of the gained results for the maximum applied strain with untreated dollies, corundum blasted dollies and glass bead blasted dollies is illustrated in figure 40. The displayed results are based on the measurements executed for the first sample lot, the BPSG from different CVD equipments.

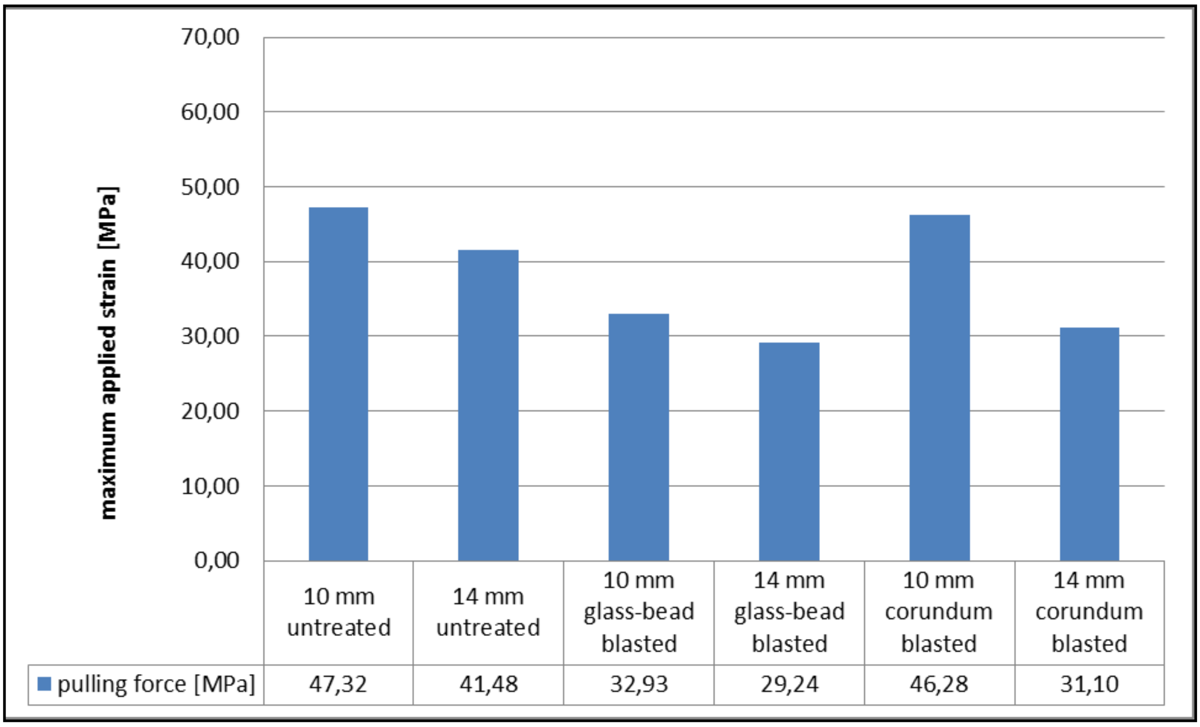

	10 mm untreated	14 mm untreated	10 mm glass-bead blasted	14 mm glass-bead blasted	10 mm corundum blasted	14 mm corundum blasted
■ pulling force [MPa]	47,32	41,48	32,93	29,24	46,28	31,10

Figure 40: Comparison of the maximum applied strain for differently treated rear sides of the utilized dollies.

Due to the improved strength of the adhesive and the application of smaller dollies the metering range of the adhesion tester could successfully be altered to higher magnitudes correlating to table 7. Furthermore, the method of blasting the rear sides of the dollies with corundum was found to be suitable for recycling the used dollies, and improving the strength of the interface between the resin and the dolly’s lower surface. For this reason the dollies with 20 mm rear side diameter have become inoperative because the achieved shear strength of the resin due to the improved curing procedure was too high to pull these dollies off with the actuator.

9. Measurement Results and Discussion

This section will deal with the four sample lots of different film stacks which have been investigated during this thesis. To begin with, the adhesion pull-off test had to be given a first trial with the boron and phosphor doped silicon oxide films on 6 inch wafers processed on different CVD equipments to find out about the potential and the limitation of the PosiTest apparatus. Beside the BPSG films, also the copper nitride samples have been used to adjust and improve this testing method for our purposes as good as possible. That's why the first puff-off tests for these two lots have been executed with all three available dolly-sizes and the tape test with the recently discovered sawing pattern has firstly been applied on the CuNIT and in addition to the other two lots processed on 8 inch wafers, the silicon nitride on various substrates as well as the amorphous hydrogenated nitrogen-doped carbon film on POLY and TEOS.

Before every single sample has been tested with respect to the adhesion of the deposited films to one another and towards the subjacent layer or substrate, all the in-line measurements introduced in chapter 7 were executed after every single process step and immediately before the adhesion tests. The circumstantial intention behind these in-line parameter measurements was to find out whether the adhesion can be associated with to high compressive or tensile stresses or not. This assumption, however, did not occur for any of the samples wherefore the tables including all these parameters can be found in the appendix and it will be referred to them if required.

For all the obtained results, especially for the pull of test, the values for the metered compound strength, as defined according to equation 2,

$$\sigma_C = \frac{F_m}{A_g}$$

will just be presented for the 14 mm and the 10 mm dollies in order to have comparable results for all the investigated samples.

9.1 Boron and Phosphor doped Silicon Glass on silicon

During the adhesion pull-off tests executed on these samples for low-dopant BPSG films the obtained adhesion by means of the measured compound strength, of the films to the substrate wafer (6 inch ground material) processed in a SA-CVD and an AP-CVD reactor (Centura and Watkins Johnson) should be compared to one another.

Before the actual sample wafers were processed, the correct amount of dilutent and especially reactant substances (TEB and TEPO) had to be found to achieve the expected doping levels for boron an phosphor (1.0%B / 2.7%P, respectively 2.3%B / 2.7%P) of the deposited films. After this calibration process 6 wafer for each doping level have been processed on the Centura, and another 6 wafers on the Watkins Johnson, with a doping level of 1.0%B / 2.7%P. As an additional widening of this experiment, two wafers from each group have been tempered inside a furnace tube at 975°C for 20 min in N_2+O_2 atmosphere with the intension to release thermal stresses in the deposited films and maybe detecting a difference of the metered compound strength.

A comparison of the values for the compound strength of the different sample groups obtained with different dolly sizes can be done by looking at figure 41 for the 10 mm dollies, and figure 42 for the 14 mm dollies.

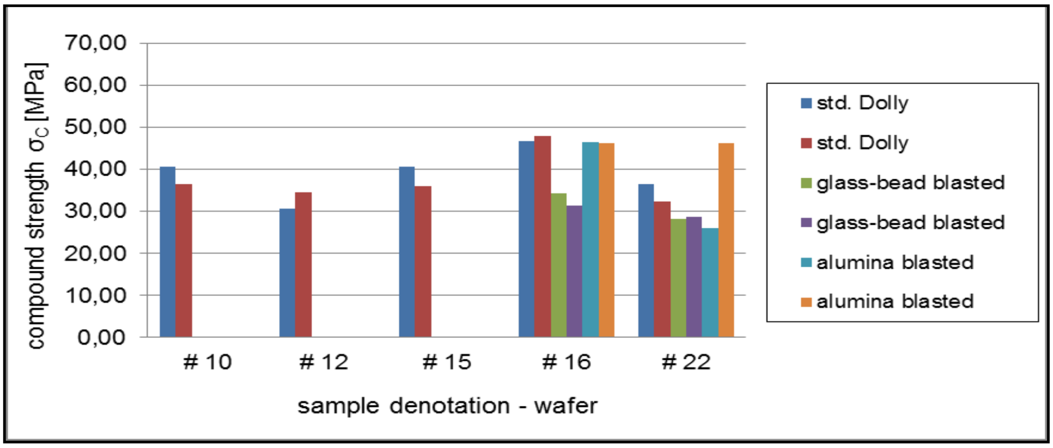

Figure 41: Compound strength for BPSG film obtained from tests with differently treated 10 mm dollies.

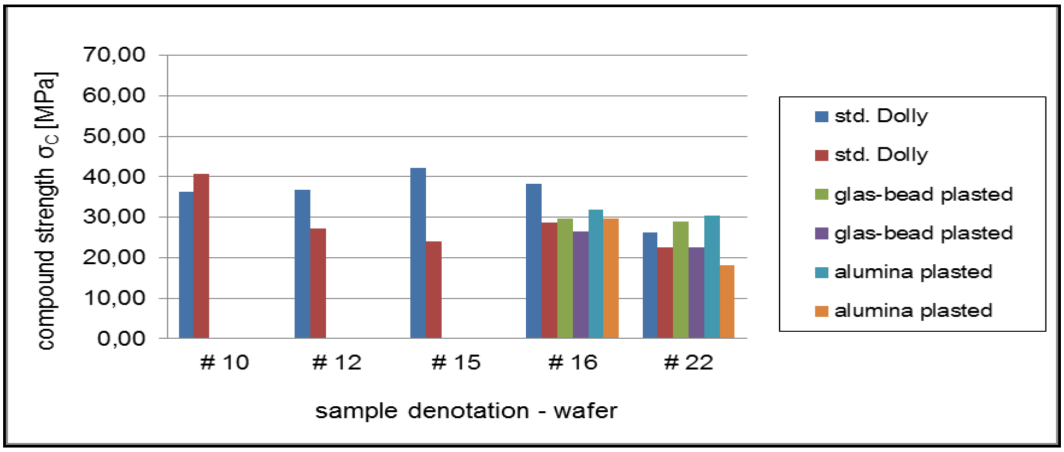

Figure 42: Compound strength for BPSG film obtained from tests with differently treated 14 mm dollies.

These two figures are based on the values for the measured values for the compound strength shown in table 9. If not noted otherwise the actual compound strength of every sample has to be regarded as being greater than the magnitudes displayed in the table, because the film was not pulled of the wafer by the actuator, but the resin-composite failed at the interface between the rear side of the deposited film. For those values which are highlighted green in table 9, the silicon composite material broke off, maybe due to hair-line cracks or because the wafer was not glued to the aluminum plate properly.

All the other metered film parameters for this lot are summarized in appendix 1 and appendix 2. The only effect of the tempering that could be detected was a densification of the deposited film explained by a reduction of the film thickness of 6.6% ± 0.6% as shown in appendix 3, so no difference of the compound strength could be recognized.

Table 9: Compound strength of boron and phosphor doped silicon oxide obtained from different dolly-sizes with variably treated rear sides.

## . . . sample denotation
Equ. . . . equipment used for depositing the film
Proc . . . type of deposition procedure
Dop. . . . doping level of the deposited films [%]
σ (14 mm) . . . compound strength for a dolly with 14 mm diameter of its lower surface
σ (10 mm) . . . compound strength for a dolly with 10 mm diameter of its lower surface
g-b b . . . glass-bead blasted rear side
cor . . . alumina blasted rear side

##	Equ./Proc./Dop	σ (14 mm)		σ (10 mm)		σ (14 mm) g-b b		σ (10 mm) g-b b		σ (14 mm) cor		σ (10 mm) cor	
# 09	Cenura SA-CVD 1.0*2.7																
# 10		36,25	40,77	40,67	36,46												
# 11																	
# 12		36,88	27,20	30,75	34,63												
# 15	Cenura SA-CVD 2.3*2.7	42,19	23,93	40,61	35,93												
# 16		38,25	28,59	46,74	47,90	29,64	26,46	34,39	31,46	31,84	29,56	46,44	46,16				
# 17																	
# 18																	
# 21	Watkins Johnson AP-CVD 1.0*2.7																
# 22		26,32	22,46	36,45	32,40	28,83	22,43	28,13	28,78	30,35	18,07	26,00	46,27				
# 23																	
# 24																	

Highlighted red = tempered film stack; highlighted light-green = silicon wafer broke during testing

9.2 Copper-Nitride Interface on a product-specific Substrate

While fabricating these samples with the stratigraphic sequence silicon wafer / 100 nm titanium-tungsten / 500 nm copper / 800 nm silicon nitride, whereas the titanium-tungsten acts as an adhesion promoter between the silicon wafer and the copper layer, the copper layer has intentionally been deposited at different powers. When raising the deposition power the residual stress of the film increases and furthermore also affects the surface appearance of the copper films by means of roughness. So, one was interested in the correlation between the surface roughness of copper and its effect on the subsequent SNIT film.
As copper can strongly contaminate the process kit of every equipment, where a wafer coated with copper is processed, only selected equipment is applied to process such wafers. Therefore it was neither possible nor allowed to measure parameters like film thickness, uniformity and residual stress.

The results of the pull-off test which were achieved by using the 10 mm and the 14 mm dollies with differently treated rear side are shown in figure 43 and figure 44. For both figures the plotted results refer to the measured values in table 10.

Table 10: Compound strength of the copper-nitride interface obtained from different dolly-sizes with variably treated rear sides.

## . . . sample denotation

P sput Cu . . . applied power during the copper deposition process

σ (14 mm) . . . compound strength for a dolly with 14 mm diameter of its rear side

σ (10 mm) . . . compound strength for a dolly with 10 mm diameter of its rear side

g-b b . . . glass-bead blasted rear side

cor . . . alumina blasted rear side

##	P sput Cu	σ std.St. (14mm)		σ std.St. (10mm)		σ (14mm) g-b b		σ (10mm) g-b b		σ (14mm) cor		σ (10mm) cor	
# 01	2 kW	40,59	44,04	57,72	46,16					31,34	41,43	38,69	32,51
# 05	3 kW	45,16	44,01	39,54	59,62	34,1	34,22	43,38	33,39	42,14	39,39	52,64	59,59
# 09	4 kW	44,52	44,49	57,88	57,17	30,21	19,71	44,59	50,6	40,43	41,16	38,05	53,44
# 13	5 kW	45,38	44,59	54,27	≥59,21					39,72	44,05	53,97	35,88
# 17	6 kW	34,87	45,18	64,28	54,49	28,14	29,95	43,4	44,87	43,87	45,29	40,12	61,61

Highlighted orange = metered values for the compound strength at which delamination has occurred;

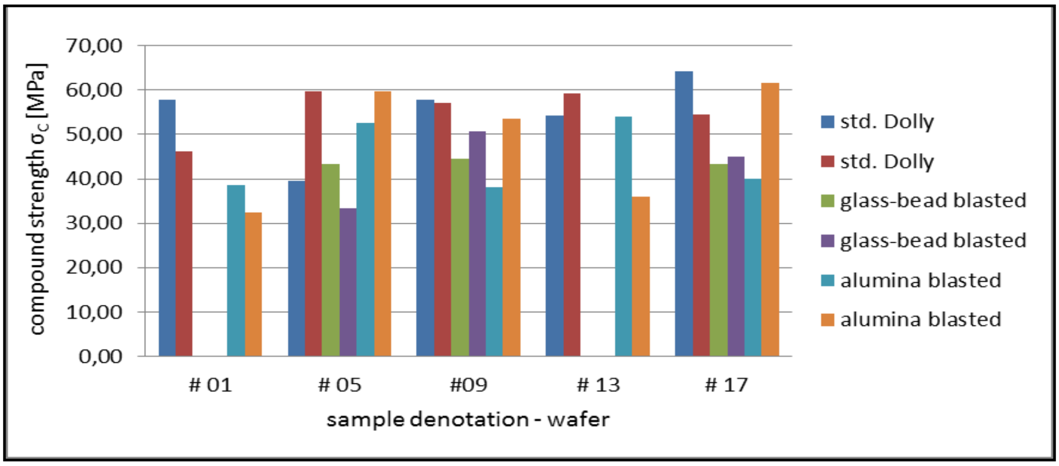

Figure 43: Compound strength for the copper-nitride interface obtained from tests with differently treated 10 mm dollies.

Like for the BPSG samples the displayed values for the compound strength indicate that the adhesion failure occurred within the composite material of the glue. But during the tests with the 14 mm dollies shown in figure 44 below, we managed to pull-off some film material at certain magnitudes of compound strength indicated with red arrows. The average compound strength at which a pull-off of the film was succeeded was found to be $\sigma_C = 43 \pm 2$ [MPa].

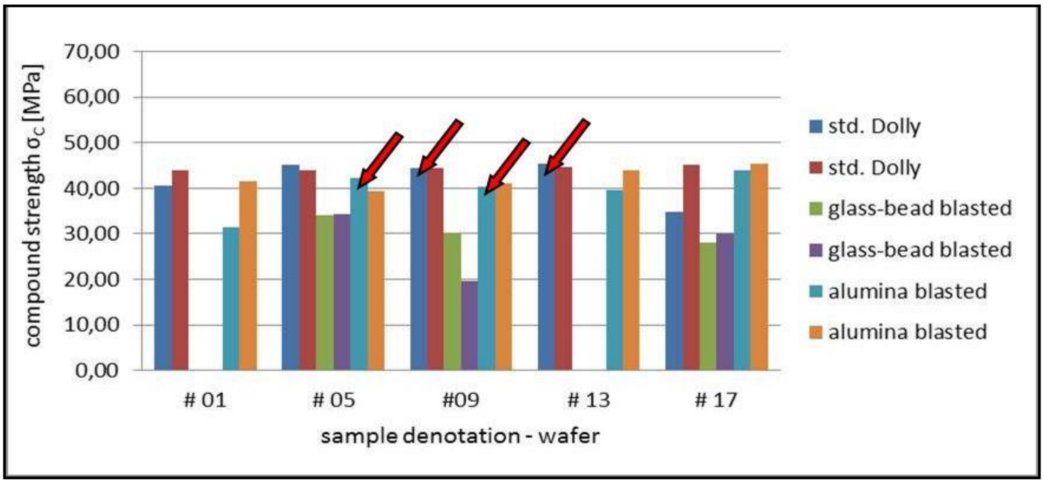

Figure 44: Compound strength for the copper-nitride interface obtained from tests with differently treated 14 mm dollies. The arrows indicate those values at which some film material was pulled-off by the actuator.

The most astonishing thing was that the failure did not occur at the suspected interface, between the SNIT film and the subjacent copper film, but the whole film stack was pulled-off the substrate. According to these results the major purpose of the titanium-tungsten film, being an adhesion promoting film between the silicon substrate and the copper, has definitely not been achieved at all. Nor a correlation between the adhesive properties of the copper film deposited at different, resulting in different ranges of thermal stresses, and the silicon nitride film could be observed.

Figure 45 shows some selected pictures of sites on tested samples, where some film material was pulled-off or even silicon shivers were broken off the compound. The red circle shall always indicate the position of the dolly with a rear side diameter of 14 mm, though the pictures are not equally dimensioned.

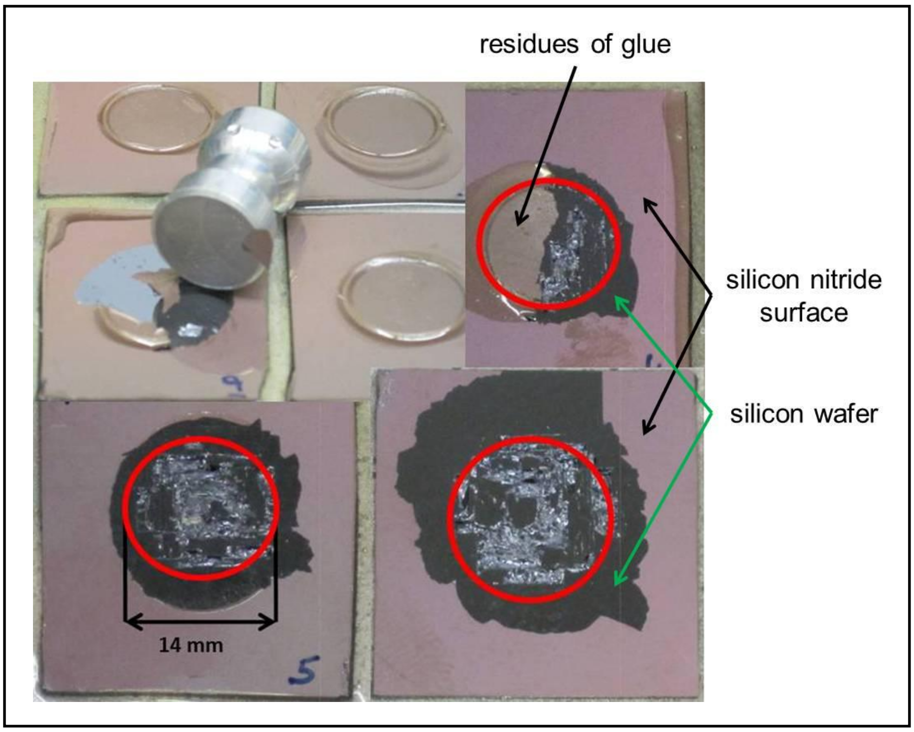

Figure 45: Pictures of sample sites where the film stack has been pulled off and the silicon compound of the wafer was broken in succession.

According to the results gained from the pull-off test some interesting results have been expected from the tape test as well, which was applied to examine the adhesive properties of the deposited film stack. In addition one expected to observe some correlation between the results gained from those two testing methods.

But the expected results did not come true, as the film stack has completely peeled off the silicon wafer during the sawing process, for which reason there was no need to evaluate and rate the adhesion corresponding to the ASTM standard. Figure 46 (a) shows a picture of the grid, 160*160 µm in size, taken with the applied microscope (Nikon ECLIPSE L200). The picture illustrated in figure 46 (b) should demonstrate how a 500 µm broad track of the sawing pattern should look like, if delamination would not have been that strongly pronounced.

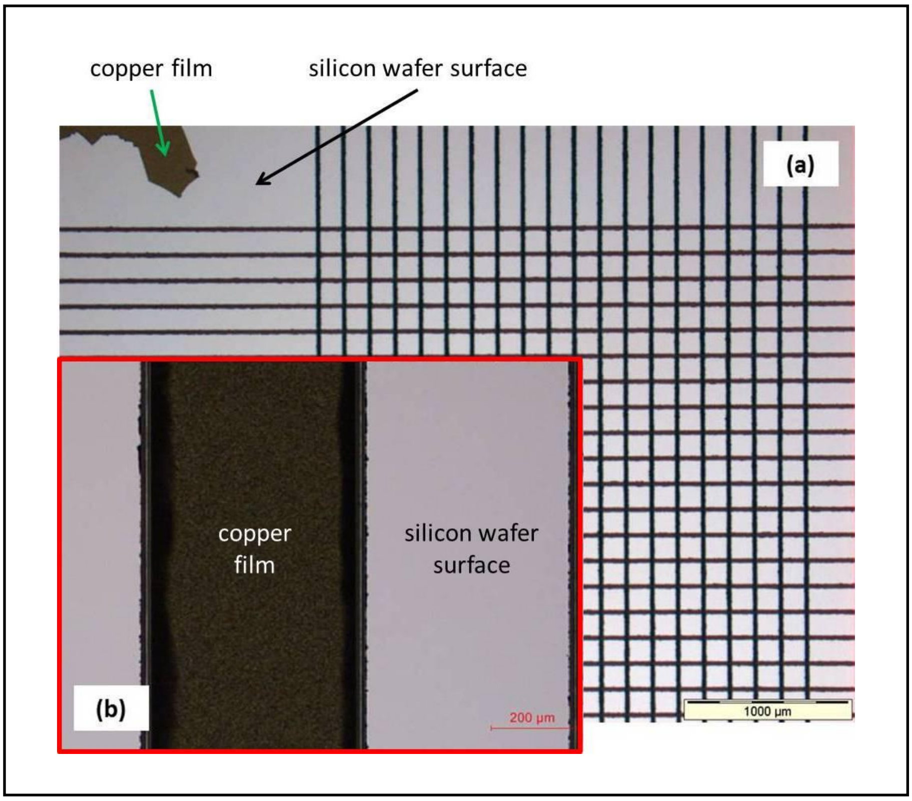
copper film
silicon wafer surface
(a)
copper film
silicon wafer surface
(b)
200 µm
1000 µm

Figure 46: Pictures of the 160*160 µm grid where the CuNIT stack has completely peeled off from the silicon wafer (a) and of a 500 µm broad track where the CuNIT stack did not delaminate during the sawing process.

In figure 46 (a) the dimension of every single square is 160 µm * 160 µm and one can see that from all these squares the whole film stack has completely been peeled-off due to the small area-to-edge ratio. Figure 46 (b) should just show how a trace looks like, when the film stack still adheres to the wafer surface. The width of this trace is 500 µm.

9.3 Silicon Nitride Films on assorted Substrates

This all-around sample lot should be the second to last one, wherefore some meaningful results gained from the pull-off test, as well as from the tape were desired. As for this lot many different sequential arrangements of the deposited films were fabricated all showing different properties, sometimes terminated with an annealing process, the tables containing the film parameter are quite voluminous. As these values were found not to have any effect on the adhesion of the silicon nitride film toward its substrate all the tables have not been included to this thesis.

It could be pointed out during earlier measurements with the adhesion pull-off tester that those tests executed with dollies, whose rear side has been blasted with alumina yielded the best results by means of preferably high values for the metered compound strength σ_C. For this reason and for purposes of recycling the dollies by blasting the rear side to remove the resin residues, all dollies used from now on were blasted with alumina.

To keep an overview, the results for the pull-off test of this lot will be summarized in two separate tables, whereas the results will be depicted in one common graph.

For the first group a SNIT film of 1800 nm was deposited either on a bare silicon wafer, or on 850 nm EOX, or on another 1800 nm SNIT film, and also on an undoped silicon oxide film (USG) being 1400 nm thick. With this group one wanted to find out whether storing some of the wafers in boxes inside the clean room has an effect on the adhesion, or not.

For the second group selected sequences from recent process plans of certain products have been processed, all including BPSG films. Though all of these BPSG films have been annealed after the deposition process, they differ in film thickness and doping level of boron and phosphor. That’s why the second table of this lot contains the results for a simple phosphor doped oxide film as well.

The following table is split into table 11 and 12. As such they include the metered values for the compound strength of the investigated samples for both of the sample groups, but the heading and the remarks refer to both of them.

Table 11: Compound strength of Silicon Nitride on various and differently treated substrates gained from different dolly-sizes with alumina blasted rear sides.

## . . . sample denotation

Sequ. Arr. . . . sequential arrangement of the films

Equ. . . . equipment used for depositing the film

Proc . . . type of deposition procedure

Spec. Treat . . . special treatment before deposition of 2nd SNIT film

3 weeks CR . . . wafers coated with first film were stored at clean room conditions for 3 weeks

σ (14 mm) . . . compound strength for a dolly with 14 mm diameter of its lower surface

σ (10 mm) . . . compound strength for a dolly with 10 mm diameter of its lower surface

cor . . . alumina blasted rear side

##	Sequ. Arr.		Spec. Treat.	σ (10 mm) cor				σ (14 mm) cor			
	Equ./Proc.	Equ./Proc.									
1	silicon wafer	1600 nm SNIT P5000 PE-CVD	3 weeks CR	53,14	35,08	45,36	57,83	42,89	🟩 31,64	42,29	42,48
3			NONE	49,78	40,81	42,58	49,8	39,94	28,26	41,28	36,51
5	850 nm EOX furnace LP-CVD		3 weeks CR	44,70	57,99	14,72	57,08	43,06	42,34	38,85	🟩 44,87
7			NONE	42,71	46,44	49,44	56,31	26,8	42,81	39,16	44,73
9	1600 nm SNIT P5000 PE-CVD		3 weeks CR	50,82	6,71	47,16	52,48	25,3	🟩 39,02	43,97	42,08
11			NONE	42,44	53,88	51,51	56,61	🟩 36,21	40,33	🟩 32,47	🟩 40,88
13	1400 nm USG P500 plasma TEOS		NONE	🟩 25,26	14,09	36,98	56,12	43,94	38,26	31,79	40,08
				x	52,92	42,66	38,58				

Highlighted light-green = silicon wafer broke during testing

Table 12: Compound strength of Silicon Nitride on various and differently treated substrates gained from different dolly-sizes with alumina blasted rear sides.

## . . . sample denotation

Sequ. Arr. . . . sequential arrangement of the films

Equ. . . . equipment used for depositing the film

Proc . . . type of deposition procedure

Spec. Treat . . . special treatment of PSG/BPSG film

Dop. . . . doping level (boron, phosphor) of the deposited films [%]

σ (14 mm) . . . compound strength for a dolly with 14 mm diameter of its lower surface

σ (10 mm) . . . compound strength for a dolly with 10 mm diameter of its lower surface

cor . . . alumina blasted rear side

##	Sequ. Arr.				σ (10 mm) cor				σ (14 mm) cor			
	Equ./Proc.	Dop.	Spec. Treat.	Equ./Proc.								
15	1600 nm USG P5000 plasma TEOS	4.55% P	NONE	1600 nm SNIT P5000 PE-CVD	7,91	x	x	48,98	41,79	45,35	37,79	39,46
					43,56	39,85	43,46	51,9				
17	910 nm BPSG Producer SA-CVD	4.0% B 4.9% P	elapsed 900°C 30 min	1600 nm SNIT P5000 PE-CVD	40,34	50,52	41,58	58,74	46,63	46,41	45,93	46,6
19					51,59	53,94	45,97	54,02	45,29	46,11	46,13	46,27
21	1350 nm BPSG Producer SA-CVD	1.8% B 2.7% P	annealed 975°C N_2+O_2 20 min	1600 nm SNIT P5000 PE-CVD	43,74	33,75	46,60	55,18	32,65	30,50	40,18	19,15
23	850 nm BPSG Producer SA-CVD	1.8% B 2.7% P	elapsed 900°C 30 min	1600 nm SNIT P5000 PE-CVD	66,46	38,11	47,16	58,85	41,75	45,46	27,41	32,04
25					54,63	38,03	57,22	41,14	40,08	29,82	34,7	37,64

Highlighted light-green = silicon wafer broke during testing; Highlighted magenta = dolly could not be pulled off during testing;

The following graph depicted in figure 47, shows only the value for the maximum compound strength that has been measured for every denoted sample good adhesion of the film resembles to the highest measured compound strength in case the dolly was not pulled off. Therefore the adhesion of every particular film stack is better or greater than the value displayed in this figure.

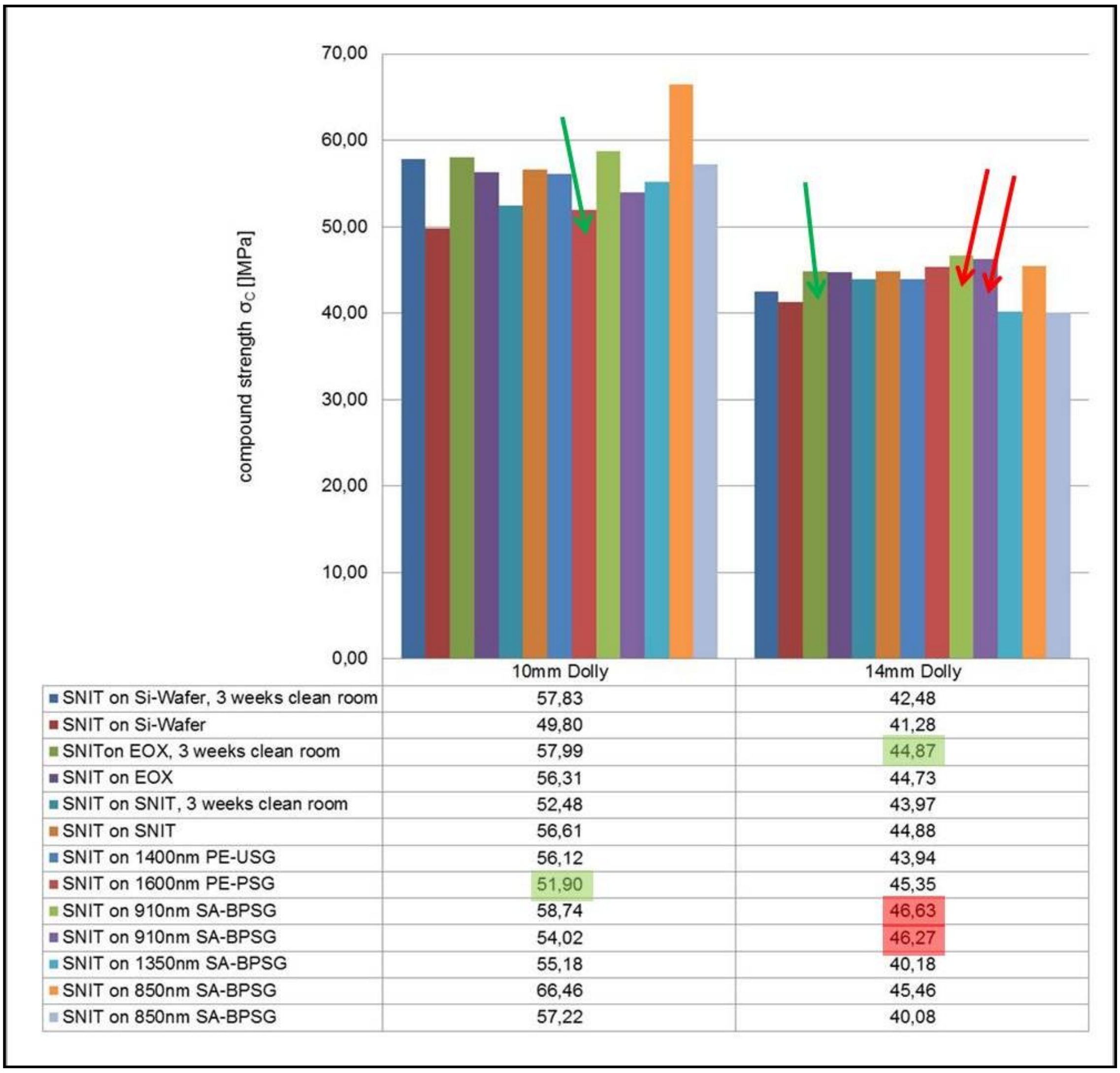

	10mm Dolly	14mm Dolly
SNIT on Si-Wafer, 3 weeks clean room	57,83	42,48
SNIT on Si-Wafer	49,80	41,28
SNITon EOX, 3 weeks clean room	57,99	44,87
SNIT on EOX	56,31	44,73
SNIT on SNIT, 3 weeks clean room	52,48	43,97
SNIT on SNIT	56,61	44,88
SNIT on 1400nm PE-USG	56,12	43,94
SNIT on 1600nm PE-PSG	51,90	45,35
SNIT on 910nm SA-BPSG	58,74	46,63
SNIT on 910nm SA-BPSG	54,02	46,27
SNIT on 1350nm SA-BPSG	55,18	40,18
SNIT on 850nm SA-BPSG	66,46	45,46
SNIT on 850nm SA-BPSG	57,22	40,08

Figure 47: Maximum values of the compound strength for Silicon Nitride on various substrates.

Just as for the previous samples no difference in adhesion of the regarded films making up the samples could be detected with the adhesion pull-off test. Anyhow, the efforts concerning the procedure of sample preparation, especially adjusting the rear side of the dollies and curing the epoxy resin properly led to very good values for the compound strength.

Some of these values almost reach or even exceed the metering capacity of the PosiTest Adhesion Tester for the particular dolly size. The two values highlighted magenta – resembling the columns in figure 47 indicated by the red arrows – have been metered for dollies which could not be pulled off with the actuator. For the values highlighted green – green arrows in figure 47 – the adhesion of the films towards each other and to the substrate has been better than the compound strength of the silicon wafer itself, notably just for these two particular cases.

Also a second success has been denoted while testing this sample lot, namely meaningful and comparative results obtained from the tape. Figure 48 shows the quality of adhesion for every sample of this lot according to the ASTM grading and table 12 contains the according sample denotations.

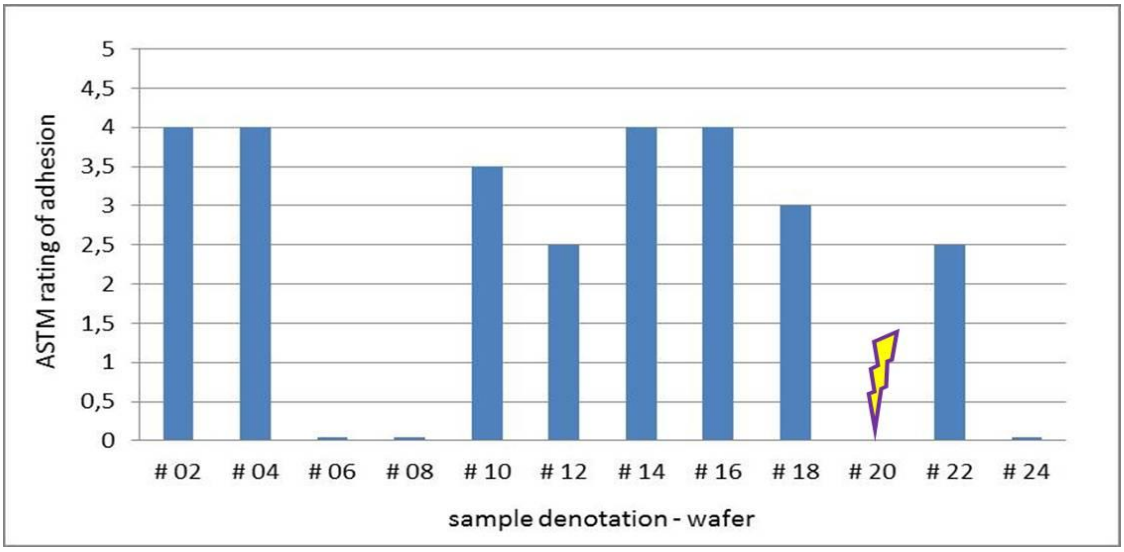

Figure 48: ASTM grading of the adhesion for Silicon Nitride films on various substrates.

Table 13: Sample denotation and sequential arrangement of the films appropriate to figure 46.

## . . . sample denotation

Sequ. Arr. . . . sequential arrangement of the films

##	Sequ. Arr.
# 02	SNIT on Si-Wafer – stored in cleanroom for 3 weeks
# 04	SNIT on Si-Wafer
# 06	SNIT on EOX - stored in cleanroom for 3 weeks
# 08	SNIT on 850 nm EOX
# 10	SNIT on SNIT - stored in cleanroom for 3 weeks
# 12	SNIT on 1600 nm SNIT
# 14	SNIT on 1600 nm USG
# 16	SNIT on 1800 nm PSG
# 18	SNIT on 910 nm SA-BPSG
# 20	SNIT on 1350 nm SA-BPSG
# 22	SNIT on 1350 nm SA-BPSG
# 24	SNIT on 850 nm SA-BPSG

For wafer #20 the adhesion could not explicitly be graded because at certain sites on the wafer, showing different dimensions of the grid, the results differed for more than the allowed two rating units. For this reason a significant evaluation was unacceptable according to the applied standard. For all the other samples the rating was quite clear and some of the results are depicted in the following figures.

According to figure 48 no difference between wafer #02 and #04 could be observed leading to the assumption, that the maintenance of wafer #02 inside the clean room did not affect the adhesion of the SNIT film. For SNIT on EOX the adhesion is quite bad for both modifications. Figure 49 compares the good adhesion of SNIT on a bare silicon wafer (#04) to the bad adhesion of SNIT on an EOX film (#06), whereas both pictures show the site with the 300*300 µm recorded with a magnification factor of 2.5.

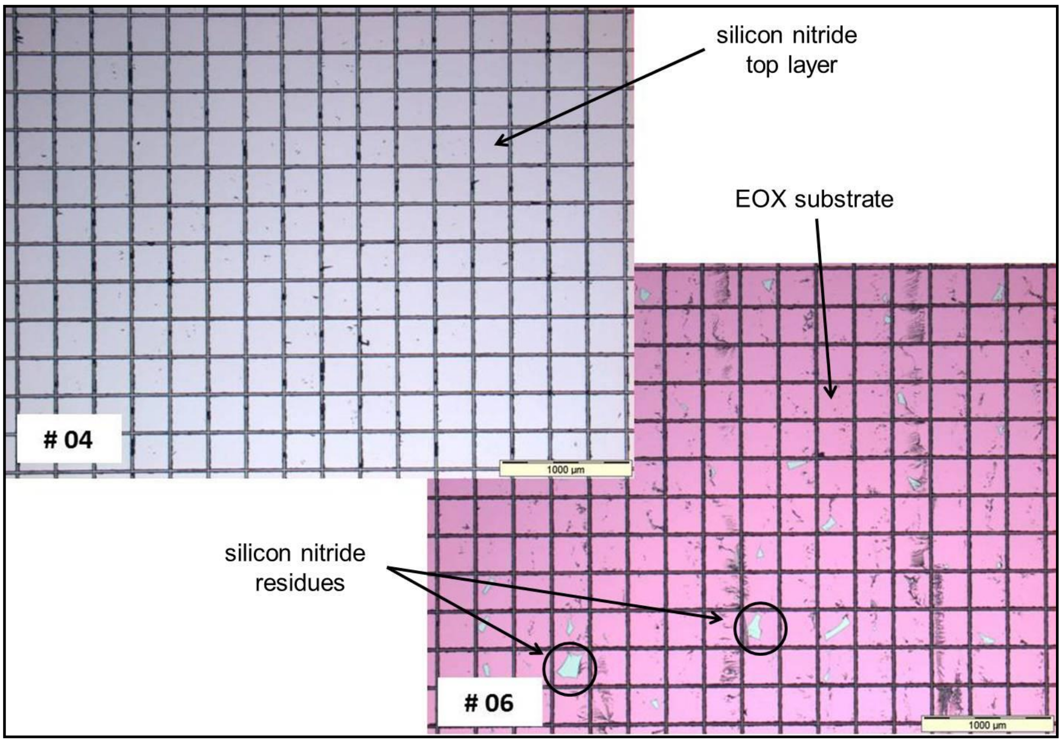

Figure 49: Comparison of SNIT on a silicon wafer (# 04) and SNIT on EOX (#06). 300*300 µm grid size, magnification factor 2.5, scale 1000 µm.

Figure 50 illustrates the different adhesion quality of silicon nitride on a silicon nitride film of same composition and same type concerning the manufacturing, whereas wafer #10 shows the better adhesion, though it was kept inside the clean room for three weeks before the second SNIT film was deposited. This might have improved the adhesive properties at the interface between those films. Both pictures show the site at which the grid is 500*500 µm large, at a magnification factor of 2.5 again.

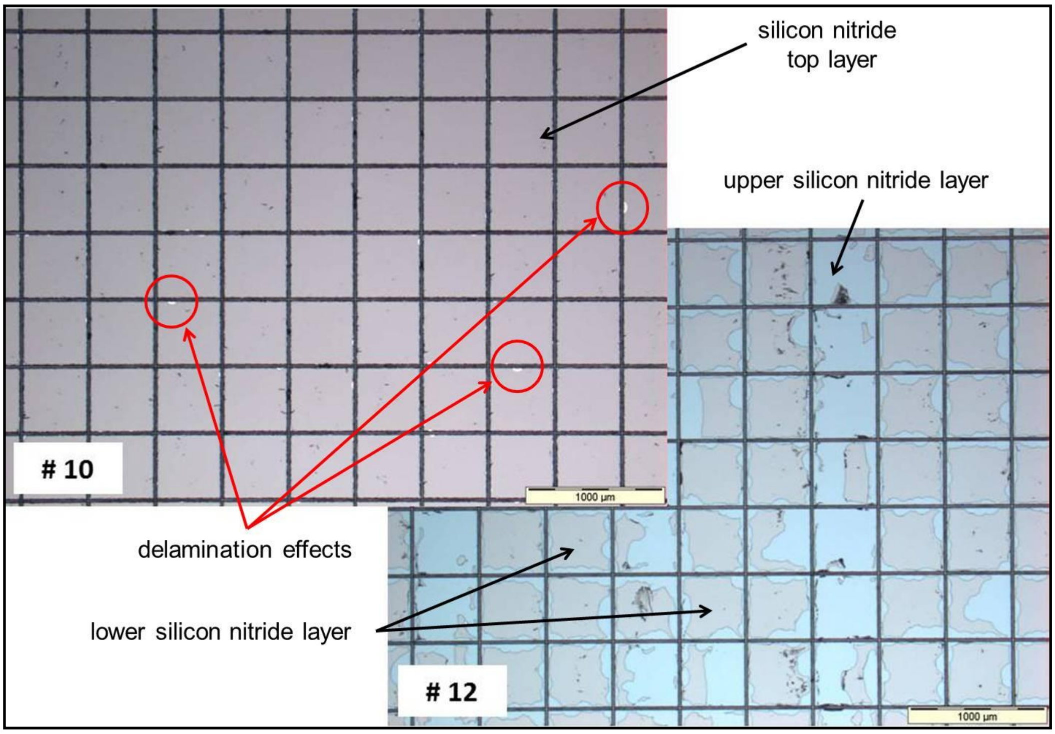
silicon nitride top layer
upper silicon nitride layer
# 10
1000 µm
delamination effects
lower silicon nitride layer
# 12
1000 µm

Figure 50: Comparison of SNIT on SNIT with 3 weeks storage inside the cleanroom (#04) and SNIT on SNIT without storing wafer (#06). The red circles indicate regions at the sawing edges where delamination slightly took place. 500*500 µm grid size, magnification factor 2.5, scale 1000 µm.

The picture of wafer #10 does not show the delamination effect that much, though at some spots, indicated by red circles in figure 50, one can recognize that small flakes of the coating detach along the edges and ad the intersections as well, leading to the grading 3.5. The more easily these delamination effects can be seen at wafer #12, where delamination also occurs on parts of the squares.

The differently coloured upper silicon nitride layer of wafer #10 and wafer #12 though they are equal to each other regarding thickness and fabrication might originate from the difference of thickness and eventually colour of the respective substrate layer. For wafer #10 this is 850 nm EOX and for wafer #12 there is 1600 nm SNIT.

9.4 Amorphous hydrogenated nitrogen-doped Carbon with different Plasma pre-treatment

Being the last lot dealt with during this master thesis the expectations towards the results have been quite high, in order to prove the statement of M. Vogt – different plasma treatments of the POLY or TEOS surface before depositing a-C:H:N, especially N_2O plasmas, have an adhesion-inhibiting effect, and furthermore include some chemical aspects into this more physically affected thesis. Also for this sample lot the film parameters of every wafer have been journalized, except the actual thickness of the a-C:H:N film as none of the available measuring devices was equipped with a suitable monitoring program. So, one had to rely on the statement of the colleague who has developed and invented this type of film whose thickness does only fractionally deviate from the expected film thickness. Nevertheless, the bow of the a-C:H:N film has been determined before and after the tempering process, leading to the awareness, that tempering processes definitely change the stress of the film stack, as apparent in appendix 4.

As usual one started the investigations with the adhesion pull-off test and after the first throughput the achieved results have been complied with the expectations: whenever the a-C:H:N film was tempered after the surface of the subjacent POLY or TEOS has been treated with N_2O plasma, the a-C:H:N film was successfully pulled off. To prove whether the obtained results can be regarded as significant, the pull-off test was repeated during another throughput, just for those samples with N_2O plasma treatment and tempered a-C:H:N film. And in fact the results from the first throughput were successfully verified, and are presented in table 13, together with those values of the compound strength, gained from the first throughput.

Table 14: Compound strength of the a-C:H:N films with respect to the kind of plasma cleaning before and the type of post-treatment after depositing the particular carbon film.

## . . . sample denotation

Sequ. Arr. . . . sequential arrangement of the films

sf . . . subjacent film

Plasma Treat. . . . denotes particular plasma cleaning before depositing a-C:H:N

p.t. . . . post-treatment of a-C:H:N film

σ (14 mm) . . . compound strength for a dolly with 14 mm diameter of its lower surface

σ (10 mm) . . . compound strength for a dolly with 10 mm diameter of its lower surface

cor . . . alumina blasted rear side

##	Seq. Arr.			p.t.	σ (10 mm) cor				σ (14 mm) cor			
	sf	Plasma Treat.			first throughput							
1	POLY	NONE	a-C:H:N - film, expected thickness ~ 1 µm	as-deposited	53,19	42,71	50,13	40,40	30,51	38,30	37,71	40,19
2		N_2O			46,52	38,66	48,59	50,52	39,57	25,85	39,82	18,90
3		NH_3			32,81	35,90	46,63	44,98	24,09	33,45	22,09	32,15
4	TEOS	NONE			50,52	56,26	50,05	32,40	40,58	42,15	29,27	26,84
5		N_2O			39,74	42,16	43,93	52,56	40,34	44,55	36,03	28,28
6		NH_3			42,91	27,82	44,15	36,21	35,83	37,21	23,80	29,52
7	POLY	NONE		tempered	47,02	46,02	30,33	44,15	31,93	33,19	33,21	21,96
8		N_2O			39,21	42,44	30,72	39,96	31,17	20,71	26,39	26,54
9		NH_3			44,48	44,54	42,77	44,12	28,44	34,04	31,19	34,39
10	TEOS	NONE			39,42	41,03	22,44	37,06	21,13	25,46	26,43	27,53
11		N_2O			40,15	26,60	50,76	12,19	24,07	20,20	23,22	30,98
12		NH_3			43,21	37,23	43,82	6,50	32,90	19,74	23,88	34,50
					second throughput							
7	POLY	NONE		tempered								
8		N_2O			47,79	50,66	42,91	53,00	37,08	38,32	40,30	38,66
9		NH_3										
10	TEOS	NONE										
11		N_2O			43,85	50,05	53,33	41,31	24,25	36,98	34,69	37,31
12		NH_3										

Highlighted light-green = silicon wafer broke during testing; Highlighted orange = metered values for compound strength at which delamination has occurred;

The values from table 14 which were used to plot the graph depicted in figure 51 have been selected under a certain aspect. For those samples where the N_2O plasma treatment and the tempering after the deposition of the a-C:H:N film has led to successfully pulling off the a-C:H:N from its subjacent film, always the smallest measured value was chosen. This value then indicates the maximal compound strength to which a-C:H:N film can withstand.

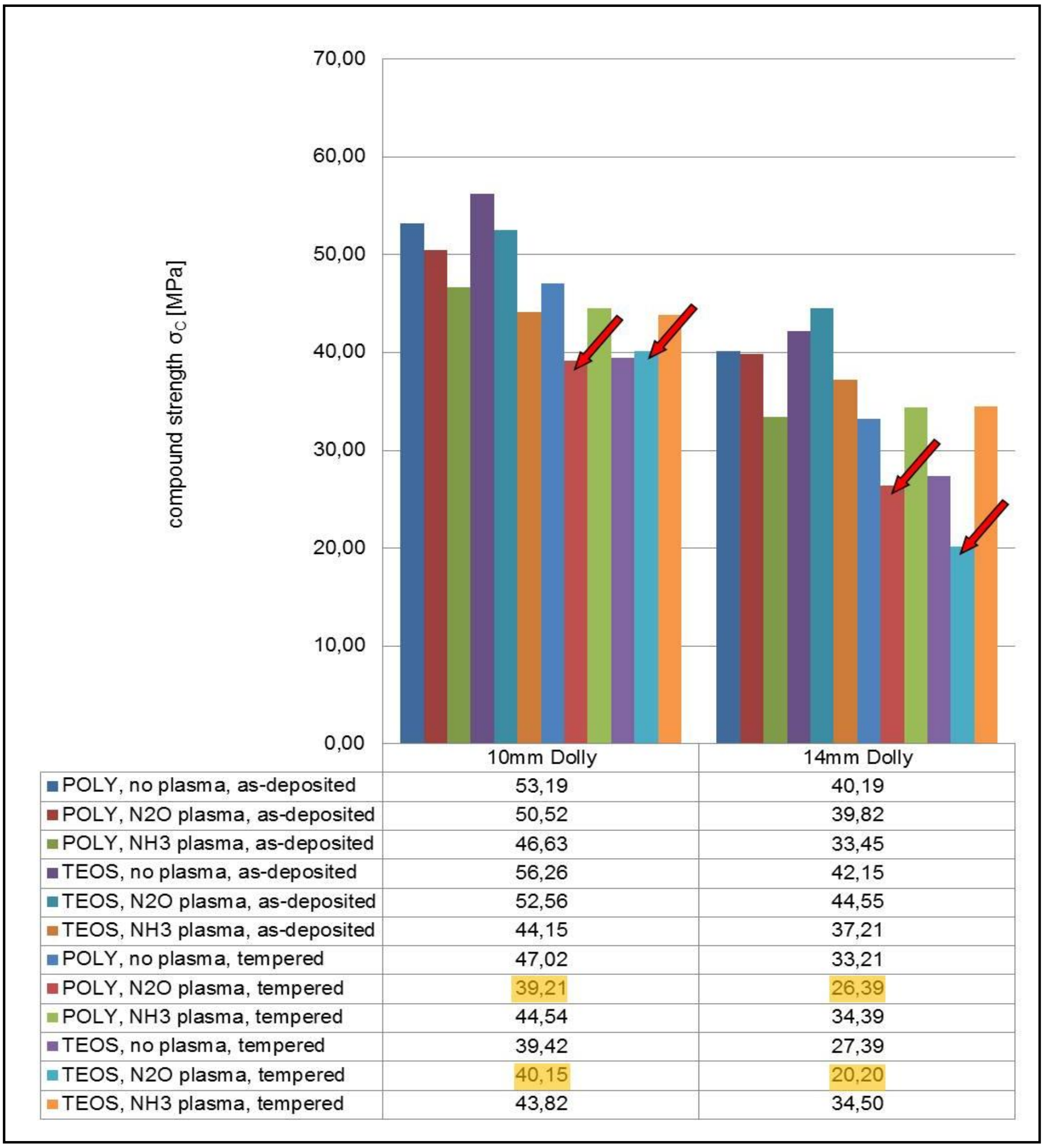

	10mm Dolly	14mm Dolly
■ POLY, no plasma, as-deposited	53,19	40,19
■ POLY, N2O plasma, as-deposited	50,52	39,82
■ POLY, NH3 plasma, as-deposited	46,63	33,45
■ TEOS, no plasma, as-deposited	56,26	42,15
■ TEOS, N2O plasma, as-deposited	52,56	44,55
■ TEOS, NH3 plasma, as-deposited	44,15	37,21
■ POLY, no plasma, tempered	47,02	33,21
■ POLY, N2O plasma, tempered	39,21	26,39
■ POLY, NH3 plasma, tempered	44,54	34,39
■ TEOS, no plasma, tempered	39,42	27,39
■ TEOS, N2O plasma, tempered	40,15	20,20
■ TEOS, NH3 plasma, tempered	43,82	34,50

Figure 51: Significant values for the compound strength describing the adhesion of amorphous carbon films on their substrate layer, affected by the post-tempering process and strongly depending on the kind of plasma pre-treatment.

The most significant values for the metered compound strength in figure 51 are indicated by red arrows and additionally highlighted orange in the list underneath the displayed graph.

Figure 52 and figure 53 show a selection of illustrative images confirming the results achieved with the adhesion pull-off test. The successful pull-offs of the tempered a-C:H:N film from the subjacent POLY film, which has been cleaned with N_2O plasma in figure 52 (a) were all achieved with a dolly whose rear side has a diameter of 10 mm, indicated by the red circle in figure 52 (b).

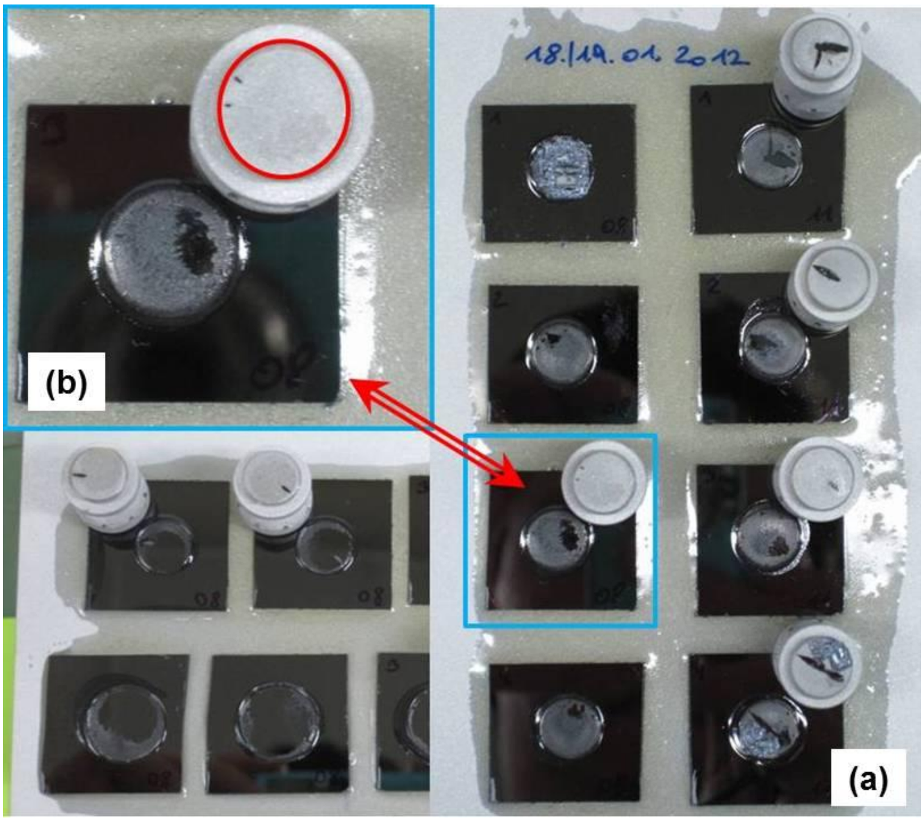

Figure 52: Images of some successful pull-offs of the amorphous carbon film from the subjacent POLY film, during testing with a 10 mm dolly. The red circle indicates the diameter of 10 mm.

The results of the pull-off test for the tempered a-C:H:N film, which was pulled off the N_2O plasma treated TEOS film - all shown in figure 53 – have been succeeded with dollies of 10 mm diameter shown by the red circle in figure 53 (c) as well as 14 mm (green circles) rear side diameter, shown in figure 53 (b). The sample depicted in insert (c) is a magnification of one of the samples from (a).

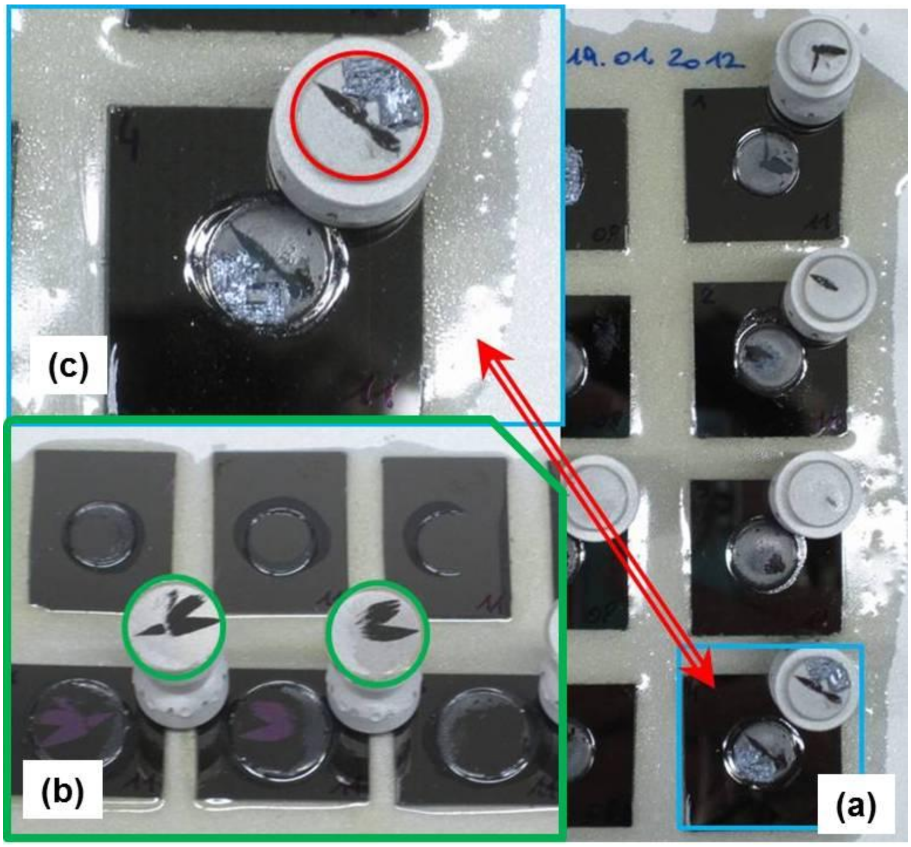

Figure 53: Images of some successful pull-offs of the amorphous carbon film from the subjacent TEOS film, during testing with 10 mm (a) as well as with 14 mm dollies. One sample in (a) is magnified in insert (c). The green circles indicate the diameter of 14 mm (b), the red circle that of 10 mm (c).

A quite similar performance for the adhesion of the a-C:H:N films on the subjacent POLY or TEOS can be observed when comparing the obtained results from the pull-off test with those gained from the tape test, depicted in figure 54. Table 15 shown underneath the figure contains the corresponding sample denotations.

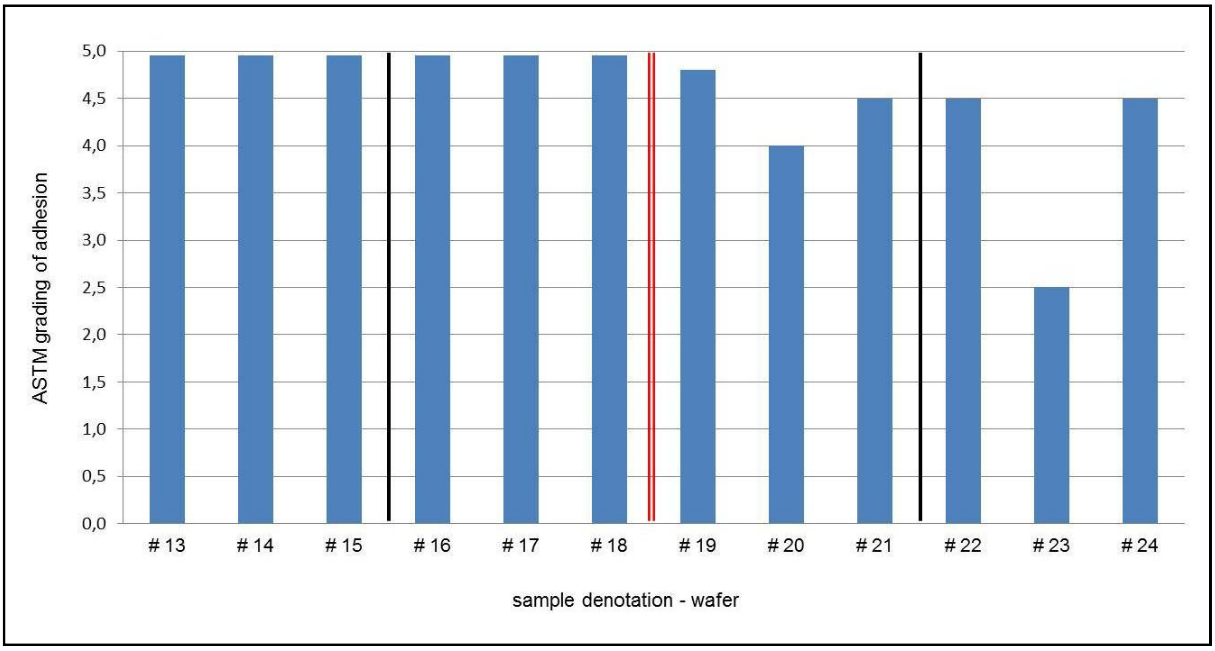

Figure 54: ASTM grading of the adhesion of amorphous hydrogenated nitrogen-doped carbon, depending on executed pre- and post-treatments.

Table 15: Sample denotation and sequential arrangement of the individual process steps.

## . . . sample denotation

Sequ. . . . sequence of substrate film, pre- and post-treatment

##	Sequ.
# 13	POLY, no plasma, as-deposited
# 14	POLY, N2O plasma, as-deposited
# 15	POLY, NH3 plasma, as-deposited
# 16	TEOS, no plasma, as-deposited
# 17	TEOS, N2O plasma, as-deposited
# 18	TEOS, NH3 plasma, as-deposited
# 19	POLY, no plasma, tempered
# 20	POLY, N2O plasma, tempered
# 21	POLY, NH3 plasma, tempered
# 22	TEOS, no plasma, tempered
# 23	TEOS, N2O plasma, tempered
# 24	TEOS, NH3 plasma, tempered

On the basis of the results shown in figure 54 one can discover the effect tempering of the a-C:H:N film has on the adhesion, especially when the POLY or TEOS film is treated with N_2O plasma. For this reason only pictures showing samples whose surfaces of the POLY or TEOS film have been pre-treated with N_2O as this type of treatment has the most severe effect on the determined quality of adhesion. Furthermore, all following pictures show the site on the wafer where the grid has the spacing of 160*160 µm, the magnifying factor was 20 and the scale shows 200 µm. These sites have been chosen as the smaller squares are more fragile concerning delamination due to the smaller area to edge length ratio.

Figure 55 compares two samples, wafer #14 and wafer #20, for both the POLY film was cleaned with N_2O plasma before depositing the a-C:H:N film, which has been investigated as-deposited (wafer #14) and tempered (wafer #20).

The delamination is even stronger distinctive for samples containing a TEOS film underneath the a-C:H:N, because TEOS itself also contains oxygen worsening the adhesion. The effects of additional oxygen at the regarded interface (TEOS/a-C:H:N) on the extent of the investigated delamination is shown in figure 56.

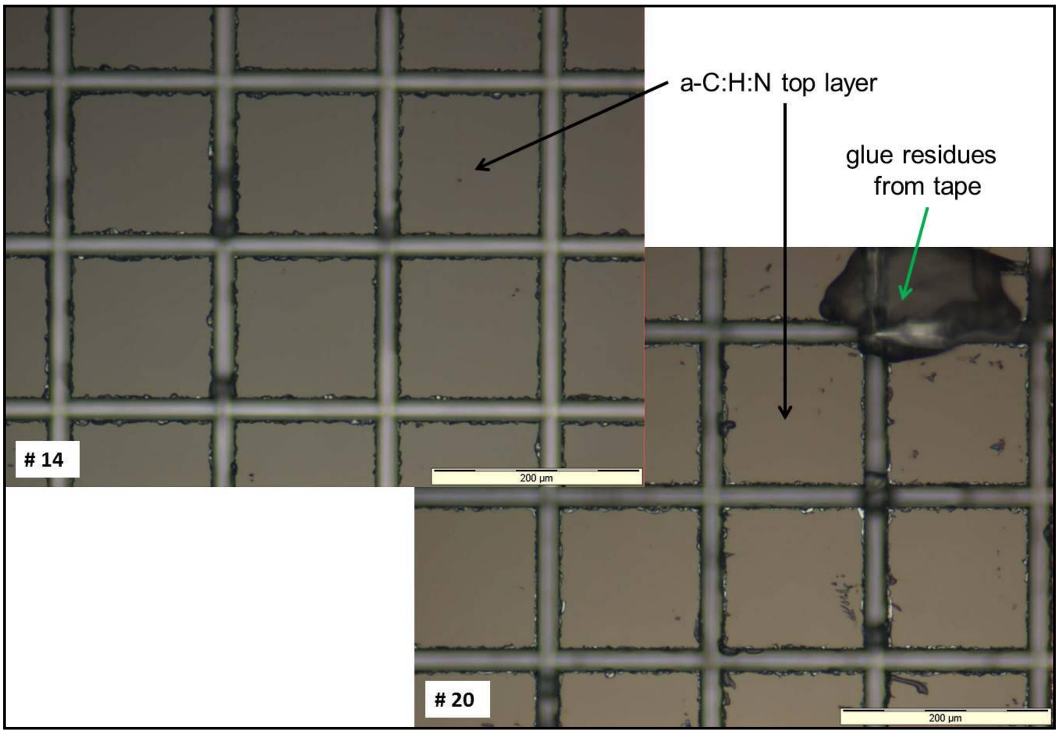

Figure 55: Comparison of the results gained by the tape test for an as-deposited (#14) and a tempered (#20) amorphous carbon film, on N_2O plasma treated POLY.

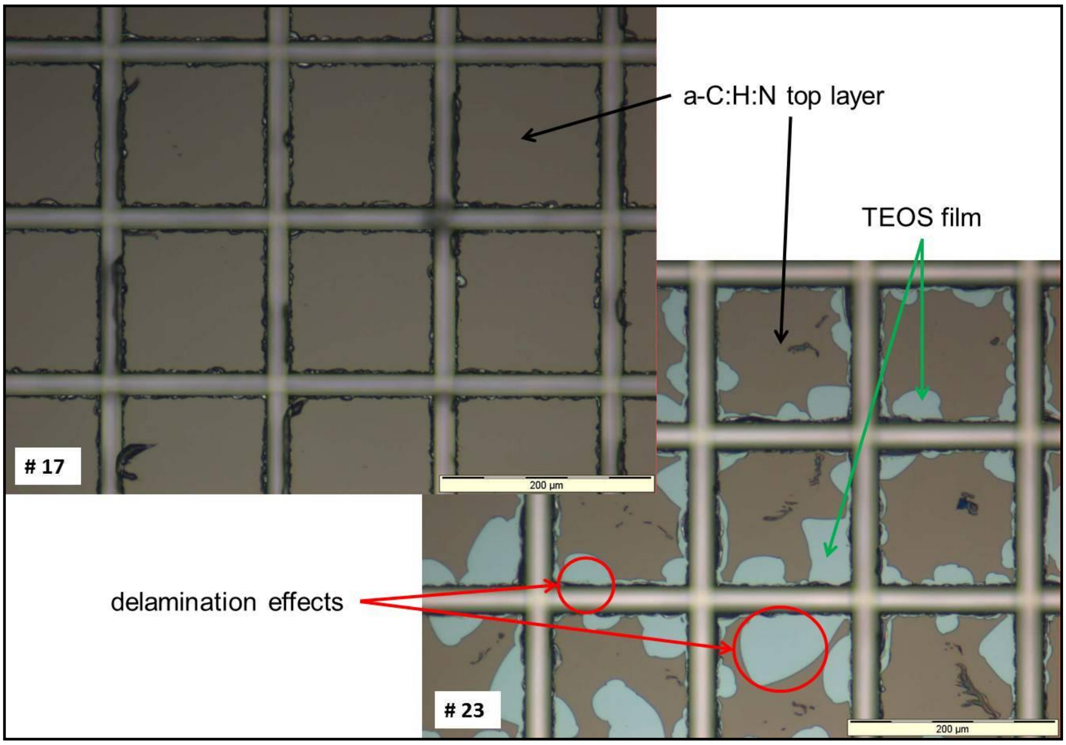
a-C:H:N top layer
TEOS film
# 17
200 µm
delamination effects
# 23
200 µm

Figure 56: Comparison of the results gained by the tape test for an as-deposited (#17) and a tempered (#23) amorphous carbon film, on N_2O plasma treated TEOS.

10. Summary and Conclusions

The presented master thesis includes an extensive insight into the various kinds and theories of adhesion, some approved and almost as many unexperienced methods to investigate and measure adhesion. Based on the awareness and the knowledge gained thereby, a selection of sample material could be investigated and studied with respect to the adhesive properties, especially the compound strength σ_C, of the particular interfaces, covering a wide range of application areas, as well as versatility of the sample specifications.

The first sample lot dealt with adhesion problems arising during and after the deposition of boron and phosphor doped silicon oxides (BPSG), originally processed under atmospheric conditions (AP-CVD), when fabricated during a sub-atmospheric SA-CVD process up to the critical film thickness of 1800 nm. The experimental results, just obtained from the Adhesion Pull-Off Test, were not that significant, as the applied test had to be developed and properly adjusted for our purposes. At this, modifying the rear side of the dollies utilized for executing the test and improving the curing procedure of the applied epoxy resin, have been the first challenges. Though, it can be recorded that the compound strength of BPSG, deposited on a bare 6'' silicon wafer yields the following averaged results:

- $\sigma_C = 32 \pm 7$ [MPa] for dollies with a rear side diameter of 14 mm
- $\sigma_C = 38 \pm 6$ [MPa] for dollies with a rear side diameter of 10 mm

The intention of the second sample lot was to investigate the adhesion of silane-based silicon nitride processed by PE-CVD on a copper substrate (CuNIT), because copper as metallization film is more convenient for applications in fields of semiconductor technology, due to its better electrical properties compared to aluminum. With the help of this lot the experimental results obtained from the Pull-Off Test should be compared to those gained with the recently discovered Tape Test, prepared with a particular sawing patter for the lattice, originally being developed for Transition Line Measurements (TLM), executed and rated according to an ASTM Standard. With the Pull-Off test which has been almost perfectly adjusted by blasting the rear side of the dollies with alumina (~70 µm granulation) and effectively changing the curing process of the resin, promising results have been achieved for those pull-off tests executed with dollies of 14 mm rear side diameter. The metered average compound strength at which some film material was pulled off was found to be:

- $\sigma_C = 43 \pm 2$ [MPa]

Unfortunately, these results could not be confirmed with the Tape-Test as the whole film stack has peeled off during the sawing process preparing the lattice pattern, in all areas of the sawing pattern. Plenty of considerations and several discussions with colleagues lead to the conclusion that something has gone wrong during the preparation processes of this sample. It is completely unusual that the adhesion fails at the interface between the surface of the silicon wafer and the titanium-tungsten film, operating as adhesion promoting agent between the silicon and the copper film.

The intention of exploring the adhesive properties of a silane-based PE-CVD Silicon Nitride film (SNIT) on various substrates lead to another sample lot comprising some miscellaneous types of film sequences according to process plans of popular semiconductor devices being manufactured at INFINEON in Villach. The consequence of the conditions predominating inside the clean room on the adhesion of PE-SNIT on bare silicon, AP-oxide (EOX) and on the same PE-SNIT has been studied and compared to the results obtained for samples with the same substrate, which have not been stored in the clean room. Furthermore, certain film stacks containing annealed BPSG films with different doping levels of boron and phosphor have been investigated, as well as the adhesion of SNIT on USG and PSG deposited from plasma TEOS. Though the Pull-Off Test did not yield very meaningful results, except some dollies which could not be pulled off due to a perfectly cured epoxy resin leading to the best achievable strength, a still explicit difference of the adhesion for the SNIT films on their substrate could be determined.

To finalize the experiments executed during this thesis a very interesting sample lot was investigated considering the adhesion and the comparison of the gained results from the Pull-Off as well as from the Tape Test. Integrating a more chemical aspect, an amorphous hydrogenated nitrogen-doped carbon film (a-C:H:N) has been deposited on two different substrate materials, POLY and TEOS, which have been treated with different plasma cleaning, N_2O and NH_3, before the a-C:H:N film was deposited. As it was assumed that certain thermally activated chemical reactions between oxygen and carbon could take place at the particular interface, half of the samples have been tempered after the a-C:H:N film deposition, to compare the results with as-deposited carbon, especially when the subjacent POLY or TEOS film has been treated with N_2O plasma.
According to the achieved results from both of the applied tests, the assumption concerning the influence of tempering processes on the adhesion of a-C:H:N on N_2O plasma treaded substrate surfaces was definitely confirmed. This worsening of the adhesion could especially be observed for samples for which the a-C:H:N film has been deposited on N_2O pre-treated TEOS, because TEOS, $Si(OC_2H_5)_4$, compared to POLY also contains oxygen, enforcing the deterioration of the interface.

After having investigated all the mentioned samples with the Adhesion Pull-Off Test and the Tape Test, applying a special sawing pattern during the preparation procedure, one can afford some statements concerning the range of application of these tests. One can definitely state that both of the applied tests yield comparative and significant results, in case the compound strength of the investigated interface or film stack does not exceed the measuring range of the PosiTest Adhesion Tester. Furthermore, one has to be aware of the upcoming issues and how to interpret the obtained results correctly. The values obtained from the Pull-Off Test just resemble the compound strength σ_C, so one can expect the “real” adhesive strength σ_A to exceed the obtained measurement results. For evaluating the Tape Test one has to be aware of side effects directly originating from the sawing process like flakes at the cut edges or intersections, or glue residues from the tape that might be kept for delamination effects and falsify the result.

Nevertheless, none of these two testing methods is suitable for routine inspections and quality testing during bulk production, as both of them are destructive and require quite some time to prepare the samples for the particular test. However, they could be identified and proven as extremely suitable for being applied for purposes of process and product development.

11. Forecast

Based on the satisfying and also significant results of the experiments which have been executed, several opportunities concerning development and research arise. During this thesis the two applied and discovered testing methods, the Adhesion Pull-Off Test and the Tape Test have been identified to be applicable for product and process developments. Especially the excellent impression which could be achieved concerning the Tape Test already affected colleagues from the department of “Entire Process Development” to apply this test for a quite extensive test series dealing with modified tempering processes in fields of reverse side metallisation.

Also the analysis of the effects on tempering a-C:H:N films after a pre-treatment of the subjacent film with N_2O, denoted as “adhesion killer”, advises to be precautious and observant whenever similar experiments or process steps are executed, especially for the enhancement and modification of the D-Sound Technology. In this context such a-C:H:N thin films were discovered to be the key component, though they are quite prone to chemical reactions with oxygen, when appearing at the considered interface.

And finally, since no correlation could be detected between the adhesion of the investigated films and thermo-mechanical stresses that appear in such thin CVD films, a further master thesis has been announced. The intention of this thesis is to judge the influence of humidity and humidity induced stresses on interfaces of thin films, which are applied in passivation layers or inter-metal oxides. For this purpose the Tape Test which has been applied, adjusted and approved during this thesis, shall be employed.

Acknowledgements

At this point I want to thank all those people who have supported me in compiling this master thesis.

First and foremost I want to acknowledge Prof. Dr. Adolf Winkler from the Institute of Solid State Physics at Graz University of Technology for agreeing to supervise this master thesis and for his steadfast guidance and support in all concerns. Through his advice during several meetings and his accordingly technical suggestions for improvement as well as thought-provoking impulses, I never lost sight of the essential and relevant aspects of my thesis. Dr. Winkler always afforded me the required and valuable tolerance for permutations and gathering the results for the existing tasks. Thank you very much for the numerous occasions of support and plenty of unselfish endeavours. It was a precious time, which I wouldn't have missed for the world.

Furthermore I want to thank all my treasured colleagues from the department of Unit Process development, UPD 3, as well as the colleagues from module M3 Deposition of Infineon Technologies in Villach. Particular appreciation is due to them for their dynamic support and their input which enabled an extremely pleasant employee attitude whilst I carried out this work.

Special thanks have to be directed to my local supervisor DI Helmut Schönherr for his steady engagement, his enduring guidance and his devotional assistance. Because of his help, his advice and his immense professional knowledge of CVD processes, it has been possible for me to better understand the scientific aspects of this thesis and to simultaneously expand my knowledge base. I always had the freedom to operate independently in the execution of my numerous test series, whereat I was led towards glancing beyond 'the edge of the plate', without losing sight of essential and important concerns.

Moreover I want to thank Dr. Markus Kahn for his help while working on my master thesis as well as for his support, especially during the development of the split plan for the sample lot dealing with the effects of plasma treatments on the adhesion of the a-C:H:N films. Thank you, Markus for your help and the always awesome collaboration as well as for the many inspiring conversations.

Regarding my former colleagues, I want to acknowledge and extend my appreciation to: Mr. Rudolf Kogler, for providing his head-workman thesis and the many schematic drawings of the several CVD reactors and the differently configured process chambers, as well as for the several conversations concerning the setup and the operating principle of such CVD

reactors, and Mr Herman Achatz, for always blasting my dollies after the pull-off tests, and his hints concerning social competence and talking to other colleagues. Thank you both.
Furthermore, I must acknowledge all my fellow employees from the production area, front end as well as back end, who have handled and dealt with the samples, which had to be prepared and processed for my master thesis.

Special thanks also to all my friends, colleagues from studies and fraternity brothers for their everlasting recourse, their support during the tougher periods of my studies and the awesome times we spent together. Thank you so much, guys.

Thanks also to all those who remain unnamed. I've been privileged to get to know such nice colleagues; I've met great people and found many new friends, each of whom has engraved my life in their own particular manner, and who might conduct me along my further path of life.

Last but not least, I want to thank my family, especially my parents, for their enduring support, their patience and for setting the cornerstone, by facilitating such an invaluable education. Thank you for so much, Mum and Dad. I also want to thank my grandfather, who unfortunately passed away much too early; for the wonderful and unforgettable time we spent together. He will always live on in my memories.

Sincere thanks to one and all!

Bibliography

[1] C. Bischof, W. Possart: Adhäsion – Theoretische und experimentelle Grundlagen, Akademie-Verlag Berlin, 1983.

[2] K. L. Mittal: Adhesion measurements of films and coatings, VSP Utrecht, The Netherlands, 1995.

[3] K. L. Mittal: Adhesion Measurement of Thin Films. Electrocomponent Science and Technology, 1976, 3, 21-42.

[4] D. M. Mattox: Handbook of Physical Vapor Deposition (PVD) Processing. William Andrew, 2nd edition. 2010.

[5] L. F. M. da Silva, A. Öchsner, R. D. Adams, (Eds.): Handbook of Adhesion Technology. Springer, 1st Edition., 2011.

[6] D.M. Mattox, D. A. Rigney: Adhesion Processes in Technological Applications. Materials Science and Engineering, 1986, 83, 189-195.

[7] D. Dunlap, J. Parekhji, A. J. Your: Interfacial Adhesion. Report on Experimental Methods in Materials Engineering, 2002.

[8] A. Pizzi, K. L. Mittal: Handbook of Adhesive Technology. Marcel Dekker Inc, Edition: Revised, Expanded, 2003.

[9] K. L. Mittal, A. Pizzi, Adhesion Promotion Techniques: Technological Applications. Marcel Dekker Inc. New York-Basel, 1999.

[10] L. Gao, T. J. McCarthy: Wetting 101°. Langmuir, 2009, 25, 14105-14115.

[11] R. Jacobsson: Measurment of the Adhesion of Thin Films. Thin Solid Films, 1976, 34, 191-199

[12] J. W. Beams, J. B. Breazeale, W. L. Bart: Mechanical Strength of Thin Films of Metal. Physical Review, 1955, 100, 1657-1661

[13] Lecture Notes, Prof. Adolf Winkler: Dünschichttechnologie. Institute of Solid State Physics, Graz University of Technology.

[14] R. A. Haefer: Oberflächen- und Dünnschicht-Technologie. Werkstoff-Forschung und Technik 5, Springer Verlag, 1987.

[15] D. M. Mattox: Interface formation and the Adhesion of the deposited Thin Films. SC-R-65-852, Metals, Ceramics and Materials, 37th edition, 1965.

[16] M. Ohring: Materials Science of Thin Films – Deposition and Structure. Academic Press, 2nd edition, 2001

[17] Yoshio Nishi, Robert Doering: Handbook of Semiconductor Manufacturing Technology. CRC Press Inc; Revised 2nd edition, 2007.

[18] http://www.halbleiter.org/abscheidung/cvd/

[19] Applied Materials: P5000 CVD Process Manual

[20] U. Höckele, T. Kunstmann, M. Müller, H. Schönherr: Thin Film Festival. Company-internal Presentation, September 2007.

[21] J. Baumgartl: Schichterzeugung. Company-Internal Presentation, 2009.

[22] J. Robertson: Diamond-like amorphous carbon. Materials Science and Engineering. 2002, R 37, 129-281.

[23] T. Kunstmann, H. Schönherr: Applied Materials Equipment Hardware Nomenclature. Company-internal Presentation, September 2005.

[24] R. Kogler: 6’’-BPSG Prozess und Hardwareentwicklung als WJ-Ersatz auf Single-Wafer Anlagen. Company-internal and confidential master-workman thesis. 2008.

[25] U. Krumbein and Team: Task Force on MEMS Robustness RPD. Company-internal presentation, April 2004.

[26] M. Kahn, private conversations.

[27] M. Vogt, private conversations.

[28] OP 3000 Series User Manual. Therma Wafe Inc., 1998.

[29] MX204 User Manual, Eichhorn + Hausmann GmbH.

[30] http://www.eh-metrology.com/products/manual-tools/mx-20x-series/mx-204-8-37-b.html

[31] Stress Evaluation Software Modul for our Contactless Wafer Geometry Gauges with three Resting Points. Article, Eichhorn + Hausmann GmbH, Revision 1.0, 2005.

[32] M. Sitarz: Rapport Stage. Company-internal Traineeship Report, July 2002.

[33] C. L. Anderson, H. L. Dunlap: Process for Annealing Semiconductor Material. United States Patent 4.135.952, 1979.

[34] Adhesion Pull-Off Tester Brochure, DeFelsko Corporation & mtv messtechnik oHG 2009. U.S. Patent #6,050,140.

[35] G. Denifl, private conversations.

[36] Araldite 2011-A/B, multiple purpose epoxy-adhesive, specifications sheet, Huntsmann Advanced Materials Americas Inc., 2006.

[37] PosiTest Pull-Off Adhesion Tester, Instruction Manual, Version 2.1.

[38] ASTM International: Standard Test Methods for Measuring Adhesion by Tape Test, D 3359-02, 2008.

[39] U. Hedenig: Sawing Instructions. private conversations.

Appendix

Appendix 1: Measurements of the BPSG film parameters.

## . . . sample denotation
TEB . . . amount of Triethylborate [mgm]
TEPO . . . amount of Triethyphosphate [mgm]
GOF . . . goodness of fit; if >0.95, then measured values are significant
Th. Av. . . . average film thickness [nm]
Th. R. . . . thickness range [nm]
Th. CP. . . thickness at the centre point [nm]
Unif. . . . uniformity of the deposited film [%]
RI Av. . . . average refractive index
RI R. . . . range of the refractive index
Av-Str. . . . average film stress [MPa]
Cnt-Str. . . . center stress [MPa]
B . . . doping level of boron [%]
P . . . doping level of phosphor [%]

##	TEB	TEBO	GOF	Th. Av.	Th. R.	Th. CP	Unif	RI Av.	RI R.	Av. Str.	Cnt. Str.	B	P
1	75	20	0,969	349,860	9,424	356,619	0,0135	1,4537	0,0027	86,30	88,00	1,44	2,99
2	40	15	0,977	307,991	7,512	313,239	0,0122	1,4161	0,0151	24,60	25,70	0,76	2,73
3	40	25	0,976	351,696	9,882	358,535	0,014	1,4547	0,0019	76,50	77,70	0,74	3,55
4	110	15	0,978	348,825	7,874	354,373	0,0113	1,4595	0,0016	6,58	6,95	2,20	2,43
5	110	25	0,968	402,682	7,229	407,719	0,009	1,4517	0,0009	57,10	57,30	2,06	3,10
6	52	15	0,985	311,072	9,379	316,833	0,0151	1,4559	0,0063	-43,9	-44,6	1,07	2,59
7	*Fall-Out Wafer*												
	Equ./Proc./Dop.												
8	Centura SA-CVD BPSG 1.0*2.7		0,971	1838,43	50,399	1829,66	0,0137	1,4412	0,0019	92,2	94,9		
9			0,972	1833,51	50,717	1801,07	0,0138	1,4413	0,0022	91,7	94,7	1,02	2,95
10			0,971	1837,37	53,447	1803,06	0,0145	1,4412	0,0022	91,4	93,9		
11			0,971	1832,48	54,257	1800,27	0,0148	1,4414	0,0024	90,6	93,4	1,04	2,95
12			0,971	1830,56	50,877	1796,72	0,0137	1,4415	0,0024	90,6	93,5		
13			0,971	1835,28	51,027	1801,97	0,0139	1,4413	0,0022	90,5	93,5	1,01	2,94

14	Centura SA-CVD BPSG 2.3*2.7	0,967	1842,74	34,26	1831,03	0,0093	1,4402	0,0014	86,4	88,9		
15		0,967	1845,74	36,71	1820,74	0,0099	1,4401	0,0013	86,2	88,7	2,11	2,81
16		0,967	1840,73	31,37	1820,4	0,0085	1,4403	0,0012	85,7	88,6		
17		0,967	1844,2	33,94	1820,24	0,0092	1,4402	0,0013	86,4	89,3	2,12	2,8
18		0,967	1844,56	33,95	1821,66	0,0092	1,4401	0,0014	86,2	88,7		
19		0,968	1837,06	32,63	1816,33	0,0089	1,4404	0,0016	86,4	89,1		
20	Watkins Johnson AP-CVD BPSG 1.0*2.7	0,962	1824,67	83,58	1867,26	0,0229	1,4455	0,0092	137	140	0,97	3,08
21		0,96	1781,08	101,64	1816,97	0,0285	1,4473	0,0031	131	134		
22		0,957	1812,93	52,52	1842,43	0,0145	1,4466	0,0065	135	138		
23		0,975	177,41	99,69	1804,44	0,028	1,4463	0,0143	132	135	1,05	3,11
24		0,963	1818,14	34,11	1833,07	0,0094	1,4461	0,0091	134	137		
25		0,954	1779,28	126,94	1825,52	0,0357	1,4488	0,0071	132	135		

Appendix 2: Measurments of the tempered BPSG films before and after the tempering process.

## . . . sample denotation
TEB . . . amount of Triethylborate [mgm]
TEPO . . . amount of Triethyphosphate [mgm]
GOF . . . goodness of fit; if >0.95, then measured values are significant
Th. Av. . . . average film thickness [nm]
Th. R. . . . thickness range [nm]
Th. CP. . . thickness at the centre point [nm]
Unif. . . . uniformity of the deposited film [%]
same comp. as app. 1 . . . same composition of the films as for the according samples in Appendix 1

##	TEB	TEBO	**results BEFORE tempering**					**results AFTER tempering**				
			GOF	Th. Av.	Th. R.	Th. CP	Unif	GOF_A	Th. Av_A	Th. R_A	Th. CP_A	Unif_A
9	same comp. as app. 1		0,972	1833,51	50,72	1801,07	0,014	0,989	1703,77	38,18	1678,30	0,012
10			0,971	1837,37	53,45	1803,06	0,015	0,989	1701,19	41,63	1680,14	0,012
15			0,967	1845,74	36,71	1820,74	0,010	0,988	1723,43	29,49	1704,00	0,009
16			0,967	1840,73	31,37	1820,40	0,009	0,988	1719,23	24,32	1703,02	0,007
21			0,96	1781,08	101,64	1816,97	0,029	0,967	1672,13	109,96	1703,05	0,033
22			0,957	1812,93	52,52	1842,43	0,015	0,961	1706,00	39,89	1725,88	0,012

Appendix 3: Percentual reduction of the BPSG film thickness during the tempering process.

## . . . sample denotation
same comp. as app. 1 . . . same composition of the films as for the according samples in Appendix 1
Th. Av. . . . average film thickness before tempering [nm]
Th. CP. . . thickness at the centre point before tempering [nm]
Th. Av_A. . . . average film thickness after tempering [nm]
Th. CP_A. . . thickness at the centre point after tempering [nm]
Δ Th. Av. . . . difference of the average film thickness [nm]
Δ Th. CP . . . difference of the film thickness at the centre point [nm]
% Th. Av. . . . reduction of the average film thickness due to tempering [%]
% Th. CP . . . reduction of the film thickness at the centre point due to tempering [%]

##		**Th. Av.**	**Th. CP**	**Th. Av_A**	**Th. CP_A**	**Δ Th. Av.**	**Δ Th. CP**	**% Th. Av.**	**% Th. CP**
9	same comp. as app. 1	1833,51	1801,07	1703,77	1678,30	129,74	122,77	7,08	6,82
10		1837,37	1803,06	1701,19	1680,14	136,18	122,92	7,41	6,82
15		1845,74	1820,74	1723,43	1704,00	122,31	116,74	6,63	6,41
16		1840,73	1820,40	1719,23	1703,02	121,50	117,38	6,60	6,45
21		1781,08	1816,97	1672,13	1703,05	108,95	113,92	6,12	6,27
22		1812,93	1842,43	1706,00	1725,88	106,93	116,55	5,90	6,33

Appendix 4: Impact of several film deposition and one tempering processes on the wafer bow.

## . . . sample denotation
Bow b. W. . . . bow of the bare silicon wafer [µm] in x- and y-direction
Th. Av. . . . average film thickness [nm]
Th. R. . . . thickness range [nm]
Th. CP. . . thickness at the centre point [nm]
Unif. . . . uniformity of the deposited film [%]
Bow ground . . . bow of the wafer with the deposited POLY or TEOS film [µm] in x- and y-direction, and in total
Bow a-C:H:N . . . bow of the film stack including the a-C:H:N film [µm] in x- and y-direction, and in total
Bow ground after. . . bow of the film stack including the a-C:H:N film [µm] in x- and y-direction, and in total AFTER the tempering process

Test	**##**	**Bow b. W.**			**Th. Av.**	**Th. R.**	**Th. Cp.**	**Unif**	**Bow ground**				**Bow a-C:H:N**				**Bow a-C:H:N after**		
		x	**y**						**x**	**y**	**total**		**x**	**y**	**total**		**x**	**y**	**total**
pull-off test	1	-2,07	0,95	**POLY**	94,56	94,76	112,99	50,64	-2,22	0,87	-1,26	a-C:H:N film, expected thickness 1 µm	50,69	49,93	29,81	**as-deposited**			
	2	-2,25	1,06		111,67	16,11	115,39	7,21	-2,20	0,94	-1,22		52,34	51,58	30,85				
	3	-1,90	1,28		92,22	95,25	114,39	51,64	-2,00	1,12	-1,09		58,19	56,86	34,20				
	4	-2,78	0,99	**TEOS**	712,63	16,19	704,74	0,05	-2,41	0,74	-1,18		52,41	51,84	30,98				
	5	-2,05	1,02		712,25	16,77	704,10	0,04	-1,85	0,98	-0,98		49,33	48,37	29,02				
	6	-2,16	0,93		711,34	17,26	703,15	0,03	-2,00	1,12	-1,00		59,25	58,01	35,00				
	7	-2,40	0,93	**POLY**	85,10	94,81	23,27	55,71	-2,49	0,82	-1,25		49,84	49,46	29,47	**tempered**	-46,01	-40,33	-27,05
	8	-2,14	0,82		113,29	15,38	117,06	6,98	-2,30	0,56	-1,32		52,83	51,55	31,04		-45,65	-40,12	-26,91
	9	-1,99	0,94		95,14	93,85	36,70	49,32	-2,51	1,22	-1,15		57,86	56,68	34,10		-47,31	-41,94	-27,95
	10	-2,10	0,55	**TEOS**	710,11	17,10	701,88	0,04	-1,99	0,42	-1,29		52,25	50,87	30,63		-45,68	-40,49	-27,08
	11	-2,96	0,89		709,33	16,94	701,36	0,03	-2,46	1,06	-1,20		50,12	49,67	29,62		-46,29	-40,45	-27,23
	12	-2,52	0,73		708,08	16,04	700,20	0,03	-2,30	0,98	-1,26		59,62	58,46	35,14		-46,49	-40,61	-27,35

tape test	13	-1,97	1,10	**POLY**	85,33	93,45	115,72	54,76	-2,15	1,07	-1,05	a-C:H:N film, expected thickness 1 µm	50,14	49,58	29,64	**as-deposited**			
	14	-2,84	0,58		80,43	93,00	113,63	57,81	-2,50	0,41	-1,45		52,63	51,28	30,61				
	15	-2,58	1,00		74,84	95,09	116,91	63,53	-2,58	1,07	-1,30		58,01	57,02	34,17				
	16	-2,54	0,35	**TEOS**	707,08	16,90	699,28	0,03	-2,29	0,36	-1,38		52,05	50,90	30,61				
	17	-2,57	0,84		705,99	17,43	698,20	0,03	-2,34	0,81	-1,20		47,17	46,35	27,77				
	18	-2,14	1,48		704,73	17,31	697,08	0,02	-1,89	1,63	-0,90		58,91	57,91	34,74				
	19	-2,69	0,81	**POLY**	82,08	93,18	115,97	56,76	-2,81	0,69	-1,49		49,36	49,11	29,09	**tempered**	-46,12	-40,31	-27,16
	20	-2,47	0,61		115,74	4,92	112,95	2,13	-2,59	0,44	-1,52		52,62	52,25	31,11		-45,66	-39,31	-26,72
	21	-2,80	0,60		116,50	4,84	115,64	2,08	-2,95	0,74	-1,49		57,59	56,28	33,83		-48,12	-42,23	-28,34
	22	-2,36	1,24	**TEOS**	703,49	16,95	696,02	0,02	-2,04	1,42	-0,96		52,20	52,24	30,78		-45,72	-39,68	-26,78
	23	-2,90	0,95		702,21	16,83	694,84	0,02	-2,60	0,89	-1,27		50,42	49,87	29,80		-46,61	-40,54	-27,31
	24	-3,05	1,35		700,71	16,46	693,56	0,01	-2,45	0,88	-1,25		59,96	59,46	35,60		-46,82	-40,71	-27,42